TEXTILE RESEARCH JOURNAL

VOLUME XX July, 1950 *NUMBER 7*

PUBLICATION OF

TEXTILE RESEARCH INSTITUTE, INC.

Editorial Office: 10 East 40th Street, New York 16, N. Y.

Rayon Reports

Avisco Introduces New Heavy Denier Carpet Staple

Avisco "15" engineered for carpet industry requirements

In response to the needs of the carpet industry, Avisco has developed a 15 denier rayon staple especially designed for use in rugs. The result of more than 10 years of study and experiment, Avisco "15" is a dull crimped staple engineered to produce a firm, sturdy surface. Tests show that carpets made from it wear exceptionally well.

Rayon brings to the carpet industry new opportunities for unlimited styling. Rayon's well-known affinity for dyes will make possible clearer, brighter rug colors. New effects in color, texture and pattern can also be achieved by cross-dyeing and by the use of variations in luster.

Already woven are carpets and rugs on Axminster, Wilton and velvet looms in a wide range of plain colors and patterns, in twist, cut and un-cut pile types. These new products will be introduced by manufacturers at floor covering shows being held this summer in Chicago and New York.

By taking advantage of the unlimited styling opportunities made available by rayon and the stable price of the man-made fiber, carpet manufacturers may well be opening up new profit possibilities for their industry. Rayon can stimulate the market for carpets just as it has for men's summer suits, women's suits and boys' wear. Avisco "15" could become as important to the carpet industry as rayon cord is to the tire industry. The reputation for versatility won by rayon in new fields benefits all users of rayon.

Avisco 15-denier carpet staple

Avisco 1.5-denier apparel staple

RAYON 20 YEARS AGO

NEW YORK, July, 1930—In spite of the general slump, rayon is holding its own, and even making progress in various fields, particularly in rayon and cotton mixtures.

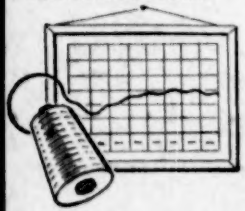

NEW YORK, July, 1930—For fall, women's wear cutters are favoring worsteds with rayon decorations.

NEW YORK, July, 1930—Leaders in the fields of knitting and weaving are welcoming the announcement of the "Crown Tested Plan" by the Viscose Company.

MAKE USE OF *Avisco* 4-PLY SERVICE

To encourage continued improvement in rayon fabrics, American Viscose Corporation conducts research and offers technical service in these fields:

1 FIBER RESEARCH
2 FABRIC DESIGN
3 FABRIC PRODUCTION
4 FABRIC FINISHING

AMERICAN VISCOSE CORPORATION

America's largest producer of rayon

Sales Offices: 350 Fifth Avenue, New York 1, N. Y.; Charlotte, N. C.; Cleveland, Ohio; Philadelphia, Pa.; Providence, R. I.

TEXTILE RESEARCH JOURNAL

VOL. XX, NO. 7 July, 1950

In This Issue

A Quantitative Study of Resilience	L. F. Beste and R. M. Hoffman	441
The Molecular Structure of Wool Keratin	A. C. Goodings	454
Measurement of Friction Between Single Fibers		
V. Frictional Properties of Viscose Rayon Staple Fibers	Bertil Olofsson and Nils Gralén	467
VI. A Theoretical Study of Fiber Friction	Bertil Olofsson	476
The Kinetics of Wool Dyeing: Part I: Simple Acid Dyes	P. Alexander and R. F. Hudson	481
INDUSTRIAL SECTION		
Gloss Measurements on Fabrics	Richard G. Quynn, Edwin J. Bernet, and Earl K. Fischer	492
The Influence of Sodium Carboxymethyl Cellulose on the Suspending Power of Built Soap Solutions	C. H. Bayley and A. S. Weatherburn	510
Laboratory Techniques		
Colorimetric Determination of Sodium Hypochlorite	Guy R. Wallin	514
Rapid Method for Determining Mildew Susceptibility of Materials and Disinfecting Activity of Compounds	R. G. H. Siu and G. R. Mandels	516

Editor: Julian S. Jacobs *Managing Editor:* Julia M. Crisp

Associate Editors

H. J. Ball
Earl E. Berkley
Henry Eyring
Gustavus J. Esselen
Earl K. Fischer
Milton Harris
K. L. Hertel
H. Mark
E. R. Schwarz
Kyle Ward, Jr.

TEXTILE RESEARCH JOURNAL, published monthly at Prince and Lemon Streets, Lancaster, Pa., is devoted to the interest of research in textile and allied industries. It is the official publication of Textile Research Institute, Inc.

Manuscripts and communications should be sent to the editorial offices, 10 East 40th Street, New York 16, N. Y.

Subscription rates (including, monthly, bound copy of the Abstracts from the *Journal of the Textile Institute*): General—$15.00 per year; additional for postage, 50 cents to Canada, $1.00 to all other countries. Special—$10.00 per year for United States and Canadian students, teachers, educational institutions, public libraries, governmental libraries and departments, plus 50 cents for postage to Canada. Single copies, $1.50 each.

Entered as second-class matter, April 27, 1945, at the postoffice at Lancaster, Pa., under the Act of August 24, 1912. Accepted for mailing at special rate of postage provided for in paragraph (d-2), Section 34.40, P. L. & R. of 1948, authorized May 9, 1950.

Contents copyrighted 1950 by Textile Research Institute, Inc.

Advertising rates supplied on request.

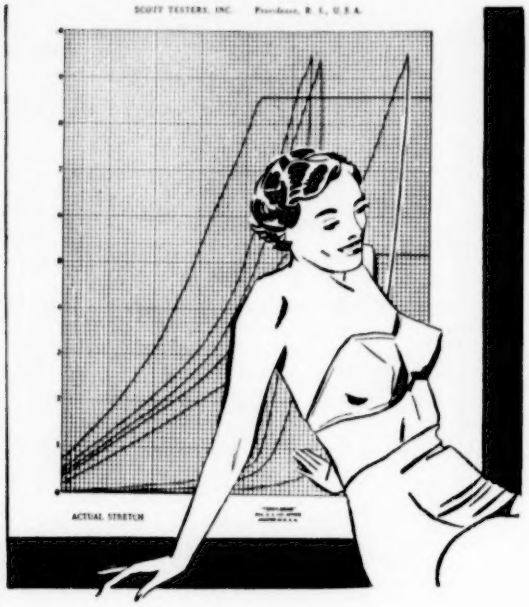

Production Control of ELASTICIZED FABRICS of all descriptions through *Scott Testers

How *Scott Testers give you three-way control of Production

1. Control of the finished product starts with controlled purchasing and production of the rubber thread. Scott makes special testers for complete analysis of rubber thread you purchase or manufacture.

2. Control in covering the thread, through testing, is an essential aid in obtaining the desired characteristics, and in maintaining uniformity.

3. In finished form, the product again requires the control analysis that physical testing provides.

Scott Testers are World-Standard for determining stretch and recovery characteristics from single end to finished fabric in various forms. Let us help you plan an adequate testing routine to detect irregularities before they get into further processing, as well as to speed production and enhance quality.

* Registered Trademark

BATHING SUIT FABRICS
GIRDLE FABRICS
GARTERS
SUSPENDERS
ELASTICIZED SUITINGS
WAISTBANDS
GUSSETS—INSERTS

TESTED IS TRUSTED

REQUEST
CATALOG 50

SCOTT TESTERS, INC., 145 BLACKSTONE ST., PROVIDENCE 5, R. I.

Scott Testers — Standard of the World

TEXTILE RESEARCH JOURNAL

VOL. XX, No. 7 July, 1950

A Quantitative Study of Resilience*

L. F. Beste and R. M. Hoffman

Pioneering Research Section, Technical Division, Rayon Department, E. I. du Pont de Nemours and Company

THE GENERAL PROBLEM of measuring fiber and fabric resilience and correlating the one with the other is of great importance to the textile industry. The purpose of this paper is to point out some fruitful lines of attack upon this problem and to give some quantitative results which have been obtained in the course of our studies. Although the methods which we shall discuss below have been extremely useful to our research on new fibers, we wish to emphasize the fact that much work remains to be done before the general problem may be considered to be solved.

Since in the present paper we continue the discussion of the theme of an earlier paper by one of us entitled "A Generalized Concept of Resilience" [1], it will be helpful to recapitulate the main points of the earlier publication. First, it was pointed out that the term "resilience" has many different meanings, the meaning in a particular instance depending upon the speaker (or writer) and the context. Much of this confusion is removed if we recognize that resilience has two aspects—namely, *type* and *extent*. Each of these aspects has its own complex factors, and, although neither one can be measured entirely independently of the other, the two should be regarded as separate entities.

It was next shown that type of resilience is separable into two factors, each of which is complex and measurable by various means. One of these factors is stiffness, or stress per unit strain: on a descending scale of inherent stiffness, glass, cotton, and rubber cover the entire range of interest to the textile world. The other factor is change of stiffness with elongation and with time. This effect is well described by the term "diminishing modulus," since the change is usually (but not always) toward lower stiffness. The diminishing-modulus effect, which is present to a high degree in the stress-strain curve of wool, explains wool's unusual ability to feel crisp but not harsh. This factor is also observed as a spontaneous decrease * of stress in a fiber which is being held at constant length.

The other aspect of resilience, its extent, is characterized by the ability of a body or substance to recover from a deformation. In considering this aspect, the time element and the environment must always be specified, because both factors play an important role in the extent of recovery.

Finally, it was shown that the three variables mentioned above—stiffness, diminishing modulus, and

* Presented at the Spring Meeting of The Fiber Society, Clemson, S. C., April, 1949.

* A spontaneous *increase* of stress at constant length can be induced by a suitable loading history; this phenomenon is called by some writers the "elastic after-effect."

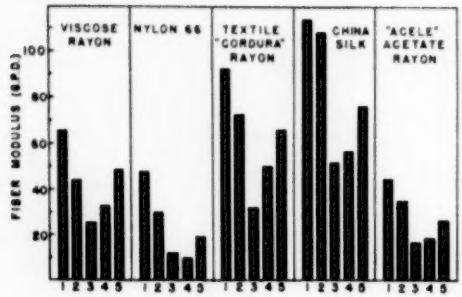

FIG. 1. *Change of fiber modulus in processing. 1—Control yarn. 2—Greige fabric. 3—Boiled-off fabric. 4—Dyed fabric. 5—Yarn boiled off in skein. (G.P.D. = grams per denier.)*

TABLE I. EFFECTS OF TIME AND TEMPERATURE IN BOILING-OFF POLYETHYLENE TEREPHTHALATE YARN *

Treatment		M	T	E
Original yarn		71	2.9	57
Boiling water	15 min.	26	2.4	41
Boiling water	30 min.	19	2.3	36
Boiling water	45 min.	22	2.2	35
Boiling water	60 min.	24	2.3	35
Water 60°C	45 min.	52	2.3	16
Water 75°C	45 min.	36	2.7	31
Water 85°C	45 min.	28	2.4	32
Water 95°C	45 min.	21	2.3	39
Oil 127°C	45 min.	9	2.0	52

* M = tensile modulus in g./den. (per 100% elongation). T = tenacity in g./den. E = percent elongation at break.

extent of recovery—may be conveniently depicted together in a three-dimensional plot or map.

In the present paper we wish to amplify some of the points of the previous one, to furnish data for several properties, and to mention some quantitative correlations which we have found between fiber properties and fabric behavior. We wish also to discuss several questions which were raised and left unanswered: (1) Should stress-strain-time relationships be measured in tension, compression, torsion, or bending? (2) Under what humidity conditions should tests be made? (3) What should be the previous history of the test sample?

We shall consider the last question first.

Previous History of the Sample

Suppose that a package of continuous-filament yarn or a bale of staple is ready for sale to the processor. How meaningful are the results if the mechanical properties are measured at this stage? Certainly from the standpoint of control they are quite meaningful. From the standpoint of predicting fabric resilience, these properties would be significant only if they suffered no change in processing. Now, it is well known that in the processing steps which lead from fiber to dyed and finished fabric a fiber is exposed to high intermittent or continuous stresses, to high temperatures, and to wetting with water. It would not be surprising if the fiber properties changed markedly under this treatment.

We have, in fact, found considerable changes in a number of properties as a result of textile processing. For example, in Figure 1 is shown the tensile modulus * for several materials at various stages of processing. These results follow a rather regular pattern: in each instance the modulus is highest for the control yarn, lowest for yarn removed from either the dyed or the boiled-off fabric, and intermediate for the boiled-off control. Other properties show similar changes, although of the properties measured the modulus exhibits proportionately the greatest change as a rule.

We conclude from these and similar data that if one wishes to correlate fabric performance with the properties of the constituent fibers he should measure these properties on fibers which have been removed from the finished fabric. When these are not available, it is preferable to boil-off yarns before testing them, since the properties of the boiled-off material are closer to the properties of the final product than are those of fibers which have not been boiled.

The time and temperature of treatment are of some importance. Effects of these variables on a particular sample of polyethylene terephthalate yarn are shown in Table I.

We conclude that the effects of boiling water on this fiber sample are essentially complete in 30 min. The effects of temperature show no leveling off in the range covered; as a practical temperature we pre-

* All modulus values given in this paper were determined at a constant rate of elongation of 10%/min., at 60% R.H. and 70°F. The modulus, determined from the slope of the linear portion of the stress-strain curve, is equal to the stress which would (theoretically) double the length of the specimen.

fer that of a bath of boiling water, since this temperature is easily maintained constant, and it is unlikely that a yarn will be exposed to higher temperatures than this for long periods of time. Because of the above considerations we have adopted a standard treatment for test yarns, which consists of immersion of the skeins in boiling water for 45 minutes. Distilled water to which had been added 0.1% by weight of detergent * was used. Unless otherwise noted, all yarns and fabrics for which data are given in this paper were prepared in this way, with the exception of cellulose acetate and polythene, which were boiled-off at 60°C.

Type of Resilience

Stiffness

Stiffness in yarn filaments may be measured by numerous means. The general definition of stiffness (stress per unit strain) applies equally well to Young's modulus when measured either in stretching or bending, to the torsional modulus, or to the bulk modulus. The rate is important; measurements of strain may be made a few microseconds after applying the stress, or the strain may be allowed to grow for days or weeks. The test may be cyclic in nature or unidirectional.

It seems reasonable to assume that of all these methods of measuring stiffness measurement of the modulus in bending is the most meaningful with respect to fabric "handle." In fact it may be said that all the stress-strain-time relationships ought perhaps to be determined in bending. With respect to the modulus, the usual practice has been to measure it in a tensile test and to assume that the same value for the measurement holds to a first approximation for the specimen in bending. Very little has been published on the validity of this practice because of the difficulty of measuring the small forces involved in bending. Khayatt and Chamberlain [2] obtained values for the bending modulus of several animal hairs which ranged from 44% to 80% of the modulus as measured in tension. By a similar method we found the ratio of bending to tensile modulus to be 86% ± 14% for a synthetic polyamide and 113% ± 12% for polyethylene terephthalate. The above limits are average deviations. From these and similar results obtained elsewhere we conclude that the tensile modulus is a sufficiently good indication of bending stiffness to make direct measurements of the latter unnecessary. However, if it ever becomes desirable to make really fine distinctions between fibers, it may be necessary to obtain these measurements.

The rate or frequency of test influences modulus results also. From one point of view, we should measure the modulus at as high a rate as possible, since we wish to account for time effects separately. From the practical point of view, elongation rates of several percent per minute are the most important. Accordingly, we have consistently employed a constant rate of elongation of 10% per minute. We briefly investigated the effect of rate upon modulus in the range 10–50% elongation per minute and found no great change in this interval.

It perhaps is not necessary to emphasize the fact that the stiffness of a fiber is a real entity which will make itself felt in any fabric construction; that is, of two fibers put into the same construction, the stiffer fiber will yield the stiffer fabric. It is sometimes claimed that modulus differences can be effectively leveled out or erased by a suitable adjustment of filament denier. This view assumes that filament denier exerts no influence in its own right as an independent variable. We can cite two harmful effects of arbitrarily decreasing the denier—namely, decrease in recovery from creasing and decrease in liveliness or "jump."

Diminishing Modulus

To illustrate the diminishing modulus as it affects the shape of the stress-strain curve, two typical curves are shown in Figure 2. In each instance the "initial modulus," or stiffness, is the slope of the dotted line. (The concave upward portion of the curve for wool is due to crimp; the dotted line is assumed to represent the true curve for the fiber substance in this region.) Aside from the difference in stiffness, the striking difference between these curves lies in their different shapes. If we examine the curve for cotton we note that the ratio stress/strain is nearly constant as the fiber is deformed. In other words, the fiber exhibits a stiffness which is almost independent of elongation. For this reason, a really crisp cotton fabric feels harsh and unyielding if crumpled tightly. On the other hand, wool becomes markedly less stiff, or more compliant, with strain. For this reason, a wool fabric with crispness and

* Duponol-WA. In some of our earliest work a technical olive-oil base soap was used.

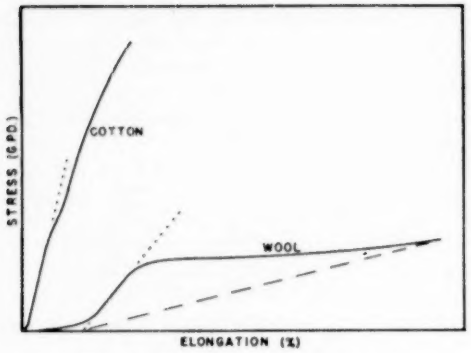

FIG. 2. *Typical stress-strain curves.*

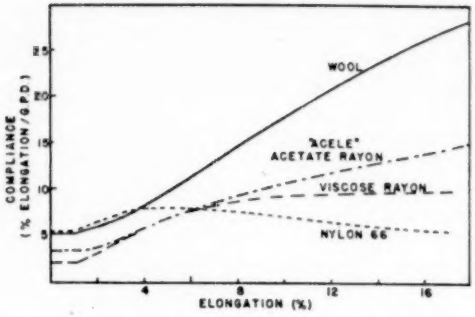

FIG. 3. *Compliance vs. elongation.*

body will not feel harsh even when it is creased sharply on itself.

Such departures of stress-strain curves from linearity are sometimes linked solely with the time variable or with a lack of "perfect elasticity." On the other hand, with simple levers or linkages and a few rubber bands one can easily construct mechanical models having zero time effects and (nearly) perfect elasticity, which will yield all manner of non-linear stress-strain curves. That such non-linear elastic elements are present in wool can be readily believed. The folds present in the wool molecule in the unstrained state provide an opportunity for hydrogen bonding, and these bonds are characterized by a rapid and reversible decrease of attractive force with elongation. This picture correlates perfectly with the fact that the recovery portion of the hysteresis loop of the wet wool filament is concave downward for the first several percent of extension. A qualitatively similar effect would be observed in a mechanical spring-and-dashpot model if it were equipped with a pair of horseshoe magnets arranged to come together at the point of zero elongation.

In the previous paper the "diminishing modulus" was measured by the ratio of the initial modulus (slope of the dotted line in Figure 2) to the average modulus at break (slope of the dashed line on the wool curve). This modulus ratio reflects some fundamental properties of the fiber substance, but in looking for a practical measure of diminishing modulus we must recognize the fact that a fiber in normal use is seldom strained to an amount approaching the breaking point. Indeed, some direct measurements of filament curvature in creased fabrics lead us to believe that the practical limit of fiber deformation is approximately 11% elongation on the outside of the bent filament and a corresponding amount of compression on the inside. We wish, then, to find some means of characterizing stress-strain behavior up to about 11% elongation.

In discussing the curves of Figure 2 we stressed the increasing compliance of wool as opposed to the constant stiffness, and hence the constant compliance, of cotton. Let us, then, examine the compliance of fibers as a function of elongation. (The term "compliance" is used here to mean the reciprocal of stiffness, or strain divided by stress.)

Figure 3 shows this property for several yarns. It is apparent that the compliance is initially constant for each yarn, as it must be where the stress-strain curve is linear. Past the 1 or 2% elongation point there follows a transition region in some of the fibers

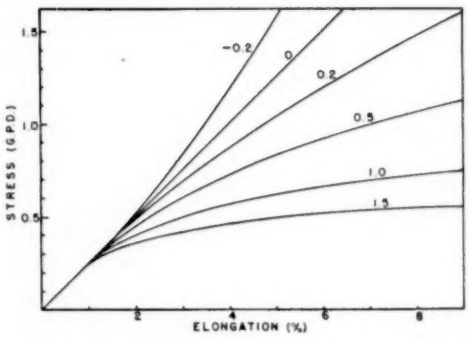

FIG. 4. *Synthetic stress-strain curves. The number on each curve indicates the rate of change of compliance with elongation.*

up to as high as 4% elongation. Past this point the compliance shows a remarkably constant rate of change with elongation.

It is of interest to ask what sort of stress-strain curves would be required to give strict linearity in the compliance *vs.* elongation plot. This is shown in Figure 4 for a number of curves having the same initial modulus. The number on each curve gives the rate at which compliance changes with elongation. Where the stress-strain curve is a straight line, the compliance is constant (zero rate of change). As the compliance changes at a higher rate the curves bend over more and more until, at a rate of about 1.5, the wool type of curve is encountered. The nylon type of curve shows a negative rate of change.

As shown in Figure 3, the compliance *vs.* elongation plots are not quite linear; therefore, it is necessary to take the differential rate of change at some arbitrary elongation or average out the change over a range of elongations. We have preferred the averaging process. Bearing in mind the upper limit previously set, and the fact that the initial modulus specifies the behavior for the first several percents of elongation, we have chosen the average rate of change of compliance between 5% and 10% elongation as our measure of diminishing modulus. As this quantity is given by a ratio, we have chosen to call it the "compliance ratio."

In mathematical terms the compliance ratio (CR) is given by

$$CR = (\text{Compliance at } 10\% \text{ elongation} - \text{Compliance at } 5\% \text{ elongation})/5$$

$$= \frac{10/L_{10} - 5/L_5}{5}$$

$$= \frac{2}{L_{10}} - \frac{1}{L_5},$$

where L_x is the stress in grams per denier at $x\%$ elongation.*

In Table II are values for the moduli and the compliance ratios for a number of fibers. In spite of the variability of most textile materials, we believe the values given are fairly typical of the various types of fiber.

* If the fiber breaks below 10% elongation, the CR may be computed between 5% and the break elongation. Where the break elongation is less than 5%, the compliance ratio may be taken as zero, since the stress-strain curve will be nearly a straight line.

The Resiliency Map

The data in Table II are easiest to study when plotted on a graph. Such a plot, embodying two dimensions of the complete resiliency* map, is shown in Figure 5A. The third dimension of the resiliency map will be treated in a later section.

In Figure 5A the fiber tensile modulus in grams/denier (per 100% elongation) is plotted as ordinate on a logarithmic scale. Choice of the logarithmic scale seems logical because it requires equal vertical distances to represent equal percentage changes in modulus. It also keeps the plot to a convenient size while avoiding crowding in the low-modulus region. The compliance ratio (horizontal axis) includes zero and negative values; accordingly, it is plotted on a linear scale.

The range of values represented on each axis in Figure 5A is nearly sufficient to include all the important textile materials. If natural rubber were included it would fall about as far below nylon as nylon falls below glass.

The various textile wools are materials with relatively low moduli and high compliance ratios. Only two materials are higher than wool with respect to this last property—namely, the man-made fibers from protein. At the left side of the map is nylon, with low modulus and low compliance ratio. Considering the great difference in "hand" between nylon and wool, it is evident that one compliance-ratio unit represents a very great change in properties. We believe that a difference of one unit corresponds to a smaller effect as higher absolute values are approached.

The highest modulus values found for the more common natural fibers are those for silk and cotton. Still higher moduli are characteristic of several fibers, including chrysotile (a type of asbestos), glass, "Fortisan," and ramie. All of these latter fibers are characterized by essentially straight stress-strain curves—that is, by compliance ratios near zero.

The effect of stretching on the properties of cellulosic fibers is of some interest. It will be seen that the series acetate rayon, viscose rayon, textile "Cordura," "Fortisan" shows a steady progression toward higher modulus and lower compliance ratio. This change in properties is no doubt due to increasing

* We use the word "resiliency" to denote an inherent property of a substance as opposed to the "resilience" of a body or structure. Where both words apply, we use "resilience" as the generic term.

TABLE II. STRESS-STRAIN PROPERTIES—60% R.H., 70°F

Material	*M* (g./den. per 100% elongation)	*CR* (dens./g.)
Japan silk	73 ± 4.1 *	0.29
Wool 50/56's	37 ± 1.3	0.86
Wool top 64's	21 ± 0.4	1.04
Wool 64's from worsted fabrics	18 to 25	1.0 to 1.7
Zein fiber	26 ± 1.0	1.80
Nylon 66, hosiery yarn	20 ± 0.3	−0.19
Casein, CH_2O-treated	18 ± 0.6	2.70
Polyethylene terephthalate C.F.†	86 ± 1.5	−0.05
Polyethylene terephthalate staple	20	1.05
Polyacrylonitrile C.F.†	83 ± 2.8	0.11
Polyacrylonitrile staple	34	0.68
Polystyrene	44	1.37
Polyvinylidene chloride	7 ± 0.2	−0.10
"Fortisan" rayon	243 ± 9.9	0
Ramie	169 ± 13.0	0
"Cordura" textile rayon	65 ± 2.8	0.37
Du Pont viscose rayon	54 ± 2.6	0.68
Cotton I‡	40 ± 3.7	0.21
Cotton II‡	35 ± 3.9	−0.04
"Acele" acetate rayon	39 ± 1.5	0.91
Glass fiber	344 ± 16.3	0
Asbestos (chrysotile)	147	0

* The fiducial limit given is the standard error of the mean. A minimum of 10 breaks was made on each synthetic and a minimum of 20 on each natural fiber.

† C.F. = continuous filament.

‡ Cotton I is 1⅛- to 1 $\frac{1}{16}$-in. American cotton removed from tire yarn. Cotton II is combed 1½-in. C.P. cotton removed from 50/1 yarn; twist multiplier 2.2.

crystallinity, and, to a greater extent, to increasing orientation, brought about by the stretching process.

In some respects the units employed in Figure 5A (g./den.) are misleading, as are all units based upon yarn or fiber weight. For example, if one should select a nylon and a wool filament of the same denier and the same modulus, he would find that they exhibited exactly the same resistance to stretch up to about 2 or 3% elongation. However, the resistance of the nylon to bending would be 35% greater than that of the wool. The reason for this discrepancy is that resistance to bending, other factors being equal, is proportional to the square of the cross-sectional area. This area, in turn, is directly proportional to denier and inversely proportional to fiber density.

The above type of discrepancy and many other difficulties could be avoided by the use of area units rather than weight units. In fact, the weight per unit area of a fabric is the *only* fabric property which is more logically related to denier, grex, yarn count, or other weight unit than to an appropriate area unit. All other fabric properties, and *all* the details of fabric and yarn geometry, are best understood in terms of fiber diameter and cross-sectional area.

In view of these considerations, the resiliency map of Figure 5A has been replotted in Figure 5B in units of kg./mm.^{2}. The rule for converting units is:

$$\text{kg./mm.}^2 = \text{g./den.} \times 9{,}000 \times \text{density.}$$

In converting, one should remember that the modulus is given in Table II and Figure 5A in g./den., but the compliance ratio is in dens./g.

A comparison of Figures 5A and 5B will show some interesting relative shifts of some of the materials.

The map is useful in defining types of resiliency. Casein, with its low modulus and high compliance ratio, should be very wool-like in hand, and it is so in fact. On the other hand, textile "Cordura" is silk-like, as shown by its position on the map. The materials between wool and silk are intermediate in type, or dual-purpose yarns. A third type of resiliency is represented by nylon, and a fourth type by inorganic materials. The chief use of this type of plot is in screening synthetic fibers before selection of the more attractive examples for scale-up into fabric. This saves considerable time and money in new-fiber research.

Recovery Characteristics of Fibers

The recovery of textile structures from deformation may be measured in many different ways, but only one of two things may be measured by each method: either the extent to which the structure returns to its original size and shape or else the proportion of the work of deformation which is returned. Each of these two types of test could conceivably be made in three ways—namely, in tension, in torsion, or in bending, a total of six combinations:

Work-recovery tests	Dimensional-recovery tests
1. Tensile	4. Tensile (controlled, creep, elastic)
2. Torsional	5. Torsional (controlled, creep, elastic)
3. Flexural	6. Flexural (elastic)

A tensile test is one in which the sample is elongated and then allowed to retract. There are only two recognized methods of carrying out tensile tests:

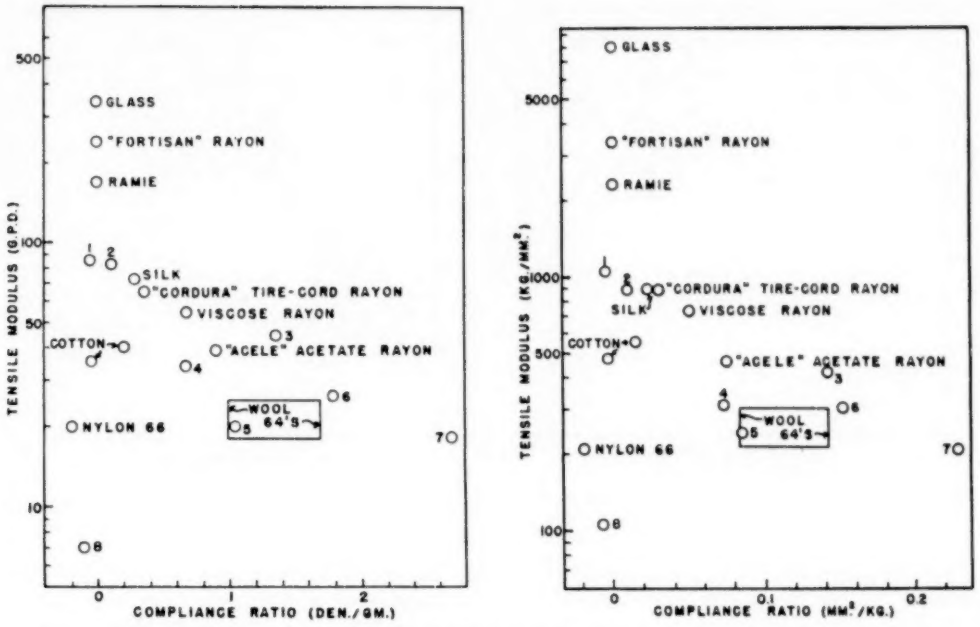

FIG. 5. *Type-of-resiliency maps, 60% R.H., 70°F. 5A (left)—Denier units. 5B (right)—Area units.*

The materials indicated by the numbers are as follows: 1—Continuous-filament polyethylene terephthalate. 2—Continuous-filament polyacrylonitrile. 3—Polystyrene. 4—Polyacrylonitrile staple. 5—Polyethylene terephthalate staple. 6—Zein fiber. 7—Casein fiber. 8—Polyvinylidene chloride.

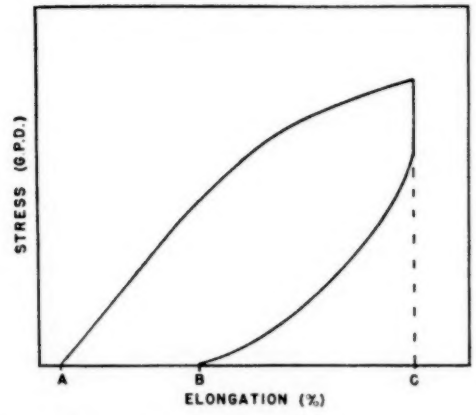

FIG. 6. *Measurement of tensile recovery. Tensile recovery = 100 BC/AC.*

either with controlled rate of elongation or with controlled rate of loading. (The controlled rate is not necessarily constant; it may be sinusoidal, for example.) It is possible to measure the tensile work recovery in a cyclic test at thousands of cycles per second. Important as this type of determination may be for fundamental reasons, we have confined our testing to the relatively slow rate of 1% elongation per minute, with retraction at the same rate.

It is possible to measure the work recovered in a torsional process also, and we have done so. The quantities of energy involved are very small. For example, the work required to twist a 3-den. acetate rayon filament 1 cm. long through an angle of 360° is about 3×10^{-5} g.-cm. This same amount of work would not elongate the same filament quite 0.2%. Since so little work is involved in this process, we believe that the torsional work recovery is of much less importance to fabric performance than is recovery measured in tension.

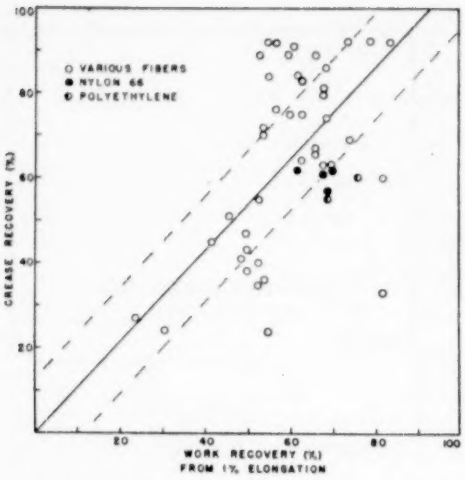

FIG. 7. *Fabric crease recovery* vs. *fiber work recovery from 1% elongation.*

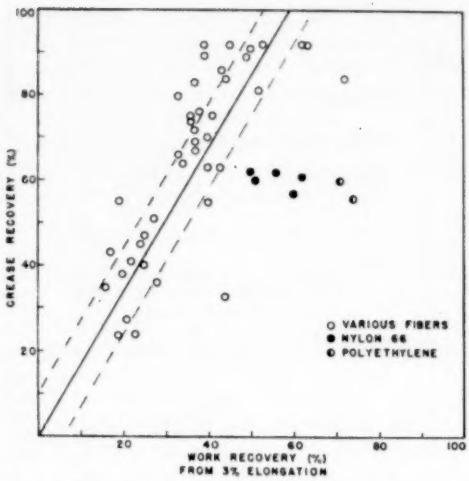

FIG. 8. *Fabric crease recovery* vs. *fiber work recovery from 3% elongation.*

It should be possible to directly measure work recovery in bending, but we have not attempted it. Some of the "compression" tests on masses of fibers measure bending work recovery indirectly as well as a certain amount of torsional work recovery.

There are three general classifications of dimensional recovery tests also, together with several subdivisions. The tensile test may be carried out at a controlled rate, as is done in the tensile work-recovery test. The measurement involved is indicated in Figure 6. The quantity of interest, which we shall term the "tensile strain recovery," or "tensile recovery," for short, is obtained by dividing the retraction BC by the elongation AC. Of course, the value obtained depends somewhat upon the rate chosen; for this test we employ the same rate as for the tensile work recovery test. There are two other possible ways to study longitudinal recovery of a fiber—namely, recovery from creep under a fixed load and recovery from a fixed elongation. The latter is often called the "elastic recovery" test.

The same three variations are possible in measuring torsional recovery; the discussion above concerning the relative importance of torsional tests applies here also. We have measured recovery from bends in only one way—namely, with the fiber re-

TABLE III. CORRELATION OF FABRIC CREASE RECOVERY WITH FIBER RECOVERY

R_{15} = 15-sec. crease recovery
TR_x = Tensile strain recovery from x% elongation
WR_x = Tensile work recovery from x% elongation
N = Number of comparisons
r = Correlation coefficient
$P.E.$ = Probable error of estimating R_{15} from the regression line
$P.E.'$ = Probable error of estimating R_{15} from best line through the origin

Equation of regression line	N	r	$P.E.$	Equation of best line through origin	$P.E.'$
$R_{15} = .90\ (WR_1) + 11.4$	43	.513	12.38	$R_{15} = 1.08\ WR_1$	12.47
$R_{15} = 1.27\ (WR_3) + 17.8$	43	.764	9.29	$R_{15} = 1.70\ WR_3$	10.00
$R_{15} = 2.32\ (WR_5) + 4.6$	28	.835	7.19	$R_{15} = 2.50\ WR_5$	7.22
$R_{15} = .92\ (TR_1) - 8.9$	38	.581	11.67	$R_{15} = 0.79\ TR_1$	11.73
$R_{15} = 1.05\ (TR_3) + 4.0$	38	.760	9.31	$R_{15} = 1.10\ TR_3$	9.35
$R_{15} = 1.26\ (TR_5) + 5.4$	25	.697	9.56	$R_{15} = 1.39\ TR_5$	9.56

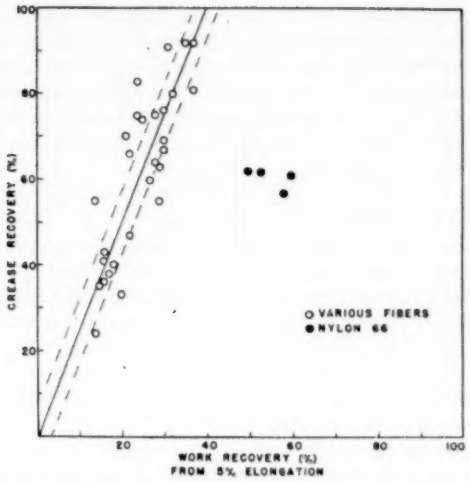

FIG. 9. *Fabric crease recovery* vs. *fiber work recovery from 5% elongation.*

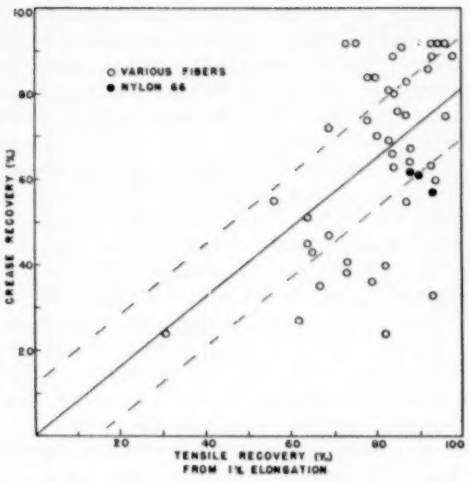

FIG. 10. *Fabric crease recovery* vs. *fiber tensile recovery from 1% elongation.*

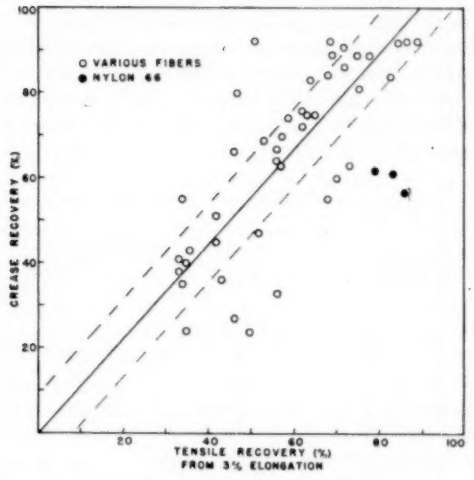

FIG. 11. *Fabric crease recovery* vs. *fiber tensile recovery from 3% elongation.*

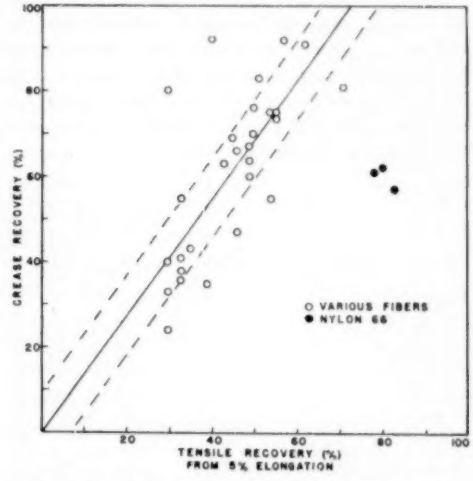

FIG. 12. *Fabric crease recovery* vs. *fiber tensile recovery from 5% elongation.*

covering freely from a fixed bend which had been held for a certain length of time. This method is thus analogous to the ordinary longitudinal "elastic recovery" test. In fact, the results from the bending recovery test for wool, acetate rayon, nylon, and viscose rayon parallel the results from the longitudinal elastic recovery test quite well. Accordingly, it seemed unnecessary to us to measure bending recovery as a routine practice.

In discussing the utility of the tensile work-recovery and tensile strain-recovery tests, we shall confine the subject to filaments intended for use in fabrics. Under this restriction, our only reason for measuring the recovery of a filament is that we may

be able to predict the recovery from creasing, wrinkling, and stretching of fabric woven from the same material. The first step has been to run various recovery tests on filaments removed from fabrics and compare the results with the crease recovery of the fabric in each instance.

The two tensile tests which we chose to compare with fabric recovery were: (1) tensile work recovery for 1%, 3%, and 5% elongation and (2) tensile strain recovery computed from the same curves. The test was run at a constant rate of elongation of 1% per minute, with the sample held for 30 seconds at the maximum elongation before it was allowed to retract. A recording tester employing a magnetic-type strain gage was utilized [3]. Each specimen was elongated successively to the three elongations specified above, with only enough pause between cycles to enable the operator to take up slack in the sample. The areas under the curves were measured by means of a polar planimeter.

The fabric crease-recovery test will be described in detail in a later publication. It will be sufficient here to state that fabric samples were creased according to a standardized technique and were then allowed to recover with the crease held vertical. This last feature minimized the effects of gravity on recovery. The recovery was measured 15 seconds after release of the sample. Recovery from a crease perpendicular to the warp was compared with the work recovery and tensile recovery of warp filaments, and where the crease was perpendicular to the filling the comparison was made with filling filaments. This made two comparisons possible for each fabric, but in some instances we made the comparison for only one direction.

All of the 28 fabrics in this study were twills from continuous-filament yarns except for two wools, which were plain weaves. Filament deniers, yarn deniers, and fabric-construction variables were quite diverse. As a result, whatever correlation was found in this preliminary study should be regarded as general and not confined to some particular construction. We are presently engaged in carrying out this same kind of study on a series of fabrics which are all of the same construction.

In each instance we obtained the rectilinear correlation coefficient and regression line in the usual way, together with the probable error of estimating the crease recovery from the regression line. It seems logical for physical reasons that the regression lines should pass through the origin—that is, that zero fiber recovery should correspond to zero fabric recovery. For this reason we also computed the best line through the origin for each case by the method of least squares. The probable error of estimating crease recovery from this line was then obtained. As

TABLE IV. TENSILE AND WORK RECOVERY

Material	Tensile recovery (%)								Work recovery (%)							
	60% R.H.				90% R.H.				60% R.H.				90% R.H.			
Elongation (%) →	1	3	5	10	1	3	5	10	1	3	5	10	1	3	5	10
Japan silk	84	60	52	34	78	65	58	45	57	32	23	17	47	30	24	23
Wool 50/56's	99	84	69	51	94	89	82	56	83	58	37	21	67	54	45	25
Wool top 64's	100	81	65	49	98	94	84	62	79	58	41	21	65	59	39	24
Zein fiber	100	74	47	—	85	59	43	28	90	36	22	—	48	31	21	15
Nylon 66	90	90	89	86	92	92	90	—	66	57	55	52	68	68	64	—
Casein fiber	90	65	47	30	76	58	43	25	74	45	23	11	53	34	18	9
Polyethylene terephthalate C.F.	98	79	65	51	92	75	60	47	82	49	35	24	76	46	30	21
Polyethylene terephthalate staple	95	75	70	—	92	73	69	—	85	44	37	—	83	43	34	—
Polyacrylonitrile C.F.	92	56	50	43	90	55	48	39	64	27	23	21	66	24	21	16
Polyacrylonitrile staple	89	66	51	—	84	62	48	—	63	33	20	—	62	30	19	—
Polyvinylidene chloride	89	86	83	70	—	—	—	—	62	60	56	43	—	—	—	—
Polyethylene	80	81	80	78	80	83	83	80	55	52	50	47	63	57	55	51
"Cordura" textile rayon	72	40	31	25	54	35	30	26	49	14	14	10	27	13	13	13
Du Pont viscose rayon	67	38	32	23	60	33	28	27	50	14	11	9	27	12	10	11
Cotton II	91	69	52	—	83	68	59	—	50	37	31	—	42	38	33	—
"Acele" acetate rayon	96	65	46	24	75	50	37	22	80	33	18	9	70	24	14	8
Glass fiber	—	—	—	—	—	—	—	—	97	—	—	—	—	—	—	—

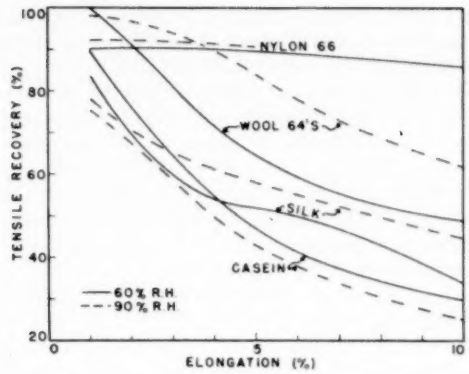

FIG. 13. *Tensile recovery of polyamide fibers.*

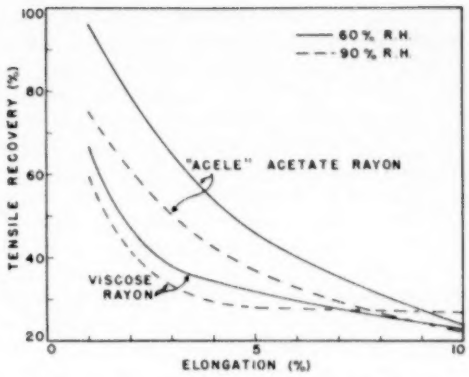

FIG. 14. *Tensile recovery of cellulosic fibers.*

is shown in Table III, the probable errors of estimate from the lines through the origin are not much greater than those from the regression lines.

The results are given in Table III and illustrated in Figures 7–12. In each figure only the line through the origin is given. The dashed lines indicate the probable errors of estimate. Since our purpose here is to discuss the utility of fiber tests, we shall not attempt to identify the separate materials except in the case of nylon (open circles) and polyethylene (half-filled circles). It will be seen that these two materials exhibit quite distinctive behavior except at the lowest elongation; for this reason they were omitted from all of the calculations.

The results of this study may be summarized as follows. First, it is evident that we can expect a fair success at predicting crease recovery from measurements on the filaments. In this connection, a determination subject to a probable error of estimate even as high as 10 can be very useful in screening new fiber candidates, and two-thirds of our probable errors were smaller than this. Next we note that, except for nylon and polyethylene, our predictions are more nearly correct when made from the work-recovery test at 5% elongation or from either type of test at 3% elongation.* Even with nylon and polyethylene included, the correlations are better at 3% and 5% elongation than at 1% elongation. Finally, these data are not extensive enough to allow a choice to be made between work-recovery and tensile-recovery tests. The results thus far slightly favor using work-recovery data for the comparison.

The tendency is to favor the tensile recovery test because in a fabric it is really strain recovery and not work recovery which interests us. However, the argument against this is that a storage of work is needed in fabrics to overcome interfiber friction in the recovery process. Just how much storage of work is needed has not been computed directly. In our testing of single filaments we have observed that strain recovery is always greater than the percentage of work recovered. For example, work recovery of 50% is almost always associated with tensile recovery of between 60% and 80%. Whether or not more than 50% of work recovery is needed to overcome interfiber friction in recovering 60–80% of the strain is a question which no one can answer at the present time. We believe that the correlation method will be extremely helpful in settling this question of work recovery *vs.* strain recovery.

We have found only one report of a similar study in the literature. This work [4] involved the correlation of tensile strain recovery (at 5% elongation) with the crease recovery of fabrics treated with various resins. It was found that a separate regression line was required for each resin, and that with non-diffusing resins the correlation was negative. This last finding is probably of no significance to a discussion of homogeneous filaments, but it should aid in

* It should be kept in mind that the present study involved the sharp creasing of fabrics; as a result, the fiber deformations were close to the maximum deformations encountered in ordinary service. Preliminary results of work in progress indicate that recovery from mild wrinkling correlates best with fiber recovery from 1% elongation, as is to be expected.

interpreting the behavior of fibers which have a macroscopic structure such as a skin-core arrangement.

One further point should be made about the above study. This is that the fiber recovery measurements were all made on the filaments *after* weaving. If we are to save the time and expense of weaving fabrics in order to evaluate fibers we must find some way of predicting what changes of properties will occur in textile processing. This consideration applies to the modulus and compliance ratio as well as to the recovery. The solution might be some sort of simulated carding, weaving, and finishing treatment which would cause a change in the properties of the fiber to those which obtain in the final fabric.

Recovery Results

It has been stated by numerous workers that wet tests are to be preferred for fundamental studies of fiber properties. We do not disagree with this view, but feel that practical studies should be carried out at ordinary humidities. Accordingly, we chose to measure recovery at 60% and 90% R.H. The temperature was 21°C throughout.

Results of recovery measurements are given in Table IV. The standard error is estimated to be about 3 for the work recovery results and about 5 for the tensile recovery results. Some of these results are plotted in Figures 13 and 14.

Aside from the absolute level of recovery, perhaps the feature of greatest practical interest in these results is the dependence of recovery upon humidity. It will be noted that the two wools and silk exhibit an *increase* in tensile recovery as the humidity is raised from 60% to 90%. This increase for wool is not reflected to a high degree in the crease recovery of wool fabrics, although, in general, conditions which raise or lower fiber recovery also raise or lower fabric crease recovery. In marked contrast to the behavior of wool and silk, the two synthetic fibers spun from proteins exhibit a marked decrease in recovery at the higher humidity. Still another type of behavior is characteristic of nylon 66, polyethylene terephthalate, and the vinyl polymers, for which recovery is practically independent of humidity. The recovery of all the cellulosic fibers deteriorates with rising humidity throughout much of the elongation range, but at some elongation above 4 or 5% a reversal takes place.

The above considerations are of great practical interest because conditions of high relative humidity are fairly common, and it is precisely under these conditions that some materials become objectionable with respect to creasing and mussing.

Another interesting feature of these results is the fact that nylon, polyethylene, and cotton show relatively little decrease in recovery with elongation. It is probably no coincidence that these materials are all highly crystalline. None of the other materials, which show considerable decrease in recovery over the range of elongations studied, is more than moderately crystalline. It was indicated in the section on correlations of fiber recovery with fabric recovery that the regression lines which are characteristic of the other materials do not apply to nylon and polyethylene. A rough comparison of the recovery characteristics of cotton fabrics with the fiber recoveries in Table IV indicates that they may not apply to cotton either. If they do not, then the three materials with relatively horizontal recovery *vs.* elongation curves are also exceptional in their fiber *vs.* fabric recovery relationships. Of course, this apparent connection may be indirect or it may be merely coincidence. There is no doubt, however, that an explanation of the somewhat peculiar behavior of nylon and polyethylene (and perhaps also of cotton) would materially advance our knowledge of the factors responsible for fabric crease recovery.

Summary

1. This paper continues, in a more quantitative way, the theme of an earlier paper [1].

2. It is shown that fiber and yarn samples for resiliency studies should be boiled-off before testing, since this treatment brings the fiber properties closer to what they would have been after weaving and finishing.

3. *Type* of resiliency is defined in terms of two factors, *stiffness* (measured by Young's modulus) and *diminishing modulus*. The "compliance ratio" is proposed as a practical measure of diminishing modulus on the stress-strain curve.

4. The results of stiffness and compliance-ratio measurements are given for a number of fibers. Wool is characterized by a relatively low modulus and high compliance ratio and silk by high stiffness and low compliance ratio. Nylon represents a third combination: low stiffness and low compliance ratio.

5. The type of resiliency of a synthetic fiber can be varied by its method of preparation. This variability is well illustrated by the cellulosic yarns acetate rayon,

textile viscose rayon, tire-cord rayon, and "Fortisan" rayon.

6. *Extent* of resiliency is characterized by ability to recover from deformation. Practical recovery tests are discussed, and the tensile strain recovery test is described.

7. The 15-second crease recovery of fabrics correlates much better with fiber recovery tests at 3–5% elongation than with those at 1% elongation. The fiber tensile work recovery correlates a little better with fabric crease recovery than does tensile strain recovery as presently measured.

8. Results of recovery measurements made at 60% and at 90% R.H. are given. Wool and silk show an increase of recovery with humidity. Vinyl polymers, nylon 66, and polyethylene terephthalate are relatively insensitive to humidity changes. The recovery of synthetic fibers made from proteins or cellulose decreases as the humidity is raised.

Acknowledgment

We wish to thank L. E. Amborski, J. W. Ballou, C. E. Black, S. K. Breslin, H. J. Kolb, and D. W. Vanas for important contributions to this work. Most of the measurements of physical properties were carried out by the du Pont Rayon Department, Pioneering Physical Test Laboratory, under Mr. C. J. Curtin.

Literature Cited

1. Hoffman, R. M., TEXTILE RESEARCH JOURNAL **18**, 141 (1948).
2. Khayatt, R. M., and Chamberlain, N. H., *J. Text. Inst.* **39**, T185 (1948).
3. Ballou, J. W., *A. S. T. M. Bull.*, No. 150, 38 (Jan. 1948).
4. Gruntfest, I. J., and Gagliardi, D. D., *Ind. Eng. Chem.* **41**, 760 (1949).

(Manuscript received January 25, 1950.)

The Molecular Structure of Wool Keratin

A. C. Goodings

Ontario Research Foundation, Toronto, Canada

Abstract

Properties of the wool fiber are considered, and the information given by density and x-ray diffraction measurements in particular is used to deduce the structural pattern in keratin. Some of the implications of this structure are pointed out, and other folded molecular configurations which are extensions of the proposed keratin structure are advanced and discussed in connection with experimentally observed facts.

Introduction

The structure of wool is complex both in chemical composition and in the physical configuration of the molecules. Silk is very simple by comparison; the protein fibroin has its amino-acid residues linked together in a straight-chain form, and these residues are largely those derived from the two simplest α-amino acids, glycine and alanine. Keratin, on the other hand, is built up in greater measure from amino-acid residues of higher molecular weight, giving rise to longer side chains projecting from the main molecular chain. Among the 18 different amino acids which have been identified in the hydrolytic products of the keratin molecule, certain residues with reactive side chains, both acid and basic, as well as that from the sulfur-containing amino acid cystine, occur with high frequency.

Despite the complexity of the problem, considerable progress has been made in the elucidation of the structure of keratin both from chemical and physical standpoints. In the latter connection, the use of x-ray diffraction technique, notably by Astbury and coworkers, has proved a most valuable tool. Wool is unique among textile fibers by virtue of its long-range elasticity, and Astbury [3] has been led to propose a folded molecular structure in which the main chain is potentially capable of slightly more than 100% extension when unfolded and made to assume a fully extended state. By introducing 3 amino-acid residues into a simple repeat of the folded structure, extending axially with the fiber over a distance of approximately 5.1Å., the prominent meridional x-ray reflection which occurs at this distance is accounted for.

A somewhat different approach to the problem of determining the molecular structure of keratin can be made by critical examination of certain other of its known physical properties—in particular, density—together with x-ray data and stereochemical considerations. The conclusions to be drawn from these arguments, which are discussed in this paper, lead to a structure for keratin differing from those previously advanced. By simple extension, the pattern may help to explain the structure of certain other fibrous proteins, as well as the molecular configuration assumed in states of contraction differing from the normal.

Density Considerations

Silk

The density of dry silk has been found to be 1.353 g. per cc. [10]. The positions of the x-ray reflections given by the crystalline regions of silk fit a unit cell, containing 8 amino-acid residues, which has the following dimensions: $a = 9.9$Å., $b = 6.95$Å., $c = 8.9$Å., $\beta = 76°40'$. The unit residue volume is therefore equal to 74.5×10^{-24} cc. These crystalline regions are probably composed largely or entirely of glycine and alanine residues [7] (possibly including some serine), although in what proportion is not known. The mean residue weight for crystalline silk fibroin may reasonably be considered to be in the region of 64 (the mean for glycine and alanine), and the density of crystalline silk would therefore be

$$\frac{64}{N \times 74.5 \times 10^{-24}} = \frac{64 \times 1.65}{74.5} = 1.42 \text{ g. per cc.},$$

where N is the Avogadro number. Although the density so calculated relates to a crystalline region composed largely of glycine and alanine residues, it is probable that the density of a hypothetical crystalline structure containing all the amino-acid residues which are present in silk in the proportion in which they actually occur would not differ greatly from the above value of 1.42 g. per cc. The density of crystalline material will be higher than that of the same material in an amorphous state, and a value of 1.42 g. per cc. for the density of crystalline silk is 5% higher than the actual fiber density, the normal silk fiber being composed of both crystalline and amorphous regions. Despite the fact that silk may be fairly high in crystalline content—estimates indicating a crystalline content of about 40–60% [11]—the difference in density between amorphous and crystalline regions cannot be very large.

Confirmation of the value derived for the density of crystalline silk may be sought from consideration of the apparent density of the fiber in water. If all of the noncrystalline regions of the fiber were penetrated by water, the apparent density of silk in water would approximate the crystalline density. If penetration is incomplete, the apparent density would be somewhat lower than the crystalline density. The actual value found for the apparent density of silk in water [10] is 1.426 g. per cc. The calculated value of 1.42 g. per cc. for the density of crystalline silk is therefore probably close to this value but slightly on the low side. The effect of this would be to make the crystalline density slightly more than 5% higher than the normal fiber density.

Nylon

The density of crystalline nylon 66 is given by Bunn and Garner [8] as 1.24 g. per cc. The density of dry nylon filaments in the drawn state has been found to be 1.145, and of undrawn nylon to be 1.141 [1]. Crystalline nylon, therefore, has a density approximately 8.3% higher than that of the normal drawn nylon filament and 9.6% higher than that of undrawn nylon. The amorphous content of nylon is believed to be higher than that of silk, a content of 65% having been indicated [1]. The somewhat larger percentage spread between the crystalline and normal filament densities in the case of nylon than that calculated for silk is therefore not unexpected.

Wool

The density of dry wool has been determined by King [13] and found to be 1.304 g. per cc. The density of crystalline wool protein is unknown, but it is clear that it will be higher than the value for that of the normal fiber. The evidence is that the crystalline regions of wool comprise only a small percentage of the total keratin material, and by comparison with the data for silk and nylon we may anticipate that crystalline keratin will have a density about 10% to 15% higher than that of normal wool. It may also be pointed out that the apparent density of wool in water given by King [13] is 1.3965 g. per cc., and, as stated in discussing silk, this value is likely to be a minimum for the density of crystalline wool keratin. Whatever the precise value is, it can be assumed with reasonable certainty that it will fall within the limits of from 5% to 15% higher than 1.304—that is, between values of 1.37 and 1.50 g. per cc. The fact that wool has a cell structure (differing from silk and nylon in this respect) does not, of course, invalidate the argument: what is being sought is the density of a hypothetical wool fiber which is identical in composition with natural wool but the molecules of which are arranged in an orderly manner which would conform to a crystalline state. The probable limits discussed within which the density of crystalline keratin should lie can, without more precise definition of the actual value, be made to serve sufficiently well for the present purpose.

In his extensive investigations on wool, Astbury [5] has differentiated between molecular configuration in the normal (α) state and in the stretched or extended (β) state. X-ray diffraction data show a clear distinction between the two, the strong meridional reflection in the former being at 5.14Å. and in the latter at approximately 6.7Å. Astbury has proposed, with strong supporting evidence, a reversible intramolecular transformation from a folded configuration in the α state to a β configuration approximating but not completely reaching the extended state of the chain molecule in silk. The carbon and nitrogen atoms which form the "backbones" of the main molecular chains are presumed to be coplanar for reasons of the conformity of such a geometrical pattern with experimental evidence and with general considerations of structure having regard for the chemical composition of keratin. The folding of the main molecular chains in normal keratin takes place in the plane of the "backbone"—that is, at right angles to

the protruding side chains, thereby not interfering with the space requirements of the latter groups.

In addition to the strong meridional reflection at 5.14Å., the photograph of α-keratin shows an intense area equatorially around 9.8Å., which is attributed by Astbury to the side-chain spacing. No separate reflection which might correspond to a spacing at right angles to this—that is, to a "backbone" spacing —is evident. In the case of β-keratin, equatorial reflections are given which correspond to about 9.7Å. and 4.65Å., interpreted by Astbury to be, respectively, the side-chain spacing and a "backbone" spacing at right angles to this. The strong meridian reflection in β-keratin appears at approximately 3.35Å., and has been concluded by Astbury to be a shortened form of the extended amino-acid residue which occurs as a 3.5Å. value in silk.

Chemical analysis of keratin has as yet neither reliably accounted for the whole of the protein nor settled unequivocally the relative amounts of each amino acid present. Existing data are sufficiently good, however, to indicate a mean weight for the amino-acid residues of between 110 and 120, more probably nearer the higher value. For the purposes of calculation required here, a value of 115 may be assumed, without being likely to introduce any serious error.

If the unit cell in crystalline β-keratin is orthorhombic, which is probable, and the single residue occupies a volume given by the space dimensions 3.35Å., 9.7Å., and 4.65Å., as suggested by Astbury [2, 5] from x-ray diffraction data, the density of crystalline β-keratin would be

$$\frac{115 \times 1.65}{3.35 \times 9.7 \times 4.65} = 1.26 \text{ g. per cc.}$$

The actual density of crystalline keratin in the β form is not known, but considering the density of normal wool and the value of 1.353 g. per cc. for the density of silk, we might suspect the above calculated value for β-keratin to be too low. This is probable, particularly in view of the fact that the "backbone" spacing of 4.65Å. is less than that for the same spacing in silk and nylon, and it is not likely to be too high. An increase in the mean weight of a residue from 115 to 120 would raise the density to 1.31 g. per cc. but this would still be lower than would be expected. Among the few possible causes for error which exist, doubt falls most heavily on the correctness of the values for the two lateral spacings.

In the development of his proposed structure for α-keratin, it has been suggested by Astbury [3, 5] that the strong meridional reflection at 5.14Å. results from a repeat of 3 amino-acid residues which are folded in such a manner that they extend over this axial distance. If the folded configuration of the main chain is represented as a wave periodicity, the 5.14Å. repeat corresponds to half of a wave length, and the full wave length of 10.28Å. corresponds to one complete geometrical repeat of the folded structure. This is illustrated diagrammatically in Figure 1; 3 amino-acid residues in Astbury's structure are contained in the molecular chain in passing from A to B.

The average axial distance occupied by a single residue would be 5.14Å./3, or approximately 1.71Å. This value, taken in conjunction with the 9.8Å. equatorial reflection and what has been deduced for the probable density of crystalline α-keratin, permits

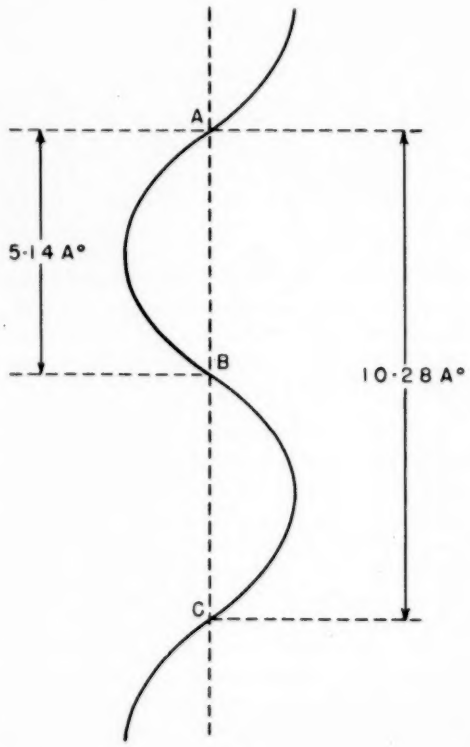

FIG. 1.

an estimation of the undetermined lateral spacing. The calculations for the two values of density which are regarded as probable upper and lower limits give the following results for this second lateral spacing (L).

$$\frac{115 \times 1.65}{9.8 \times 1.71 \times L} = 1.37, \quad \text{or} \quad L = 8.27\text{Å}.$$

$$\frac{115 \times 1.65}{9.8 \times 1.71 \times L} = 1.50, \quad \text{or} \quad L = 7.55\text{Å}.$$

Such distances in the plane of the fold are too small to accommodate the proposed structure if adjacent chains are to be linked through hydrogen bridges, the value required being of the order of 9.3Å. Taking the value for density which is regarded as the lowest possible (namely, 1.37) and raising the average residue weight to 120, it is further necessary to reduce the side-chain spacing to a value of 9.1Å. in order to provide a spacing equal to 9.3Å. at right angles to it. It would appear, therefore, that there is good reason to doubt the correctness of this structure.

Consideration of the Molecular Fold in Keratin

In his extensive physicochemical studies of the wool fiber, Speakman [17] has shown that under conditions of slow loading a fiber in saturated air or water at room temperature can be made to extend from 50% up to as much as 70% before rupture occurs. Under suitable conditions, such as the application of tension in the presence of steam, a wool fiber can be extended to a maximum of approximately twice its original length and subsequently, on removal of the stretching force, recover completely or contract to a length shorter than the original. This latter phenomenon of supercontraction has been extensively investigated by Woods and collaborators [5, 19, 20], and, as suggested by these investigators, some even more folded form of molecular configuration than that which exists normally in the wool fiber is probably involved. The high reversible extension possible for wool differentiates this fiber from other textile fibers in their normal states and, as suggested by Astbury, is to be attributed to the folding and unfolding of the main molecular chains in keratin. Fibers such as viscose rayon, silk, and nylon, which have extended, straight-chain molecular configurations, can, however, be stretched 25% and more, and under suitable conditions they exhibit remarkable powers of recovery. It has been shown in unreported work carried out in this laboratory, for example, that nylon can be extended 29.5% and will subsequently recover to within 4% of its original length. Similarly, a viscose rayon filament which had been stretched 23% in air recovered by simple immersion in water to only 4% over its original length. It may in fact generally be stated that filaments such as nylon, rayon, and silk, when stretched and allowed to recover in air, can be made to recover appreciably further by immersion in water, and there is reason to believe that deformations which have perhaps been regarded as permanent are in large part elastic extensions recovery from which is blocked. Under suitable conditions the elastic-recovery forces can reassert themselves. In the case of wool, the existence of the phenomenon of supercontraction does not permit the recovery from high extensions, such as those obtained in steam, to be ascribed to simply a reversal of the stretching process. That is to say, there must be doubt that the keratin returns only and wholly to an α configuration, duplicating a state in the fiber identical with that which originally existed. Indeed, there is evidence that such is not the case, and extents of recovery from extension do not provide the best basis from which to draw conclusions regarding α-β intramolecular folding.

The fact that wool fiber under suitably favorable conditions can be stretched to twice its original length, whereas other fibers such as silk, rayon, and nylon can be extended only about 30%, suggests, in agreement with Astbury's conclusions, that a large part of the ability of wool to show long-range extension resides in an intramolecular folding. In view of the behavior of other fibers, however, there is no reason to assume that the whole of the total extension possible in wool is to be attributed to the unfolding of molecular chains. Such is indeed highly improbable. It is much more probable that the contribution of molecular unfolding to the maximum extension which it is possible to realize in wool—*i.e.*, approximately 100%—is of about the same order as that of the difference between this figure and the maximum extension possible in silk or nylon. This would suggest a rough value attributable to molecular uncoiling in keratin of about 70%. In this case, the average residue length in the folded α configuration which when extended will account for a length of 3.35Å. observed in β-keratin would be approximately 2.0Å. In the axial repeat distance of 5.14Å. which is exhibited in α-keratin by x-ray diffraction

photographs, the number of residues would therefore be $\frac{5.14}{2.0} = 2.57$. Each amino-acid residue comprises 3 main-chain atoms, and the probability indicated by the rough estimation of 2.57 residues is that the molecular chain corresponding to half of a wave length of the folded structure contains 7 or 8 such atoms. Having due regard for bond angles, however, an even number of atoms in one-half wave length of the molecular chain would not provide a structure in which consecutive half wave lengths were symmetrical. In view of the strong 5.14Å. meridional reflection, this is unlikely, and it is to be concluded as probable, therefore, that each portion of the fold corresponding to an axial distance of one-half wave length contains 7 main-chain atoms.

This conclusion might have been reached perhaps more simply in the following way. The construction of a folded structure which is symmetrical about its long axis requires that the total number of main-chain atoms in a half wave length be odd. Nine such atoms are equivalent to 3 amino-acid residues which in the straight-chain configuration of silk extend over an axial distance of 10.5Å. The potential extensibility of 9 main-chain atoms when folded to occupy an axial distance of 5.14Å. is therefore 104%. If the extension due to molecular unfolding is to be less than 100%, the number of atoms to be considered in one-half wave length must therefore be 7, 5, or 3. Five or fewer, however, are inadmissible because the distance occupied by 5 atoms in a fully extended protein chain can be only 6.1Å., which would not provide for an adequate amount of molecular extension.

The configuration necessary to include 7 atoms of a polypeptide chain in an axial distance of approximately 5.1Å. can be constructed readily. The average axial spacing between atoms in a straight chain is 1.21Å. (or as small as 1.17Å., depending upon whether or not there is hydrogen bonding between adjacent chains). The distance 5.1Å. therefore requires 4 atoms lying axially with the fiber, with the remaining 3 lying in a more lateral direction. Due observance of the direction of valence bonds provides the molecular chain configuration shown in Figure 2. A complete repeat of the fold, which is one wave length, is shown marked from A to C, and a half repeat, or one-half wave length, is from A to B.

Taking interatomic distances as 1.5Å. and the bond angles as 109°, an approximate calculation for

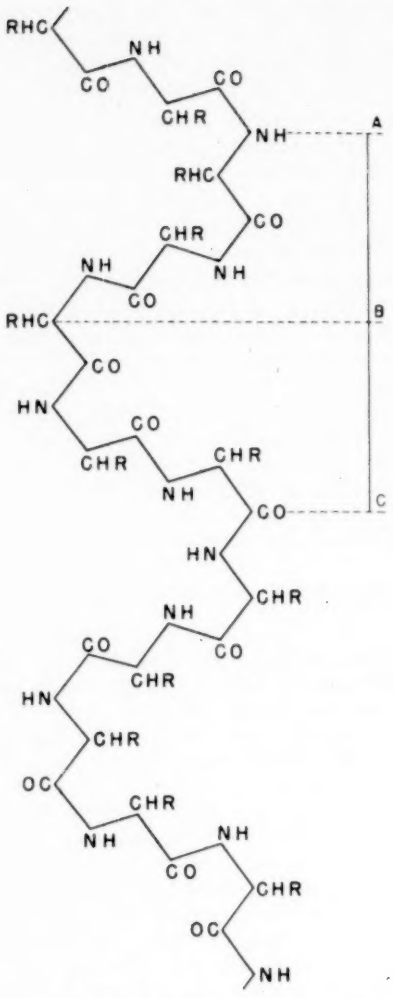

FIG. 2. *The folded configuration of the keratin molecule.*

one-half wave length can readily be made as follows:

$$3 \times 1.5 \times \sin\left(\frac{109}{2}\right)^\circ + 4 \times 1.5 \times \sin\left(\frac{109}{2}\right)^\circ \times \sin\left(\frac{109}{2} - \frac{71}{2}\right)^\circ = 5.25\text{Å}.$$

If the average axial interatomic distance is taken to be that found for silk (namely, 3.5Å./3), the above

calculation gives a value of 5.02Å. It is apparent, therefore, that some form of this configuration is not unlikely to meet the necessary requirement of the prominent meridional reflection shown by x-ray diffraction photographs. This will be discussed with greater regard for stereochemical accuracy later in this paper.

The Structural Pattern in Wool Keratin

The number of amino-acid residues in the portion of the molecular chain equivalent to one-half wavelength is $2\frac{1}{3}$. Since it has been concluded that the density of crystalline α-keratin will fall within the limits 1.37 to 1.50 g. per cc., and that the structure is orthogonal, the area ($L \cdot L'$) associated with each molecular chain in a plane at right angles to its lengthwise direction can therefore be calculated:

$$\frac{115 \times 2.33 \times 1.65}{L \times L' \times 5.14 \times 10^{16}} = 1.37,$$

whence $L \cdot L' = 62.8\text{Å.}^2$;

or, for the higher value of density, $L \cdot L' = 57.4\text{Å.}^2$.

The lengths L and L' are to be regarded as the lateral side-chain and "backbone" spacings, and if the value of one of these is 9.8Å., the value of the other must be between 6.4Å. and 5.9Å. In view of the work of MacArthur [15], in which the strong area around 9.8Å. on the diffraction photograph shows a strong component at 9.2Å., the calculated value for the second spacing might conceivably be raised to as high as 6.8Å. If it is accepted, in accordance with Astbury's suggestion, that the 9.8Å. (or 9.2Å.) value is the side-chain spacing, then this second spacing must be that in the plane of the "backbone." The width of the deduced folded molecular structure in this plane, considering only the main-chain atoms, is, however, in the region of 5.4Å. In order for hydrogen bonding to occur, a distance of roughly 4Å. is required between the carbon and nitrogen atoms of carbonyl and imino groups of adjacent chains. It is clear, therefore, that in order for adjacent folded chains to be fitted together within an average distance of 6.8Å. or less, and at the same time allow sufficient space for the formation of hydrogen bonds, the molecular pattern would have to be one in which the folds pack within each other after the manner shown in Figure 3A, rather than occupy the maximum space necessary for an association of the kind depicted in Figure 3B.

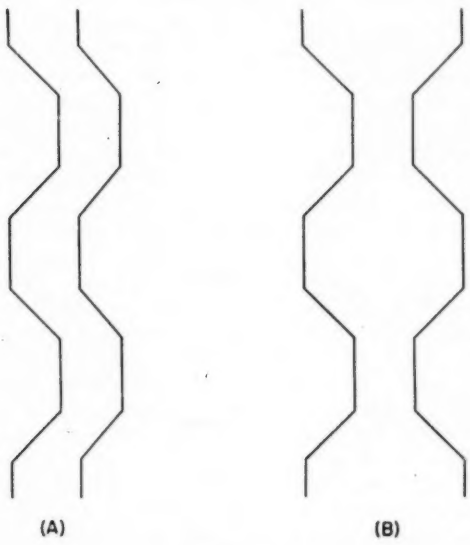

FIG. 3.

Arrangement of molecules at the required distance apart according to pattern A or at positions intermediate between A and B does not, however, provide a positioning of atoms suitable for hydrogen bonding to occur, and is therefore improbable. The alternative conclusion to be reached is that the wider spacing corresponding to the strong area shown in x-ray diffraction photographs around 9.8Å. cannot be a side-chain spacing but must itself be the "backbone" spacing—that is, the spacing between molecular chains in a direction at right angles to the side chains. To accord with a structure of the type B, with adjacent chains linked together through hydrogen bonds, the mean "backbone" spacing would have to be approximately 5.4Å. plus 4Å., or in the neighborhood of 9.4Å.

The relative position of similar atoms in the chains of the molecular pattern introduces a number of possibilities to be considered. Directing attention to the vertical plane containing the "backbones" of the molecules, a nitrogen atom, for example, may occupy one of three positions in relation to a nitrogen atom in the adjacent chain; the sequence of the carbon atom which carries the side chain, the carbonyl carbon, and the nitrogen may be the same or reversed in adjacent chains; alternate chains may be

identical, or the lateral repeat of the pattern may take place over 6 molecular chains. In the latter case the atoms in lateral planes repeat over every 3 molecular chains, the first and fourth, second and fifth, third and sixth being identical except for rotation around the chain axis through 180°. Certain of these possibilities can be discarded immediately by virtue of the improbable structures to which they give rise, and others may be rejected on grounds of incompatibility with experimentally known facts. The prominent 5.14Å. meridional spacing in α-keratin, for example, would suggest a pattern in which lateral planes separated by this distance are similar. Each such plane must, for example, contain side chains.

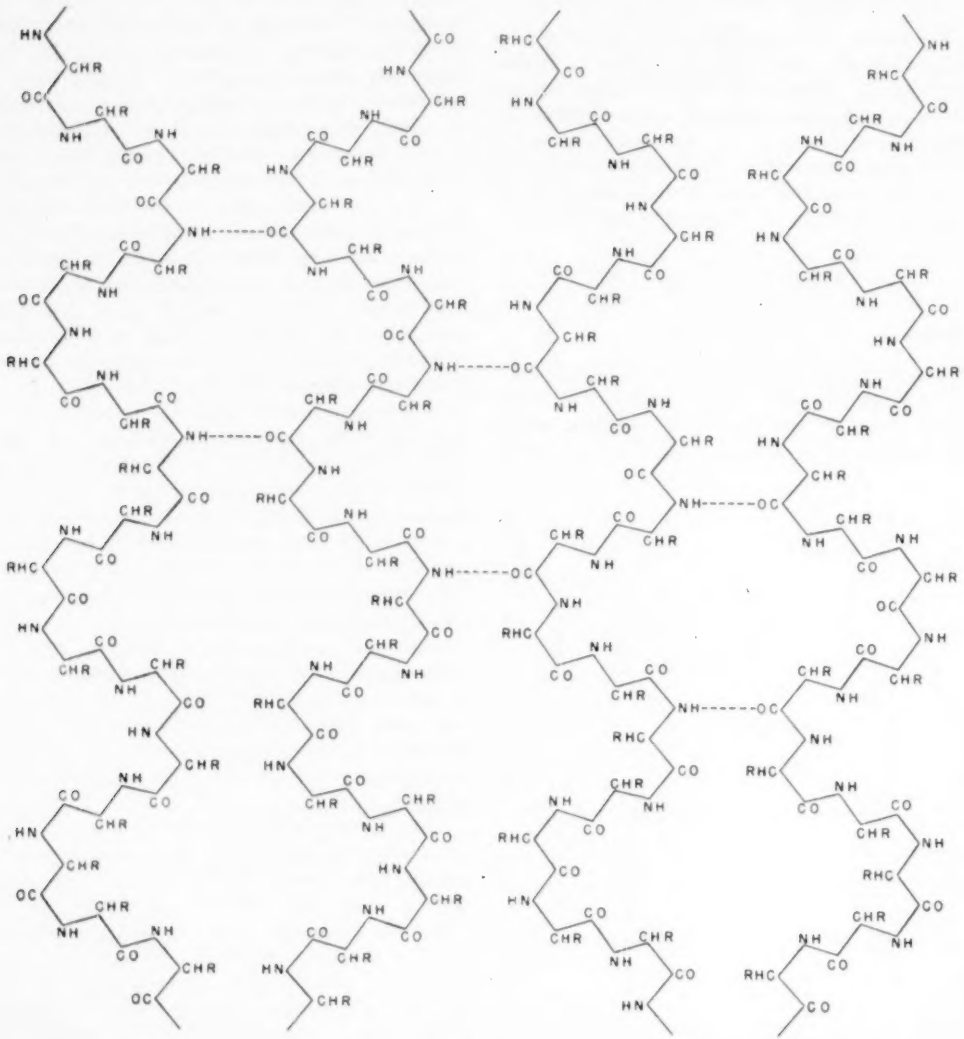

FIG. 4. *The structural pattern in wool keratin.*

If the molecular arrangement were such that alternate chains were identical, this would not be the case. Of the four remaining possibilities which fall within the bounds of a pattern of reasonable repetitive simplicity, two are inadmissible because like groups from adjacent chains are brought together and no hydrogen bonding can take place. The other two structures are simply mirror images of each other, and in the present connection are therefore to be considered the same. The structural pattern to which they give rise, viewed in the plane containing the atoms of the main chains, is that shown in Figure 4.

Further Consideration of the Proposed Structure of Wool Keratin

The Lateral Spacings

It has been pointed out that the width of the folded molecule in the plane of the "backbone" shown in Figure 2 is 5.4Å., and in order for adjacent chains to be linked together through hydrogen bonds, the lateral space requirement of each molecule in this plane must be approximately 9.4Å. In addition to the series of planes spaced at this distance which would give rise to a strong equatorial reflection, other parallel planes arise from the proposed structure, among which it may be observed that a spacing approximately 10.3Å. should also be strong. The average of these two approximates the 9.8Å. value assigned by Astbury to this lateral spacing. Density considerations have indicated that the area occupied by a molecular chain in a plane at right angles to its long axis is between 62.8Å.^{2} and 57.4Å.^{2}. If the "backbone" spacing is 9.4Å., the average side-chain spacing must therefore be in the range 6.7Å. to 6.1Å.

It is of interest at this point to consider the lateral spacings in certain other fibers. In silk, these are 4.95Å. and 4.45Å. Polythene has lateral molecular space dimensions of 3.70Å. and 2.47Å. In nylon 66 the "backbone" spacing is 4.8Å. and the side-chain spacing is 4.03Å. Where hydrogen bonding between chains is possible, as in silk and nylon, the value of the "backbone" spacing is about 4.8Å. or 4.9Å. In polythene, where no hydrogen bonding can take place, a closer approach of the molecular chains results. The fact that the value is somewhat lower in nylon than in silk is probably to be attributed to the fewer hydrogen bonds in the structure of the former fiber. In the extended β-keratin, the x-ray diffraction photograph shows a spacing 4.65Å. not to be seen in the case of the normal folded configuration, and which has been attributed to a new "backbone" spacing formed in the α-β transformation. If there were considerable hydrogen bonding between adjacent chains in the case of β-keratin, the value of 4.65Å. would appear to be slightly low, and indeed suggests, as will be discussed more fully later, that the amount of such bonding is very limited. In connection with the average side-chain spacing which has been calculated to lie in the range 6.7Å. to 6.1Å., no prominent equatorial reflection other than the heavy area around 9.8Å. appears on the α-keratin photograph. Although the atomic planes at right angles to the side chains would not be expected to give rise to as intense reflections as those evidencing the "backbone" spacing, the absence of any readily recognizable reflection corresponding to a side-chain spacing would suggest that uniform spacing of the side chains does not exist. The distance between 2 molecular chains which are joined together through a cystine bridge is approximately 7Å. The number of cystine amino-acid residues in wool keratin is of the order of 1 in 9 or 1 in 10 of the total, and it is clear, therefore, that a wide deviation of the average side-chain spacing from the value of 7Å. is improbable. Where no covalent linkage of the type of cystine exists between adjacent main chains, the latter, dependent upon the size of the side chains, tend to approach more closely, as shown by corresponding values for silk and nylon. The largest side-chains in wool are those resulting from the amino acids arginine, lysine, glutamic acid, and tyrosine, which have lengths approximating 6½Å., 7Å., 4½Å., and 5½Å., respectively. The largest of these, lysine, accounts, however, for only about 2 residues in every 100. Glycine, alanine, valine, leucine, serine, threonine, and aspartic acid together comprise approximately 55% of the total number of residues present in keratin, and these amino acids have relatively short side chains. The probability is, therefore, that the side-chain spacing of 7Å. required by cystine is a maximum, and closer approach of main chains will occur provided large side groups from 2 molecules do not give rise to hindrance by falling together at the same position. Some variation in the spacing between main chains in the plane of the side chains would, in addition to explaining the lack of any evidence of this spacing on an x-ray diffraction photograph, result in an average value somewhat less than the 7Å. maximum necessary for the cystine

linkage. Density considerations indicate this to be the case, and the cystine bridge is to be regarded as forcing the chains slightly further apart at intervals. It follows also that in the proposed structure salt linkages of the type postulated by Speakman [18] are inadmissible, at any rate in a crystalline region. A salt linkage between glutamic acid and arginine, for example, calls for a space requirement of the order of 12Å. Having regard for the density of the fiber as a whole and the relatively small difference between the densities of amorphous and crystalline regions, that any side spacings of large magnitude exist in wool at all would appear to be improbable, and, indeed, impossible except to a very limited extent. The possibility of linkages between free amino groups of diamino acids and carbonyl groups of the main chain, and of carboxyl groups of dicarboxylic acids with imino groups, cannot, however, be overlooked.

The Axial Repeat

In order for any proposed structure to be satisfactory it must be capable of explaining in terms of known stereochemical facts the repeat which occurs longitudinally along the molecular axis at 5.14Å. Although the proposed folded configuration of the molecular chain has been shown to give rise to a repeat (half wave length) approximating this distance, more critical examination can suggest further detail in the structure. The values which are quoted below are based on stereochemical calculations using bond angles equal to the tetrahedral angle, a C—C interatomic distance of 1.54Å., a C—N interatomic distance of 1.47Å., and that of C=N equal to 1.26Å.

In a fully extended polypeptide chain with no hydrogen bonding between adjacent chains, the axial distance occupied by one amino-acid residue is 3.65Å. In silk, where hydrogen-bond formation occurs, the residue length is found to be 3.48Å. It has been pointed out by Huggins [12] that in order for the imino hydrogen to lie in the plane of the "backbone" atoms and to participate in hydrogen-bond formation, it is necessary that a double bond be substituted for a single bond between the carbonyl carbon and the adjacent imino nitrogen. Huggins shows that it is to be expected that the electron distribution would correspond to a state of resonance between (a) and (b) of Figure 5, and the hydrogen-bonded structure of an extended protein chain may be depicted as in Figure 5(c). Using 1.26Å. for the distance between double-bonded C and N atoms instead of 1.47Å. for the same atoms with a single bond, the calculated axial distance occupied by one amino-acid residue is reduced from 3.65Å. to the value of 3.48Å., which is actually found for silk. It is justifiable, therefore, in further calculations on keratin structure to associate this reduced length of an amino-acid residue with the presence of a hydrogen bond, or, alternatively, to assume that a hydrogen bond should result in a decrease in the length of an amino-acid residue from 3.65Å. to 3.48Å.

In the folded keratin structure shown in Figure 2, the complete repeat of the molecular pattern occurs over a distance equal to 3 wave lengths, or 14 amino-acid residues. For purposes of calculation this complete repeat may be considered to consist of 6 amino-acid residues lying axially with the molecular chain and 6 portions of a polypeptide chain, each containing 4 atoms, lying in a transverse direction. The axial distance occupied by these latter 4 atoms varies slightly, depending upon the order in which the carbons and nitrogens are involved. The calculated values for the three possible arrangements of these are 1.64Å., 1.65Å., and 1.58Å., and in the complete repeat each appears twice. Of the 6 residues lying axially, 4 are capable of engaging in hydrogen-bond formation (See Figure 4). The total distance axially occupied by the 14-residue repeat is therefore:

$$2(1.64 + 1.65 + 1.58) + 4 \times 3.48 + 2 \times 3.65,$$

or 30.96Å., or an average of 5.16Å. for the half wave length of the molecular fold. The close correspondence of this value with that recorded by x-ray diffraction suggests a correctness in the positioning of

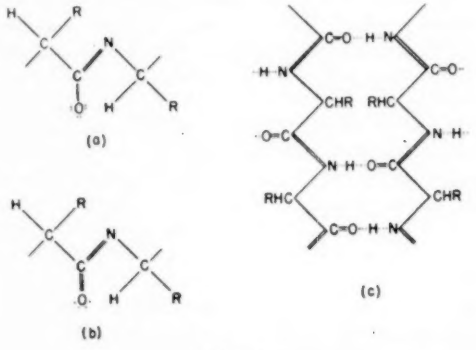

FIG. 5.

the hydrogen bonds as well as in the basic structural configuration of the molecular chains. Distortion of the main chains out of axial planes transverse to the side chains due to a variable side-chain spacing would have a shortening effect on the axial repeat. It can be calculated, however, that if the side-chain spacing varied from 7Å. at the cystine linkages to a minimum of 4.5Å. between them, the influence on the average axial spacing would not exceed 0.6%.

It has been pointed out that the complete repeat of the molecular pattern, taking into consideration the type and position of the main-chain atoms, extends over 14 amino-acid residues, and each half wave length of the folded α-keratin structure contains $2\frac{1}{3}$ residues. The strong reflection shown by x-ray diffraction photographs at a meridional spacing of 5.14Å. is not to be sought in a single molecular chain but is to be found in the repeat of the structural pattern, viewed both axially and laterally. From an examination of Figure 4 it will be seen that there is a series of planes at right angles to the axial direction of the molecules which have similar groups repeating over a unit of 3 molecular chains. It has been pointed out by Astbury [5] that a small diffuse spot from a lateral spacing around 27 ± 2Å. is evident, which would indicate such repetition in groups of three. Equidistant lateral planes, corresponding to the 5.14Å. axial spacing, occur at the position of every atom in the main chain, and a strong meridional reflection is therefore to be expected. Other weaker meridional reflections are also possible, and it is to be noted that reflections of lesser intensity observed by MacArthur [15] in his detailed study of porcupine quill—*e.g.*, 6.16Å., 10.44Å., 12.35Å.—can be readily identified in the proposed structure.

The Extended State (β-Keratin)

When wool fibers are stretched, a structural transformation begins to be evidenced in x-ray photographs at about 20% fiber extension; the reflections intensify and become progressively more clearly defined as high fiber extensions, of 70% or 100%, are reached. A new meridional spacing of 6.7Å. and an equatorial spacing of about 4.65Å. which is not present in the case of the unstretched fiber result from this transformation.

The structure of α-keratin discussed here would suggest that stretching would result in rotation in each half wave length of that part of the molecular chain which lies transverse to the molecular axis. This would involve 4 atoms rotating as a unit. Inability, for reasons of steric hindrance, to rotate through the full 180° required to bring all the main-chain atoms into one plane would cause the average axial distance occupied by each residue to be shorter than that found for silk. The 6.7Å. meridional reflection in β-keratin would, as suggested by Astbury, appear to be a shortened form of 2 amino-acid residues.

It can be assumed that the side-chain spacing present in α-keratin, stabilized as it is by the numerous cystine linkages, will be retained in the stretched β-keratin state. The new lateral spacing of 4.65Å. is of the order (slightly less) to be expected for a "backbone" spacing from polypeptide chains linked through hydrogen bonds. Although on stretching a wool fiber the first evidence of the β structure is exhibited at about 20% extension, the fact that x-ray photographs become progressively stronger in β-keratin reflections as the extensions are increased clearly indicates that the α-β transformation in the fiber is a discontinuous process. There is good reason to believe, therefore, that both old and new "backbone" spacings should be evidenced by x-ray diffraction. Whether or not transformation to the β state is necessarily accompanied by a reduction in the "backbone" spacing between adjacent chains, or whether some chains in the crystal may assume an extended configuration without drawing closer together, is uncertain. Some diminution in the intensity of the larger lateral spacing is, however, to be expected as stretching proceeds.

The fact that the new lateral spacing of 4.65Å. is somewhat less than the "backbone" spacing in silk and nylon is itself of interest. It has been pointed out that where no hydrogen bonding can occur, as with polythene, there is a closer approach between adjacent chains than would be the case if hydrogen bonds existed. In silk the "backbone" spacing is slightly larger than in nylon, and the number of hydrogen bonds for the same length of molecule is greater. Each residue in silk participates in hydrogen-bond formation, as shown by stereochemical calculation of its length, although it is not certain whether or not each imino and carbonyl group is directly involved after the manner depicted in Figure 5(c). More probable, perhaps, is an arrangement in which hydrogen bonds, one from each residue, alternate on either side of the main chain, giving rise to one bond between a pair of chains for every 2

residues. This latter arrangement requires that there be 1 bond between adjacent chains for every 6 main-chain atoms. In nylon there may be 2 bonds between adjacent chains for every 14 main-chain atoms, being unevenly spaced at 6 and 8 atoms apart, but possibly there may be only 1. In the proposed structure of α-keratin 2 hydrogen bonds occur in every 42 main-chain atoms, and these are unequally spaced at 12 and 30 atoms apart. The low value of the "backbone" spacing in β-keratin would suggest that few hydrogen bonds exist in the plane of the "backbone" as it is formed, lending support to the view that rotation around the valence bonds in the α-β transformation is prevented from attaining a full 180°. It may be pointed out that even if rotation were complete and all possible hydrogen bonds were formed, the structure of β-keratin would still differ from that of silk with respect to the positions of atoms in adjacent molecular chains and to the disposition of the hydrogen bonds.

In connection with the α-β transformation it should also be noted that if the side chains in α-keratin are disposed alternately on either side of the main chain, the rotation of a portion of the chain necessary for an extended configuration would result in the side chains adjacent to the bond of revolution being made to point in the same direction.

Contraction in Protein Fibers and Additional Folded Configurations

Recognizing that folded molecular-chain structures are possible, it might be anticipated that proteins which normally exist in an extended configuration could, under the right conditions, be induced to assume some folded state, with attendant contraction in length. Farrell [9] in 1905 published his observation that silk filaments when treated with strong hydrochloric acid could be made to contract about one-third of their original length. Similar and more extensive observations on this behavior of silk have since been made by other investigators [6, 16]. In this laboratory it has been found possible to effect contractions in silk filaments up to as high as 60% of their original length, and in the case of one filament a value of 70% was recorded. Using different acid reagents at various concentrations, it has been observed that there is a tendency for contractions to approach certain definite levels rather than for the values to be merely random. Two of these levels which have been observed by us conform to values

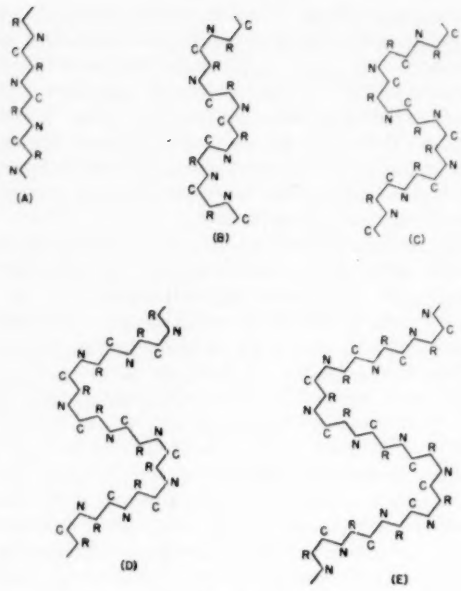

FIG. 6.

quoted in the literature by other observers—namely, 27% contraction [6] and 46% contraction [16], a third notable one being around 39%. Further details of these contraction experiments on silk will be given in a later paper. The ability of wool fibers to contract to less than their normal length has been extensively investigated by Woods and colleagues [19, 20], and similar contraction phenomena have been studied by Astbury [4] for myosin. The conclusion reached by these authors is that protein chain configurations can exist in a higher state of folding than that of normal keratin.

It is of interest to consider some geometrical extensions of the folded structure suggested here as being the normal keratin configuration. The number of atoms disposed axially in one repeat is maintained constant and those positioned transversely are varied in minimum steps. In Figure 6 is shown the fully extended molecular chain (A) and the first four types of fold ((B) to (E)). For the sake of simplicity and clarity, the carbon to which the side chain is attached is marked R; the carbonyl carbon, C; and the imino nitrogen, N. The first possible folded configuration is that shown in (B), which, allowing for hydrogen bonding, has a half wave length of 4.35Å.

Type (C) is that suggested for normal keratin, the half wave length being 5.16Å. Type (D) is the next extension of the number of atoms in the fold lying laterally, and has a half wave length of 5.85Å., while in type (E) the value is 6.70Å. In connection with long folds, it is doubtful whether or not geometrical exactitude would be maintained and the possibility of a closer approach of the laterally placed chains would not appear improbable. Such an effect would, of course, give rise to much higher contractions than would occur with a rigid structure of the kind being considered. Type (D) differs from the other three by virtue of having similar atoms repeatedly falling at the innermost part of the fold in any one molecular chain, and the arrangement shown in Figure 6(D) is one of three which are possible. The contractions from the fully extended form (A) to the other configurations (B), (C), (D), and (E) may be calculated approximately from the formula

$$\text{Contraction} = \frac{2n - 6}{3n},$$

where n is the number of main-chain atoms in one-half wave length of the fold. The percentage contractions calculated for (B), (C), (D), and (E) are 27%, 38%, 44%, and 48%, respectively. The corresponding figures for potential extensibility from the folded to the fully extended configuration (A) can be calculated from the approximate formula $\frac{2n - 6}{n + 6}$; values of 36.5%, 61%, 80%, and 94% for (B), (C), (D), and (E), respectively, are obtained.

It will be observed that the contraction values for the different configurations bear a striking similarity to the contraction levels observed for silk under the influence of acid reagents. Recently Kratky, Schauenstein, and Sekora [14] have reported the existence of an unstable lattice in silk fibroin which provides an x-ray photograph differing from the normal. The strong meridional reflection given by this newly found lattice corresponds to a spacing of 4.5Å. In a structure similar to type (B) (Figure 6), but with no hydrogen bonds between adjacent chains, the calculated half wave length fluctuates between the values 4.44Å., 4.46Å., and 4.52Å., depending upon the order of occurrence of the atoms in the chain. A strong meridional reflection would therefore occur around the mean value of 4.47Å. It is pointed out by Kratky and coworkers that the unstable silk lattice gives x-ray reflections very similar to those reported by Astbury for actin, and the possibility that this latter protein conforms in structural pattern to molecular chains having a type (B) configuration appears to be reasonable.

Discussion

Both straight-chain and folded configurations are exemplified by naturally occurring proteins, and it is possible, under suitable conditions, to transform one configuration into some other. This change may be either to a simpler form, as in the stretching of a normal wool fiber, or to one more complex, as in the case of supercontraction. The question arises as to why some proteins like silk adopt an extended chain configuration, while others such as keratin prefer a folded structural pattern. Some light may be thrown on the matter through the following considerations.

In the case of silk fibroin the groups forming the side chains are very largely nonreactive. Adjacent molecular chains can be linked together in the plane of the "backbone" through hydrogen bonds, and the number of bonds in fibroin, spaced at close intervals, is large. If folding occurs in a protein, a lesser number of hydrogen bonds must be operative, because of either some other stronger tendency or a reduced ability to form such bonds. Differences between proteins which bear on this must have their origin in the composition of the amino-acid residues—that is, in the nature of the side chains. Size or weight of a side chain is not likely in itself to be of primary importance, but its reactivity is important. It has been suggested in the discussion of lateral spacings that linkages may occur between carboxyl groups present in the side chains and imino groups of adjacent main chains, and also between side-chain amino and main-chain carbonyl groups. Such bonding would effectively prevent participation of the involved carbonyl or imino group in hydrogen-bond formation, including also the nitrogen or carbon adjacent to the reacting group. It is possible therefore that freedom of a protein molecule to assume a folded configuration may be associated with its reactive side groups, and suggests that the differences in the normal structural pattern of different proteins may perhaps be correlated with differences in chemical composition, particularly the dicarboxylic and diamino acid contents.

Acknowledgment

The author wishes to acknowledge helpful discussions with his colleagues Mr. N. J. Abbott and Mr. M. L. Staples during the preparation of this paper.

Literature Cited

1. Abbott, N. J., and Goodings, A. C., *J. Text. Inst.* **40**, T232 (1949).
2. Astbury, W. T., *J. Chem. Soc.*, p. 337 (1942).
3. Astbury, W. T., and Bell, F. O., *Nature* **147**, 696 (1941).
4. Astbury, W. T., and Dickinson, S., *Nature* **135**, 95, 765 (1935).
5. Astbury, W. T., and Woods, H. J., *Phil. Trans. Roy. Soc., Series A*, **232**, 333 (1933).
6. British Silk Research Assoc. experiments referred to by Astbury, W. T., and Woods, H. J., *J. Text. Inst.* **23**, T17 (1932).
7. Bunn, C. W., in "Fibre Science," Manchester, England, The Textile Institute, 1949, p. 176.
8. Bunn, C. W., and Garner, E. V., *Proc. Roy. Soc. (London), Series A*, **189**, 39 (1947).
9. Farrell, F. J., *J. Soc. Dyers and Colourists* **21**, 70 (1905).
10. Goodings, A. C., and Turl, L. H., *J. Text. Inst.* **31**, T60 (1940).
11. Harris, M., and Brown, A. E., in "Symposium on Fibrous Proteins," Leeds, England, Soc. Dyers and Colourists, 1946, p. 203.
12. Huggins, M. L., *J. Org. Chem.* **1**, 449 (1937).
13. King, A. T., *J. Text. Inst.* **17**, T53 (1926).
14. Kratky, O., Schauenstein, E., and Sekora, A., *Nature* **165**, 319 (1950).
15. MacArthur, I., *Nature* **152**, 38 (1943).
16. Nutting, G. C., Halwer, M., Copley, M. J., and Senti, F. R., TEXTILE RESEARCH JOURNAL **16**, 599 (1946).
17. Speakman, J. B., *J. Text. Inst.* **17**, T457 (1926); **18**, T431 (1927).
18. Speakman, J. B., and Hirst, M. C., *Trans. Faraday Soc.* **29**, 148 (1933).
19. Whewell, C. S., and Woods, H. J., in "Symposium on Fibrous Proteins," Leeds, England, Soc. Dyers and Colourists, 1946, p. 50.
20. Woods, H. J., *Nature* **132**, 709 (1933).

(Manuscript received May 5, 1950.)

Measurement of Friction Between Single Fibers*

V. Frictional Properties of Viscose Rayon Staple Fibers

Bertil Olofsson and Nils Gralén

Swedish Institute for Textile Research, Gothenburg, Sweden

Introduction

In a previous communication by Gralén and Olofsson [2] a description was given of a new apparatus for the measurement of single-fiber friction, its construction, and theory. Some preliminary results were also given.

In the case of wool fibers a very great dispersion of the separate readings was found, as regards anti-scale friction. The reason for this is that relatively small differences in the height and the shape of the scales can give rise to rather large differences in friction. Smooth fibers give less dispersion of the values. Using the stick-slip apparatus is more time-consuming and laborious than using the twist friction meter described by Lindberg and Gralén [6], but in other respects the former has some advantages over the latter apparatus. Firstly, the distribution of the load on the contact surface is better defined; secondly, the form and area of the fiber cross section certainly does not influence the precision of the measurements; thirdly, rather short fibers can be used.

As pointed out [2], we intended to compare the frictional properties of different fibers with their spinning qualities. First we wanted to determine the effect of treatments with different auxiliaries on the fiber frictional properties. The present communication gives a survey of our work on viscose rayon fibers.

Experimental Procedure

The method of measurement has been completely described in [2]. Usually, no photographic records were taken; these curves would always have the ordinary saw-tooth shape. Instead, slip and brake points were observed directly. From these values the static and the kinetic (the word "kinetic" is more nearly adequate than the word "dynamic," which was used in [2]) frictional coefficients (μ_s and μ_k) were determined. In order to obtain figures for load dependence, measurements were always made at the nominal loads 30 mg. (corrected normal pressure, $N = 27$ mg.) and 51 mg. ($N = 48$ mg.). In special cases a still greater range of loads was used. Depending upon the dispersion of the values, at least 4 pairs of fibers were measured in both directions of movement for each kind of treatment. We used uniform fibers about 20 microns in thickness and about 30 cm. in length. These were obtained from Svenska Rayon AB, Älvenäs, Sweden.

We have collected the following information about the different finishing agents.

Vapoline in oil consistency is an anion-active, brown, 100% oil from a mineral oil base. It has no water content and no free fatty acid. It is emulsified with pure water at 70°C and is easily washed away.

Vapoline 300% is cation-active, has salve consistency, and is easily emulsified with water at 70°C.

Perma Par R is a light salve, a cationic acetate of a substituted secondary amine. It gives a faintly opalescent, slightly acid solution in water at 70°C.

Velvamine K 90% is a light, anion-active salve, a fatty-acid amine that gives a clear, alkaline solution with water at 80°C.

Veicol M 50, a light yellow, faintly alkaline salve, is an organic condensation product, containing no soap.

Veicol S is a nonionic polymerization product which gives an opalescent, neutral solution in water.

Spinol + triethanolamine.

* Parts I–IV of this series appeared in the September, 1947, May, 1948, August, 1948, and April, 1949, issues of TEXTILE RESEARCH JOURNAL, and also in issues No. 3 (1947), No. 6 (1948), No. 8 (1948), and No. 10 (1949), respectively, of the *Proceedings of the Swedish Institute for Textile Research*. Part VI follows in this issue.

TABLE IA. FIBER FRICTION COEFFICIENTS USING DIFFERENT FINISHING AGENTS

Finishing agent	Handle	μ'_e	μ'_k	μ''_e	μ''_k
None	Coarse, crunching	0.333	0.199	0.320	0.178
Vapoline oil, 0.5%	Soft	0.386	0.314	0.360	0.285
Vapoline 300%, 1%	Soft	0.172	0.114	0.157	0.111
Vapoline 300%, 0.5%	Soft	0.194	0.120	0.167	0.113
Perma Par R, 1%	Soft	0.167	0.096	0.144	0.089
Perma Par R, 0.5%	Soft	0.145	0.086		
Velvamine K 90%, 1%	Soft	0.190	0.114	0.168	0.102
Veicol M 50, 1%	Soft	0.228	0.138	0.211	0.122
Veicol S, 0.25%	Coarse, crunching	0.356	0.165	0.353	0.165
Spinol + triethanolamine, 0.5%	Coarse, crunching	0.317	0.165	0.315	0.151
Varkaus, 1%	Crunching	0.371	0.242	0.339	0.218
Sodium soap, 0.5%	Soft	0.369	0.217	0.361	0.207
Kerosene, direct application	Crunching	0.338	0.172	0.329	0.162
Pendulum oil, direct application	Soft	0.204	0.179	0.166	0.150
Woolrex, direct application	Crunching	0.307	0.244	0.288	0.220

TABLE IB. FIBER FRICTIONAL PROPERTIES USING DIFFERENT FINISHING AGENTS

Finishing agent	μ_e	μ_k	$(\alpha S)_e$	$(\alpha S)_k$	$\mu_e - \mu_k$	$\frac{\mu_e - \mu_k}{\mu_e + \mu_k}$
None	0.327	0.189	0.8	1.3	0.138	0.27
Vapoline oil, 0.5%	0.373	0.300	1.6	1.8	0.073	0.11
Vapoline 300%, 1%	0.165	0.113	0.9	0.2	0.052	0.19
Vapoline 300%, 0.5%	0.181	0.117	1.7	0.4	0.064	0.21
Perma Par R, 1%	0.156	0.093	1.4	0.4	0.063	0.25
Velvamine K 90%, 1%	0.179	0.108	1.4	0.8	0.071	0.25
Veicol M 50, 1%	0.220	0.130	1.1	1.0	0.090	0.26
Veicol S, 0.25%	0.355	0.165	0.2	0.0	0.190	0.33
Spinol + triethanolamine, 0.5%	0.316	0.158	0.1	0.8	0.158	0.33
Varkaus, 1%	0.355	0.230	2.0	1.5	0.125	0.21
Sodium soap, 0.5%	0.365	0.212	0.5	0.6	0.153	0.27
Kerosene, direct application	0.334	0.167	0.6	0.6	0.167	0.33
Pendulum oil, direct application	0.185	0.165	2.4	1.8	0.020	0.06
Woolrex, direct application	0.298	0.232	1.1	1.5	0.066	0.12

TABLE IIA. INFLUENCE OF HUMIDITY ON FRICTION COEFFICIENTS

Fiber	Relative humidity (%)	μ'_e	μ'_k	μ''_e	μ''_k
Fiber treated with Perma Par R, 1%	50	0.167	0.096	0.144	0.089
	65	0.178	0.101	0.151	0.090
	85	0.178	0.101	0.168	0.099
	89–90	0.279	0.144	0.275	0.144
	100% (wet fiber)	0.287	0.145	0.278	0.143
Crunching rayon	65	0.445	0.212	0.442	0.200
	87	0.528	0.285	0.496	0.279

TABLE IIB. INFLUENCE OF HUMIDITY ON FRICTIONAL PROPERTIES

Fiber	Relative humidity (%)	μ_e	μ_k	$(\alpha S)_e$	$(\alpha S)_k$	$\mu_e - \mu_k$	$\frac{\mu_e - \mu_k}{\mu_e + \mu_k}$
Fiber treated with Perma Par R, 1%	50	0.156	0.093	1.4	0.4	0.063	0.25
	65	0.165	0.096	1.7	0.7	0.069	0.26
	85	0.173	0.100	0.6	0.1	0.073	0.27
	89–90	0.277	0.144	0.3	0.0	0.133	0.32
	100% (wet fiber)	0.283	0.144	0.6	0.1	0.139	0.33
Crunching rayon	65	0.444	0.206	0.2	0.8	0.238	0.37
	87	0.512	0.282	0.4	2.0	0.230	0.29

TABLE IIIA. INFLUENCE OF APPLICATION OF AGENT ON FRICTION COEFFICIENTS (BEROIL 204)

Method of application	μ'_s	μ'_k	μ''_s	μ''_k
Emulsion, 30%	0.614	0.321	0.620	0.281
Directly	0.620	0.354	0.605	0.309

TABLE IIIB. INFLUENCE OF APPLICATION OF AGENT ON FRICTIONAL PROPERTIES (BEROIL 204)

Method of application	μ_s	μ_k	$(\alpha S)_s$	$(\alpha S)_k$	$\mu_s - \mu_k$	$\frac{\mu_s - \mu_k}{\mu_s + \mu_k}$
Emulsion, 30%	0.617	0.301	0.4	2.5	0.316	0.34
Directly	0.613	0.332	0.9	2.8	0.281	0.30

Varkaus is a Finlandic preparation containing olein + some amine.

Sodium soap.

Kerosene (refined petroleum).

Pendulum oil is a pure, light mineral oil.

Woolrex is a sulfonated spinning oil.

Svenol is a sulfonated mineral oil.

Beroil 204 is a mineral oil with emulsifying agent.

The treatments with Vapoline, Velvamine K, Perma Par R, Veicol S, and Spinol were carried out at Älvenäs. The samples were dried at 50°C for 3 hours and were then transferred to a room of constant temperature and humidity, where the measurements were performed. Varkaus, Veicol M 50, and soap were applied from 0.5–1% solutions; the various oils were applied directly. The results are given in Table I.

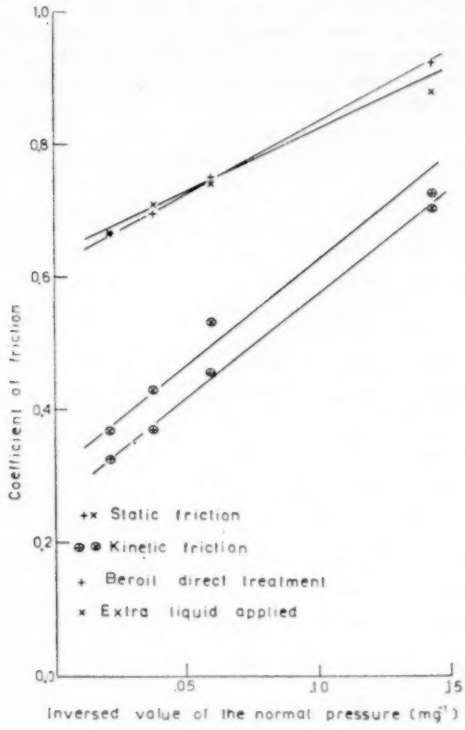

FIG. 1. *Relationship between* μ *and* $\frac{1}{N}$ *for fibers treated with Beroil 204.*

It seemed to be necessary to investigate the influence of some other factors on the frictional properties. A wetted fiber generally gave higher frictional values than a dry one. We used fibers treated with Perma Par R to investigate the effect of varying relative humidity (Table II).

Regarding spinning oils, it should be of interest to investigate the influence of concentration and method of application.

Some fibers were treated in a 30% water emulsion of Beroil, pressed, and dried (50°C). Other fibers were treated with this reagent directly (Table III).

There is no difference between the two methods of treatment. However, because of the great difference between $(\alpha S)_s$ and $(\alpha S)_k$ (see Discussion) it was desirable to make a more careful study of the μ *vs.* N curves. For this purpose measurements at different loads (7–50 mg.) were made on one fiber which had been treated directly with Beroil 204 and then pressed free from superfluous liquid (series A). Then we added still more oil, so that small drops were seen on the fiber, and we made new measurements (series B). The results (Figure 1) will be discussed later. With the spinning oil Svenol, which gives a very high friction also, we investigated the effect of varying the concentration. One emulsion of 1% and one of 20% concentration were used (Table IV).

The influence of the conditions of treatment was further investigated with preparations of Varkaus. This auxiliary was chosen because of its characteristic high static and low kinetic friction, which is accompanied by a typical "crunching" handle. Soap was more thoroughly investigated since it has about the same frictional constants as Varkaus has but gives a rather soft handle. As seen from the results (Table V), there are no remarkable differ-

TABLE IVA. INFLUENCE OF CONCENTRATION OF AGENT ON FRICTION COEFFICIENTS (SVENOL)

	μ'_s	μ'_k	μ''_s	μ''_k
Emulsion, 1%	0.478	0.253	0.443	0.220
Emulsion, 20%	0.514	0.254	0.481	0.218

TABLE IVB. INFLUENCE OF CONCENTRATION OF AGENT ON FRICTIONAL PROPERTIES (SVENOL)

	μ_s	μ_k	$(\alpha S)_s$	$(\alpha S)_k$	$\mu_s-\mu_k$	$\frac{\mu_s-\mu_k}{\mu_s+\mu_k}$
Emulsion, 1%	0.461	0.237	2.2	2.1	0.224	0.32
Emulsion, 20%	0.498	0.236	2.1	2.3	0.262	0.36

ences between the soap and the Varkaus treatments. However, we thought it necessary to repeat the measurements on rayon, which had not been squeezed after treatment, and use a wider range of loads. The crunching effect of Varkaus was very great after this treatment, whereas the soap-treated samples were still very soft when they had been conditioned at 65% R.H. for one day. After storing both sets of samples for several days at 65% R.H. the crunching effect seemed to be less pronounced for the Varkaus-treated ones. And so another series of measurements was taken (Table V). Figure 2 gives average curves for the dependence of μ on $\frac{1}{N}$.

Discussion of Measurements

In [2] we proved the validity of the equation

$$\mu = \mu_o + \frac{\alpha S}{N},$$

where N = normal pressure, S = contact area, α = constant, and $\mu = \mu_o$ for $N \to \infty$. Then we could use μ_o and αS (S is not measurable separately but αS is almost constant in the region of our measurements) as characteristic constants, but because of the error of extrapolation we prefer using $\mu = \frac{\mu' + \mu''}{2}$ and $\alpha S = \mu' - \mu'' \Big/ \frac{1}{27} - \frac{1}{48}$, where μ' and μ'' are the coefficients at 27 and 48 mg. normal pressure, respectively. Table I shows that samples treated with Vapoline 300%, Perma Par R, and Velvamine K 90% all have about the same char-

TABLE VA. COMPARISON BETWEEN THE EFFECT OF VARKAUS AND SODIUM SOAP ON FRICTION COEFFICIENTS

Treatment	Finishing agent	μ_o $N=7$	17	27	48	μ_k $N=7$	17	27	48
1% solution, pressed off and dried, measured immediately	Varkaus			0.554	0.541			0.263	0.258
	Soap			0.489	0.475			0.212	0.205
1% solution, dried and conditioned (65% R.H.)	Varkaus		0.484	0.460	0.433		0.325	0.286	0.246
	Soap	0.478	0.459	0.452	0.427	0.262	0.238	0.227	0.211
Same samples after storing 4–5 days (65% R.H.)	Varkaus		0.505	0.477	0.436		0.366	0.336	0.284
	Soap		0.470	0.421	0.402		0.277	0.250	0.226

TABLE VB. COMPARISON BETWEEN THE EFFECT OF VARKAUS AND SODIUM SOAP ON FRICTIONAL PROPERTIES

Treatment	Finishing agent	μ_s	μ_k	$(\alpha S)_s$	$(\alpha S)_k$	$\mu_s-\mu_k$	$\frac{\mu_s-\mu_k}{\mu_s+\mu_k}$
1% solution, pressed off and dried, measured immediately	Varkaus	0.548	0.261	0.8	0.9	0.287	0.35
	Soap	0.482	0.209	0.3	0.4	0.273	0.40
1% solution, dried and conditioned (65% R.H.)	Varkaus	0.447	0.266	1.4	1.6	0.181	0.25
	Soap	0.440	0.219	0.7	0.8	0.221	0.34
Same samples stored 4–5 days (65% R.H.)	Varkaus	0.457	0.310	2.3	2.5	0.147	0.19
	Soap	0.412	0.238	1.6	1.5	0.174	0.27

acteristics: μ_s is $\simeq 0.17$, $\mu_k \simeq 0.10$, and $\mu_s - \mu_k \simeq 0.07$. For untreated fiber, and fibers treated with Veicol S, and Spinol + triethanolamine, on the other hand, $\mu_s \simeq 0.32$, $\mu_k \simeq 0.18$, and $\mu_s - \mu_k \simeq 0.14$. Fiber treated with Vapoline oil has $\mu_s = 0.37$, $\mu_k = 0.30$, and $\mu_s - \mu_k = 0.07$. Thus, we can distinguish between three groups of treatments: (I) μ_s, μ_k, and $\mu_s - \mu_k$ are all small; (II) μ_s is large, μ_k is small, and $\mu_s - \mu_k$ is large; (III) μ_s and μ_k are large and $\mu_s - \mu_k$ is small. The effect of finishing agents should be to give the fibers good spinnability and a good handle; the handle can be very soft or it can be crunching. As seen from Table I, all preparations belonging to group I give a soft handle, preparations of group II give a crunching handle, and Vapoline oil (group III) gives a soft handle. Thus, we suggest that this crunching effect is always accompanied by a large value of $\mu_s - \mu_k$ and it can probably be explained as an acoustic effect: When the fibers move along against each other, the large value of μ_s necessitates a rather large force for slippage. When started, the slip will occur at a high velocity because the frictional force of movement (μ_k) is small. During this rapid movement the crunching sound, just as from a resined bow, is heard.

The crunching effect is obtained [3] by using olein sulfonates which are treated afterwards with acid, or by using fatty-acid derivatives corresponding to the products Soromin SG or Sebosan GM.

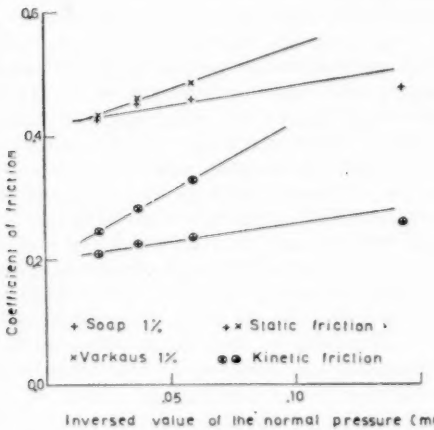

FIG. 2. *Relationship between* μ *and* $\frac{1}{N}$ *for fibers treated with soap and Varkaus.*

TABLE VI. COMPARISON BETWEEN FRICTIONAL COEFFICIENT, RELATIVE VISCOSITY, AND SURFACE TENSION FOR SOME LIQUIDS

Liquid	μ_s	μ_k	Relative viscosity	Surface tension
Water	0.40	0.21	1.0	72
Kerosene	0.33	0.17	1.1	25
Pendulum oil	0.19	0.17	161.8	31
Woolrex	0.30	0.23	165.2	30
Beroil 204	0.61	0.33	137.1	30
Svenol	0.50	0.24	67.6	30

However, the relationship between crunching effect and chemical constitution does not seem to be clear. The cationic or anionic character alone of an auxiliary does not give specific differences, as is seen from the similarity between the cationic reagents Vapoline 300% and Perma Par R and the anionic reagent Velvamine K 90%. The agent Veicol S, on the other hand, should give a crunching effect because of its constitution. And triethanolamine added to spinning oil is often the basis for "crunching" agents. Varkaus gives a typical crunching effect, and it has a large value of $\mu_s - \mu_k$ too. Like Spinol, it contains olein plus some amine. Woolrex and Svenol, which are sulfonated oils, could be included in group II. But pendulum oil, which is a pure mineral oil, should be included in group I; it has an extremely small value of $\mu_s - \mu_k$. However, refined liquid paraffin (kerosene), which has a nonionic character also, clearly belongs to group II. We measured the viscosity of the different liquids with an ordinary Ostwald viscosimeter and got the values listed in Table VI. There is a very large viscosity difference between paraffin oil and pendulum oil, and this difference is probably the reason for the frictional differences. Of the sulfonated oils, Woolrex has a viscosity which is more than twice that of Svenol, and Svenol has a μ_s value which is 1.7 times that for Woolrex. For the last two spinning oils listed in Table VI the friction-viscosity relationship is of different form from that for the liquids of low viscosity.

The surface tension was measured by means of a du Noüy tensiometer, according to Harkins *et al.* [4].

As seen from Table VI, there is only small variation between the surface tensions of the different oils, but the frictional properties vary considerably. As seen from Table IVB, there is a small increase of μ_s when the concentration of Svenol has increased from 1% to 20%, but this increase is not very significant. Concentration changes of 0.5–

1% give no changes in friction at all (Table IB). In fact, very small quantities of agent on the fibers are sufficient to change friction. According to a rough calculation [5] a cotton fiber should contain 10% soap in order to have its whole surface covered with a monomolecular layer, but calculations from irreversible absorption of direct dyestuffs give the considerably lower figure of 0.6% (unpublished data by Lange). Some of the finishing agents are absorbed to 0.5–2% of the fiber weight; only spinning oils are present in a much greater quantity. Thus, a monomolecular layer is sufficient to affect friction.

The influence of humidity is interesting. Table IIB gives some measurements on fibers treated with Perma Par R. Friction increases rather slowly when humidity increases up to 85–87% R.H. Then it increases very rapidly up to 100% R.H. Also, for a "crunching rayon," the friction increases in about the same manner. Extensive drying gives a rather high friction, which decreases on conditioning to 65% R.H. (see Table VB).

In order to be assured that the friction-increasing effect of a spinning oil was not attributable to the method of application, we compared Beroil treatments made directly and those made in water emulsion after drying. As seen from Table IIIB, there is no noticeable difference.

Special attention was paid to the ordinary soap treatment. If a 0.5–1% solution is used, a rather soft feeling of the fiber mass is obtained. But the frictional properties are typical for group II agents, and are not very different from those of Varkaus. Some samples were first treated with 1% solutions at room temperature, the liquid pressed off, and the samples dried. Other samples were treated with the same solutions at 70°C and allowed to dry without pressing. In both cases the Varkaus samples gave slightly higher values than the soap samples for static as well as for kinetic friction. However, the differences were not significative. After some days of storage at 65% R.H. the crunching effect of Varkaus seemed to have decreased a little. The corresponding frictional effect was an increase of μ_k and thus a decrease of $\mu_s - \mu_k$, which agrees with our theory.

In the tables $\frac{\mu_s - \mu_k}{\mu_s + \mu_k}$ is also calculated as a measure of the relative difference between static and kinetic friction values. This quantity is a little smaller for group I than for group II agents, and is still smaller for group III agents.

Of special interest are the slopes (αS) of the curves of μ *vs.* $\frac{1}{N}$. These values are not very accurate, but in some cases they may give valuable information. As shown in [2], a smooth viscose fiber gives $(\alpha S)_s = (\alpha S)_k$, and from this it was concluded that the kinetic friction is not much influenced by small changes in velocity. If there is any influence, the curve μ_k *vs.* $\frac{1}{N}$ should differ in curvature from the curve μ_s *vs.* $\frac{1}{N}$ because of the different average velocities and hence the different μ_k values for different loads. However, the values are not accurate enough to account for small deviations from straight lines. Therefore we can draw straight lines and use their αS values for some quantitative considerations. A large value of αS should mean that there are appreciable attractive forces between the fibers or an intimate contact between them. A small value of αS should mean that the surface forces are not very important. If the difference between $(\alpha S)_s$ and $(\alpha S)_k$ is large, we could presume that there are great differences in surface forces when the fibers stick together and when they slip. From Table IB we see that for the softening agents of group I $(\alpha S)_s$ is $\geq (\alpha S)_k$, which means that the fibers are not in such intimate contact when slipping as when sticking together. However, this relationship does not hold for the fibers of group II. There $(\alpha S)_k$ is often larger than $(\alpha S)_s$. This also may be related to the crunching effect. It is probable that this effect is associated with an intimate contact between the fibers during slippage. For Beroil the difference $(\alpha S)_k - (\alpha S)_s$ is very large (Figure 1). This could give a new view on the effect of this spinning oil. Although $\mu_s - \mu_k$ is very great for the loads used here, this difference will decrease as N decreases, owing to the magnitude of $(\alpha S)_k - (\alpha S)_s$. The results for soap and Varkaus also give some interesting information. For Varkaus as well as for soap $(\alpha S)_k \simeq (\alpha S)_s$, but both $(\alpha S)_s$ and $(\alpha S)_k$ for Varkaus are actually larger than the corresponding values for soap. This may be an explanation for the absence of the crunching effect in the case of soap. When this effect is observed in practice, there are possibly very small normal pressures in action, and this is represented by the part of the μ *vs.* $\frac{1}{N}$ curve where the μ values are much larger for Varkaus than for soap (Figure 2).

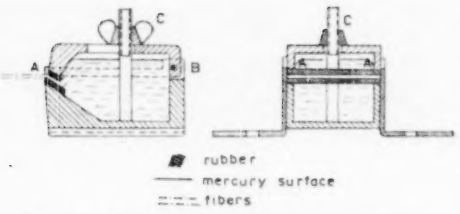

FIG. 3. *Clamp for conductivity measurements.*

Measurement of Conductivity

It is well known from industrial experience that a high humidity is necessary for drawing and spinning operations. As shown here, the frictional coefficients are not much influenced by humidity variations up to 85% R.H. The principal effect of a high humidity should be to increase the electrical conductivity of the fiber material, which raises the question of whether or not the finishing agents could change the electrical conductivity to such an extent that this conductivity becomes more important for the spinning qualities than the different frictional effects.

To investigate this we made two special metal clamps for holding a fiber bundle. They consisted of nickel-plated bowls with lids (Figure 3). The lids were hinged at B and could be pressed against the bowl edges at AA. There the fiber bundle was fixed tightly by means of the screw C. The holder surfaces at AA were supplied with plates of rubber which were smeared with a plastic paste ("Metal Fix") containing powdered graphite. The fibers were first parallelized and then fixed to a pair of pincers. One end was cut with a safety-razor blade and fixed in one holder at this end. This holder was fastened to an isolating Bakelite plate; the other end of the fiber bundle was cut off and fixed to the other holder, which had also been fixed to the plate. Then the two bowls were filled with mercury through holes in the lids. By the use of mercury and graphite-coated rubber we got a good conduction between the clamps and the fiber ends. The "free" length of the fiber bundle was 2 millimeters, and the resistance R, which had a magnitude of 50–500 megohms, was measured by means of an electronic voltmeter. Afterwards, the fiber bundle was weighed and the weight of the free conducting part, V, was calculated as proportional to its length. Since the average thickness of the fibers was the same for all samples, the weight V should be proportional to the number of fibers in every sample; therefore, the quotient $\frac{R}{V}$ gives a measure of the relative conductivity of a sample. All the experiments were made in a room with constant humidity (65% R.H.). The measurements were reproducible under these conditions. As seen from Table VII, the samples treated with group I agents have possibly a little higher electrical resistance than those treated with group II agents. However, this difference is not significative. The conductivity is probably due to the fibers themselves and the water used for the treatment. Only when there is a considerable amount of auxiliary present is there a definite decrease in resistance. This is probably always the case for treatments with spinning oils in emulsion.

TABLE VII. ELECTRICAL RESISTANCE OF FIBER BUNDLES AFTER DIFFERENT TREATMENTS (RELATIVE VALUES)

Treatment	Electrical resistance
None	20
Vapoline oil, 0.5%	34
Vapoline 300%, 1%	32
Perma Par R, 1%	55
Velvamine K 90%, 1%	45
Veicol S, 0.25%	36
Spinol + triethanolamine, 0.5%	24
Soap, 1%	23
Woolrex (direct application)	3
Svenol, 1%	21
Svenol, 20%	4

Wool-Rayon Fiber Friction

As rayon staple is often used in mixtures with wool, we measured the friction between untreated rayon fibers and wool fibers. Table VIII gives the results.

There is always a difference in friction between with-scale and anti-scale movements. When the apparatus is moving in the anti-scale direction and the fibers stick together (before the fiber movement has started) the scales will press into the rayon fiber surface, and we can say that due to the impression the smooth surface itself forms an edge, directed against the wool scale edge (Figure 4). When the fibers are sliding, the rayon surface is probably not irreversibly deformed by the ploughing action of the wool scales because the surfaces are elastic and the pressure is small. When the apparatus is moving in the with-scale direction,

TABLE VIII. FRICTION COEFFICIENTS BETWEEN WOOL AND SMOOTH FIBERS

Fiber mixture	Direction of movement (fibers)	μ_s	μ_k	$\mu_s - \mu_k$
Wool-wool	With-scale	0.13	0.11	0.02
Wool-wool	Anti-scale	0.61	0.38	0.23
Wool-wool	Same direction of fibers	0.21	0.15	0.06
Wool-rayon	With-scale	0.11	0.09	0.02
Wool-rayon	Anti-scale	0.39	0.35	0.04
Wool-nylon	With-scale	0.26	0.21	0.05
Wool-nylon	Anti-scale	0.43	0.35	0.08
Rayon-rayon		0.35	0.26	0.09
Nylon-nylon		0.47	0.40	0.07

the scale impression gives considerably smaller form resistance.

It is well known that a smooth surface will give a low friction when it rubs against a rough surface, and this is true also for the fibers investigated here. The value for rayon-wool with-scale friction is close to that for wool-wool friction, both with-scale and in the same direction of the fibers (lines 1 and 3 in Table VIII), but much smaller than rayon-rayon friction. The value for rayon-wool anti-scale friction is close to that for rayon-rayon friction, but much smaller than that for wool-wool anti-scale friction.

In order to check on these results we also measured wool-nylon friction (Table VIII). These figures are also in agreement with our interpretation, although the difference between the anti- and the with-scale friction for wool-nylon is smaller than that for wool-rayon. This could be attributed to differences between elastic properties of nylon and rayon.

Relationship Between Frictional Values and Spinnability

In order for a yarn to have good tensile strength it is of course valuable to have a large value of μ_s between the fibers. In order to get a good slipping movement in drawing and spinning operations, it should be valuable to have small μ_k values. However, for the evenness of slivers and yarns it should perhaps be most important to have a small difference between μ_s and μ_k.

Figure 5 shows two pairs of drawing rollers moving at different velocities, V_0 and V_1. Löfgren has shown (unpublished data) that the position-velocity curve of a fiber in the region of "free swimming" between the grips is a hyperbole if the accelerating and retarding forces are proportional to the corresponding lengths of grasping by those fibers, which are fixed by the rollers. Acceleration should not set in until the accelerating grasping length is larger than the retarding length, if the action of other free-swimming fibers is neglected. Generally, there seems to be a more or less sudden change of velocity when a fiber is taken on by the rapid rollers. In this moment the frictional force evolved, $F_s = (\mu_s \cdot N + \alpha_s \cdot S) \cdot l$ (N = normal pressure per unit length, S = contact area per unit length, l = grasping length for surrounding fibers), may give an impulse to other free fibers. However, the force momentarily diminishes to $F_k = (\mu_k \cdot N + \alpha_k \cdot S) \cdot l$; if F_s is considerably greater than F_k, this force cannot put other fibers into increased movement; possibly it will keep in motion those fibers already moving. But there is great possibility that the whole acceleration of a fiber's movement begins at the moment when it is grasped by the roller, thus making the sliver thin just at this point. In this case the sliver is well controlled, and the chance that unevenness will result from irregular

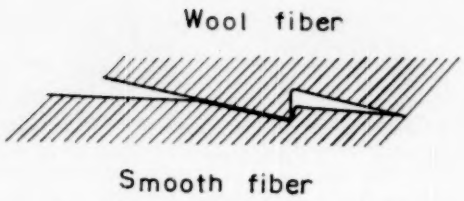

FIG. 4. *Section showing the contact wool fiber-smooth fiber.*

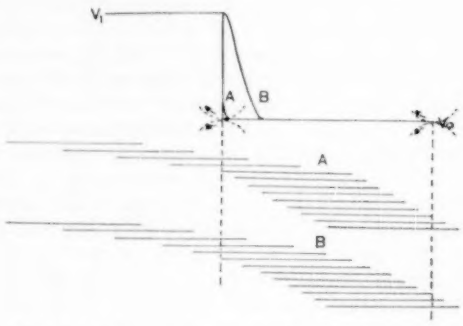

FIG. 5. *Fiber- and fiber velocity-distribution in a drawing frame. A—Discontinuous movement. B—Continuous movement. The pairs of tangent arcs represent the two pairs of rollers.*

sliding of loose fibers is not great. This should also be valid for short fibers, and the formation of drafting waves [7] probably decreases. If $F_s \simeq F_k$, the movement would be more nearly continuous, but this condition is probably not so important for the evenness as the condition of controlled sliding in the case $F_s > F_k$.

Analysis of Variance [1]

We assume that $\Sigma_j n_{ij} = n_i$ measurements are made on the fiber pair i, giving an average $\bar{\mu}_i$, and that k fiber pairs are used for the total average $\bar{\mu}$. (n is the total number of measurements $= \Sigma_i n_i$.) Then we get "variance within fibers," V_E:

$$V_E = \frac{\Sigma_i \Sigma_j (\mu_{ij} - \bar{\mu}_i)^2}{n - k}.$$

Further, we get "variance between fibers," V_B:

$$V_B = \frac{\Sigma_i n_i (\bar{\mu}_i - \bar{\mu})^2}{k - 1}.$$

V_E is attributed to apparatus errors and to variations within the contact surfaces for the single fibers. The "true variance" between average values for the different fibers, V_S, is calculated from

$$V_B = V_E + \frac{\left(n - \frac{\Sigma n_i^2}{n}\right) \cdot V_S}{k - 1}.$$

From these variances we calculate the standard error of the mean for single fibers, $\sigma_E^2 = \frac{V_E}{n_i}$, which is taken as an average for all the fibers, and the standard error of the total mean, $\sigma_S^2 = \frac{V_S}{k}$. If V_E is large, there is poor evenness for small surface regions. If V_E is small but V_S is large, there is great unevenness between the different fibers treated, even though the single fiber surface is evenly treated. If both V_S and V_E are small, the evenness is high.

The results (for static friction) obtained with the various finishing agents are given in Table IX. It was found that V_B is always significantly higher than V_E, which means that the variance V_S is real. Group I agents give less dispersion of values than those of group II. Most oils, as well as soap and Varkaus, give more dispersion. The standard error in the measurement in percent of the frictional coefficient is about the same for all fibers ($\simeq 3.5\%$ for σ_E and 4.0% for σ_S).

TABLE IX. STANDARD DEVIATIONS IN μ_s OF MEANS FOR SINGLE FIBERS (σ_E) AND CALCULATED TRUE STANDARD DEVIATIONS OF MEANS BETWEEN FIBERS (σ_S)

Finishing agent	σ_E	σ_S
None	0.010	0.015
Vapoline oil, 0.5%	0.008	0.007
Vapoline 300%, 0.5%	0.007	0.009
Vapoline 300%, 1%	0.009	0.010
Perma Par R, 1%	0.005	0.011
Velvamine K 90%, 1%	0.008	0.009
Veicol M 50, 1%	0.019	0.008
Veicol S, 0.25%	0.015	0.025
Crunching rayon, 65% R.H.	0.011	0.020
Crunching rayon, 85% R.H.	0.017	0.019
Varkaus, 1%	0.013	0.015
Soap, 1%	0.013	0.018
Pendulum oil	0.005	0.007
Woolrex	0.008	0.006
Svenol, 1%	0.020	0.016
Svenol, 20%	0.017	0.012
Beroil 204 (direct application)	0.015	0.020

Summary

1. Using a stick-slip arrangement, measurements of friction coefficients were made on viscose rayon fibers which had been treated with different finishing agents, spinning oils, etc.

2. The agents could be classified in three groups: (I) low static, low kinetic friction; (II) high static, low kinetic friction; (III) high static, high kinetic friction.

3. The difference between the static and kinetic friction is related to the handle of the fiber sample, a large difference giving a "crunching" handle.

4. Influence of humidity on friction is small if air humidity does not exceed 85–90%. High humidity as well as extensive drying increases friction.

5. Concentration and method of application (directly or in suspension) does not influence friction.

6. The dependence of friction upon load, which gives a measure of the attractive forces between the fibers, differs with the treatment. For agents of group I this dependence is greater for static than for kinetic friction; for agents of group II the opposite is often true; for other agents the dependence is about the same for static and kinetic friction.

7. Friction between rayon and wool is influenced by the wool scales, which are impressed into the surface of the rayon fiber, thus causing higher

friction in the anti-scale than in the with-scale direction.

8. The electrical conductivity of rayon fibers is only slightly influenced by the application of spinning auxiliaries if the amount of auxiliary added is not very great.

9. A theoretical study of the influence of frictional properties on sliver movement in drawing frames was made.

10. The variation of frictional coefficients measured on a bulk of fibers is always significantly higher than the variation of measurements on one fiber.

Acknowledgment

We wish to thank Dr. J. Lindberg, of MAB och MYA, Malmö, Sweden, for valuable discussions, and Mr. E. Tengquist, Svenska Rayonaktiebolaget, for kindly supplying raw materials and making some finishing treatments.

Literature Cited

1. Davies, O. L., "Statistical Methods in Research and Production," London, Oliver and Boyd, 1947, p. 71.
2. Gralén, N., and Olofsson, B., TEXTILE RESEARCH JOURNAL **17**, 488 (1947); *Proc. Swed. Inst. Textile Research, Gothenburg, Swed.*, No. 3 (1947).
3. Götze, K., "Kunstseide u. Zellwolle," Berlin, Julius Springer, 1940, p. 500.
4. Harkins, V. D., and Jordan, H. F., *J. Am. Chem. Soc.* **52**, 1751 (1930).
5. Harris, J. C., TEXTILE RESEARCH JOURNAL, **18**, 669 (1948).
6. Lindberg, J., and Gralén, N., TEXTILE RESEARCH JOURNAL **18**, 287 (1948); *Proc. Swed. Inst. Textile Research, Gothenburg, Swed.*, No. 6 (1948).
7. "Wool Research 1918–1948," Vol. 6 (Drawing and Spinning), Leeds, England, W.I.R.A., 1949, p. 46.

(*Manuscript received December 7, 1949.*)

Measurement of Friction Between Single Fibers

VI. A Theoretical Study of Fiber Friction

Bertil Olofsson

Swedish Institute for Textile Research, Gothenburg, Sweden

Introduction

The measurements of fiber friction reported by several authors show clearly that, in general, frictional coefficients depend upon the load applied. It should be of interest to compare the relationships obtained by these workers and then to consider them in connection with the general points of view on the nature of friction. The relationship between static and kinetic friction is also of interest for the interpretation of friction phenomena. The possible influence of viscous sliding should also be considered.

Dependence of Friction on Load

The equation

$$\mu = \mu_o + \frac{\alpha S}{N} \qquad (1)$$

(μ = frictional coefficient, N = normal pressure, S = contact area, α = constant, $\mu = \mu_o$ for $N \to \infty$) for the dependence of friction on load gives a good explanation of a number of results on fiber friction hitherto obtained. It has been used in earlier papers in this series [3–5, 10], also by Morrow [9] and later by Mercer and Makinson [8]. Martin and Mittelmann [7] used fibers curled over a circular rod and loaded with P_o grams at one end; the force P_1 necessary for slipping at a constant velocity was measured at the other end. They found the empirical relationship

$$\mu = a - b \log P_o, \qquad (2)$$

where a and b are constants.

Breazeale [2], using the same principle for measuring yarn friction, found the same relationship to be valid. As was observed by Mercer and Makinson, this method gives a variation of N and thus of μ along the fiber. A more exact treatment of this relationship will show that equation (1) is really valid in all cases.

Figure 1 shows a periphery element dl of the friction cylinder or rod with its center angle $d\varphi$. P is the tension, dN is the normal pressure, and dF is the frictional force of the corresponding fiber part (in the plane of the paper).

$$\mu = \frac{dF}{dN} = \frac{dP}{Pd\varphi}. \tag{3}$$

If μ were a real constant, integrating would give the well-known relationship

$$P = P_o e^{\mu\varphi} \tag{4}$$

if $P = P_o$ when $\varphi = 0$. And for the tension P_1 at the other end of the fiber ($\varphi = \pi$)

$$P_1 = P_o e^{\mu\pi}. \tag{4a}$$

But if equation (1) is valid we can write

$$\mu = \mu_o + \alpha\frac{dS}{dN} = \mu_o + \frac{\beta d\varphi}{Pd\varphi} = \mu_o + \frac{\beta}{P}, \tag{5}$$

since dS is proportional to dl, which is = constant $\cdot d\varphi$; β is a new constant.

Instead of equation (3) we get

$$\frac{dP}{Pd\varphi} = \mu_o + \frac{\beta}{P}$$

or

$$\frac{dP}{d\varphi} - P\mu_o = \beta. \tag{6}$$

This equation is integrated after multiplying by $e^{-\mu_o\varphi}$:

$$P\,(e^{-\mu_o\varphi}) = -\frac{\beta}{\mu_o}(e^{-\mu_o\varphi}) + C.$$

C is determined from the value $P = P_o$ for $\varphi = 0$:

$$C = P_o + \frac{\beta}{\mu_o}.$$

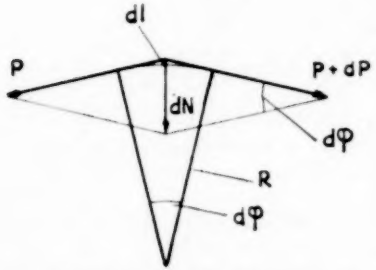

FIG. 1. *Section of a circular rod with a fiber element.*

Thus, we get

$$P = (P_o + \frac{\beta}{\mu_o})\, e^{\mu_o\varphi} - \frac{\beta}{\mu_o}; \tag{7}$$

and for $\varphi = \pi$ and $P = P_1$ we get

$$P_1 = (P_o + \frac{\beta}{\mu_o})\, e^{\mu_o\pi} - \frac{\beta}{\mu_o}. \tag{7a}$$

Breazeale and Martin and Mittelmann have used the value of μ from equation (4a). If we compare this equation with equation (7a) we get

$$\frac{P_1}{P_o} = e^{\mu\pi} = -\frac{\beta}{\mu_o P_o} + \left(1 + \frac{\beta}{\mu_o P_o}\right)\cdot e^{\mu_o\pi}; \tag{8}$$

or

$$e^{\mu\pi} = k_1 + \frac{k_2}{P_o}, \tag{9}$$

if we define the constants

$$k_1 = e^{\mu_o\pi} \text{ and } k_2 = \frac{\beta}{\mu_o}(e^{\mu_o\pi} - 1). \tag{9a}$$

This equation should replace equation (2) in the papers [2] and [7]. If $e^{\mu\pi}$ is then plotted against $\frac{1}{P_o}$ we should get a straight line, and from this line we could determine k_1 and k_2. We are thus able to draw curves for μ plotted against P_o or log P_o according to equation (9). Figure 9 from [2], with its curves for glass and "Alsimag," is copied in Figure 2 (full lines); our curves according to equation (9) are also drawn (broken lines). For glass the experimental points fit excellently to the curve. For Alsimag the three top points, but not the lowest, fit very well to a curve. To some extent this deviation may be explained from the assumption that the real contact area decreases as load decreases. This means that β, and thus k_2, decreases when P_o decreases. According to equation (9), for a fixed value of P_o μ should then be smaller than the curve value. However, in the case of Alsimag it should probably be necessary to get additional experimental values.

Figure 7 from [7] is copied in Figure 3 (full lines). (In the figure, T_o stands for P_o.) When single wool fibers are measured, the dispersion of values, especially in the case of anti-scale friction, is rather great. This is also shown when the different values of $e^{\mu\pi}$ are plotted against $\frac{1}{P_o}$. However, a straight line may be drawn and the constants k_1 and k_2 determined. The curves for μ

plotted against log P_o, calculated from equation (9), are drawn. Evidently the with-scale curve fits very well to the experimental points. For the anti-scale friction a curve may also be drawn which fits most of the points well. For decreasing tension, the curve evidently gives an increasing deviation from the experimental results. However, this is in good agreement with the results of Lindberg and Gralén [4] and Lindberg [5]. These authors have given the relationship

$$\mu_2 = \mu_1 + \frac{cAQ}{N}, \tag{10}$$

where μ_2 is the anti-scale and μ_1 the with-scale frictional coefficient, cA is the number of active scales hooking onto each other, and Q is scale resistance. cAQ is a function $f(N)$ of N; for decreasing pressure cAQ decreases more and more rapidly in one region, then decreases almost linearly to the limit $\lim_{N\to 0} f(N) = 0$.

Substituting equation (5) for μ_1 in equation (10):

$$\mu_2 = \mu_o + \alpha\frac{dS}{dN} + \frac{df(N)}{dN}. \tag{11}$$

Between appropriate limits of N we may approximate $\frac{df(N)}{dN} = K$. Substitution in equation (11) changes μ_o to $\mu_o + K$, if $\frac{\alpha dS}{dN}$ is used as before. Thus k_1 and k_2 are calculated as before, and from equation (9a) we get $\mu_o + K$ and β. From with-scale dots in Figure 3 we get $\mu_o = 0.116$ and $\beta = 19$ (loads in mg.). From anti-scale dots for the larger N values ($\mu < 0.45$) we get $\mu_o + K = 0.169$ and $\beta = 151$. Thus K in this region is small ($K = 0.053$), which is in agreement with the results in [5]. The large difference $\beta_{\text{anti-scale}} - \beta_{\text{with-scale}} = 132$ is a little astonishing, as it should mean a large difference in the closeness of contact. But it is probably related to the form resistance when scales are pressed into a smooth surface, as explained on p. 473. From the few anti-scale dots at low normal pressure ($\mu > 0.45$) we get from Figure 3 $\mu_o + K = 0.454$ and $\beta = 23$. Thus $K = 0.454 - 0.116 = 0.308$ is great in this region and $\beta_{\text{anti-scale}} - \beta_{\text{with-scale}} = 4$ is extremely small. This agrees very well with the results in [5] as well as

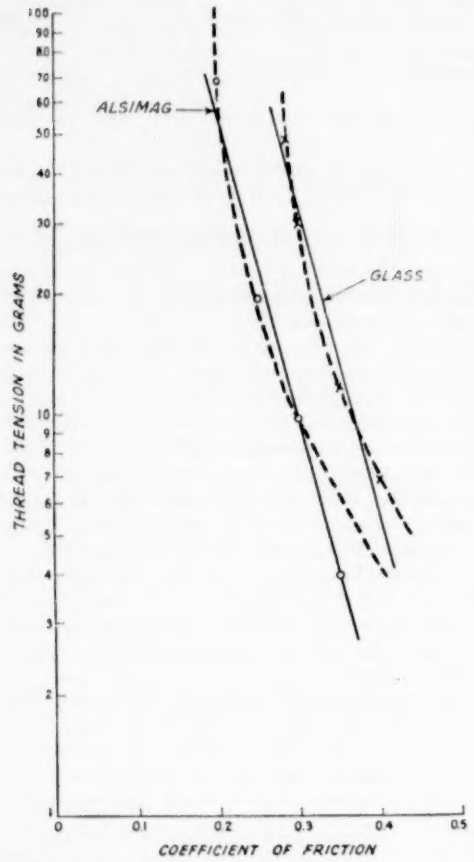

FIG. 2. *Copy of Figure 9 in [2] with theoretical curves according to equation (2) —— and equation (9) – – –.*

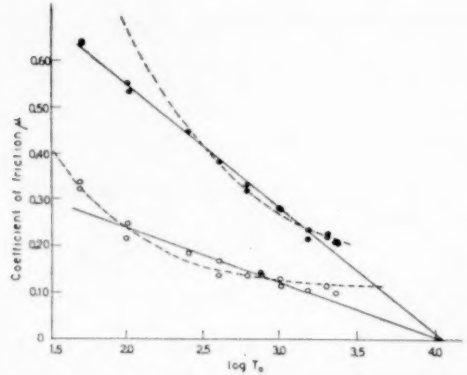

FIG. 3. *Copy of Figure 7 in [7] with theoretical curves according to equation (2) ——— and equation (9) – – –.*

with the assumption of decreasing closeness of contacts for decreasing load. All figures are of course significative only qualitatively.

Mercer and Makinson [8] plotted μP_o against P_o for Martin and Mittelmann's results and found a sharp bend in one point of the curve. There seems to be no justification for this on our plots; the curve should be continously bent.

Nature of Fiber Friction

Equation (1) thus seems to be of very general applicability. It is valid for fibers rubbing against each other and against other material, for static as well as for kinetic friction. Then we may ask how this relationship can be explained. It should be of interest to compare our results with those of different theories of friction. The first investigators (Amonton, Coulomb, *et al.*) suggested that friction was caused by moving the sticking surfaces over small asperities. If so, μ should be a function of surface structure but not of normal pressure. Some later workers, using carefully polished and clean surfaces, supposed adhesion forces to exist between bodies which stuck together. However, there are not many results for the dependence of μ upon N. Bowden and coworkers [1] have made extensive measurements on metal surfaces using the stick-slip method. They give the relationship

$$F = S + P = As + A'p, \tag{12}$$

where S is the shearing force for real junctions and P is the force necessary for displacing material from the path of the slider. If s is shear strength, p is "flow pressure," A is the real contact area, and A' is the cross section of the track, we get the second relationship in equation (12). When an increasing load N is applied, plastic flow occurs until the pressure per unit area of contact reaches the value p; then $N = Ap$. If the value for A is substituted in equation (12) and we divide by N we get

$$\mu = \frac{F}{N} = \frac{s}{p} + \frac{A'p}{N} = C_1 + \frac{C_2}{N}. \tag{13}$$

This is analogous to our results, since it is probable that A' is practically independent of N.

However, there are some important objections as regards our results. It seems improbable, firstly, that surface deformations are of a plastic and not of an elastic character, and, secondly, that there is a real ploughing from the impressed part of one fiber through the surface layer of the other. We could make another suggestion. Assume that the load is balanced by a normal pressure of the type

$$p = a_o + a_1x + a_2x^2 + \ldots,$$

where p = pressure on the area dS (that is, $N = \int p dS$) and x is the corresponding surface impression. If $p = a_o$ we have only adhesion forces (or pure plastic flow corresponding to Bowden's assumption); if $p = a_1x$ we have elastic forces of the simple harmonic kind, and if additional terms are used, we could get the value of N with sufficient accuracy. If we now suppose that F is proportional to the contact area, we get new relationships for μ. If only the first two terms of p are taken into consideration, and the depressions are assumed to be small in comparison to the fiber radius, we get a relationship for μ of the form

$$\gamma\mu N + \delta = \frac{1}{\mu}, \tag{14}$$

where γ and δ are constants. These may be determined so that the curve fits to our experimental curve as well as possible. However, since equation (14) gives $\mu \to 0$ for $N \to \infty$ it is not valid for higher loads. Furthermore, the deviation from our straight line μ *vs.* $\frac{1}{N}$ should not be neglected. The most important objection is, of course, that in the deduction above F is considered to be proportional to S, regardless of the kind of deformation. From the assumptions of a deformation which is partly elastic and partly plastic and of direct proportionality between contact area and force, Ramsauer [11] has recently tried to give an explanation of the load dependence of metallic friction. He has used a special parameter for the quotient $\frac{\text{area of plastic contact}}{\text{area of elastic contact}}$, which was calculated from experimental curves, and in this way he obtained good agreement between theory and experiment. However, his curves satisfy our equation (1) just as well.

Our results are most easily, although not exhaustively, explained in the following manner. We assume the equation $F = \mu N$ to be valid. Now N is composed of the applied load N_1 and the attraction force N_2 (*e.g.*, $N = N_1 + N_2$). N_2 is proportional to the contact area S, which gives the relationship of equation (1).

The difference between static and kinetic friction might depend upon the closer contact in the static

case. If μ_o is principally dependent upon surface shearing and α on ploughing, as given in equation (13), it is not easy to explain why $\mu_o > \mu_k$. If, according to the ordinary view, the influence of asperities is considered, we could assume that generally there are smaller differences between peaks and valleys of the contact surface in the kinetic than in the static state, in which during application of the force the surfaces are well stuck together.

There are few indications of slippage of a viscous character in the case of treated fibers. This should give a time dependency of the movement [3]. If the speed were increased the slipping should occur after greater slider deflection—*i.e.*, for higher μ values. In reality the μ values are almost independent of the velocity of the apparatus (or they decrease to some extent for higher velocities because the fibers are not allowed to "stick together" sufficiently).

However, the theory of plastic flow could, of course, be used in this connection if the slip point is regarded as the "yield point." But this gives no further explanation of the nature of the frictional forces because we are working with inhomogeneous systems. The slight dependence of μ upon velocity is not in good accord with this theory. But if there is much liquid agent and differences between μ_s and μ_k are small the friction may be due partly to viscous flow. This is the case for pendulum oil (high-viscosity mineral oil), which should be compared with kerosene (low viscosity) and Woolrex (high viscosity but of an ionic nature) (see Table VI, page 471). It seems that all ionic reagents are fixed to the surfaces, giving a layer which causes nonviscous slipping. Another consequence of liquid agent in contacts is the large αS values for pendulum oil and the spinning oils Svenol and Beroil [10]; this phenomenon is probably related to swelling and surface tension, which should increase the real contact area.

Summary

1. The relationship $\mu = \mu_o + \frac{\alpha S}{N}$ is proved to be valid for a number of friction measurements on fibers by different workers.

2. The meaning of this relationship is discussed from points of view of general friction theories. The relationship is most easily explained if surface attraction forces are considered.

3. The difference between static and kinetic friction is assumed to be due to the closer surface sticking in the static case. The possibility of viscous sliding of fibers is discussed.

Acknowledgment

The author wishes to thank Prof. Nils Gralén for his kind interest in this work.

Literature Cited

1. Bowden, F. P., Moore, A. J. W., and Tabor, D. J., *J. Applied Phys.* **14**, 80 (1943).
2. Breazeale, F., TEXTILE RESEARCH JOURNAL **17**, 27 (1947).
3. Gralén, N., and Olofsson, B., TEXTILE RESEARCH JOURNAL **17**, 488 (1947); *Proc. Swed. Inst. Textile Research, Gothenburg, Swed.*, No. 3 (1947).
4. Lindberg, J., and Gralén, N., TEXTILE RESEARCH JOURNAL **18**, 287 (1948); *Proc. Swed. Inst. Textile Research, Gothenburg, Swed.*, No. 6 (1948).
5. Lindberg, J., TEXTILE RESEARCH JOURNAL **18**, 470 (1948); *Proc. Swed. Inst. Textile Research, Gothenburg, Swed.*, No. 8 (1948).
6. Makinson, K. R., *Trans. Faraday Soc.* **44**, 279 (1948).
7. Martin, A. J. P., and Mittelmann, R., *J. Text. Inst.* **37**, T269 (1946).
8. Mercer, E. H., and Makinson, K. R., *J. Text. Inst.* **38**, T227 (1947).
9. Morrow, J. A., *J. Text. Inst.* **22**, T425 (1931).
10. Olofsson, B., and Gralén, N., TEXTILE RESEARCH JOURNAL **20**, 467 (1950) (this issue).
11. Ramsauer, R., *Kolloid-Z.* **111**, 83 (1948).

(*Manuscript received December 7, 1949.*)

The Kinetics of Wool Dyeing

Part I: Simple Acid Dyes

P. Alexander and R. F. Hudson

Department of Inorganic and Physical Chemistry, Imperial College of Science, London

Abstract

It is shown that the rate controlling mechanism of dyeing wool with the simple acid dye Acid Orange II can be diffusion through an unstirred film of liquid or diffusion through the fiber. At low concentrations of dye, the diffusion of dye through an unstirred film of liquid is the slower of the two processes, whatever the degree of agitation. At higher concentrations of dye, the rate controlling step changes from diffusion through liquid film to diffusion through solid when the stirring of the solution is increased beyond the point at which the reaction becomes stirring-independent and the activation energy, determined from the temperature coefficient, changes from approximately 5 to 13 kg.-cal./mole.

At high concentrations of dye the diffusion of dye through the fiber proceeds from a saturated concentration on the fiber surface, which action can be readily treated quantitatively. At low dye concentrations the diffusion through the unstirred liquid film can also be treated by the simple diffusion law. In the intermediate range of dye concentrations, however, the diffusion into the fiber proceeds from a varying concentration on the fiber surface and is treated on the basis of a semi-empirical relationship.

From consideration of the diffusion coefficient and the apparent energy of activation it is concluded that dye is not transported through pores, but rather that the swollen fiber behaves like a gel and diffusion occurs by displacement of peptide molecules.

Introduction

Although extensive equilibrium studies have been made on the adsorption of dyes by wool and other protein fibers [21, 35, 38], there is a surprising lack of data on the rate of the process. Speakman and Smith [39] have recorded limited rate data using the simple nonaggregated dye Acid Orange II [42], and have shown that dyeing seems to proceed from a surface layer of constant dye concentration, even though the concentration of the bath decreases almost to zero. Curves of Q_t plotted against $\sqrt{t}$ were found to be linear for approximately 70% of the reaction, in agreement with the parabolic rate law [4, 14] for diffusion into a semi-infinite solid.

$$Q_t = 2C_sA\sqrt{D_st/\pi}.$$

The mechanism of acid dyeing has been discussed by Speakman and Clegg [37] in terms of the fiber molecular structure and the fiber modification by swelling with changes in temperature and pH. Plotting D_s against T, Speakman and Smith [39] obtained two straight lines which intersected at 37°C; they believed this demonstrated that the rate of dyeing increases rapidly above 37°C because of disulfide-bond breakdown, which causes increased swelling. The minimum fiber swelling at 40°C reported by Speakman [36] was considered to support this view. This view is untenable since Gilbert [11] showed that the rate obeys the Arrhenius equation between 0°C–80°C, without interruption at 37°C, showing that no irreversible change in the fiber structure occurs and tending to prove that the system is insensitive to temperature changes over this wide temperature range. It is thought, however, that extensive modification of the fiber structure may occur at temperatures near 100°C, due to hydrolysis. That the physical state of the fibers affects the rate of dyeing was shown by Speakman and Smith, who removed the outer fiber scales and obtained a faster rate of dyeing, and by Lemin and Vickerstaff [20], who investigated briefly the rate of dyeing of damaged fibers.

The role of diffusion in the reaction between wool and oxidizing agents has recently been studied in detail by the authors [2, 3]. Depending upon the conditions of temperature, agitation, and concentration, the over-all rate of reaction is governed either by transport of reactant in solution to the fiber surface or by diffusion within the fiber. The effect of agitation, the value of the apparent activation energy, and the shape of the kinetic curves were used to differentiate between the two mechanisms. The dyeing of fiber with a simple acid dye is a similar reaction, but in this case no degradative reaction occurs, although strong adsorption of the dye molecules on particular sites is analogous to the removal of diffusing molecules by chemical reaction.

The kinetics of cellulose dyeing have been studied extensively [12, 27, 28, 41, 45], and the mechanism is generally considered to be a process of diffusion through micropores, with deposition of dye on the fiber surface. The correlation between experimental and theoretical results is very poor [10], probably because the charge on the fiber changes as dyeing proceeds. In contrast, the dyeing of protein in a solution of low pH is an ion-exchange process in which the dye anion slowly replaces a small inorganic ion being held as a gegenion to the charged amino groups of the protein. Hence, unlike the case of direct cellulose dyeing, the charge on the fiber remains constant. The kinetics of base exchange have received much attention recently [7, 19], and in most cases it has been shown that the rate of exchange is governed by the uniform diffusion of ions through the solid phase. Consequently, a simple theory of diffusion with adsorption is expected to be more applicable for the dyeing of wool than for the dyeing of cellulose.

By using the same dye as that employed by Speakman and Smith [39] it has been found that the rate of dyeing is governed by diffusion across a liquid film at the fiber surface or by diffusion within the fiber, depending upon temperature, agitation, and the concentration of dye in solution. As in the oxidation of wool, the two mechanisms are characterized by different temperature coefficients, leading to greatly different activation energies.

The following factors affect these mechanisms so as to render the one or the other rate-determining:

1. Temperature influences D_i, D_s, and δ in such a way that increase in temperature favors liquid-film diffusion, which has the smaller activation energy, as the controlling mechanism.

2. Stirring rate affects δ only; high agitation promotes the fiber-diffusion mechanism.

3. Concentration does affect the relative values of the two rates, although it might not be expected to owing to the change in distribution coefficient K between adsorbed and mobile reactant. K is incorporated in D_s, which may be replaced by D_i/K, where D_i is the true internal diffusion coefficient.

Thus, the relative concentrations of solute on opposite sides of the phase boundary are governed, in general, by some form of adsorption isotherm. For dilute solutions the concentrations are given by a distribution coefficient K, but K decreases with increasing concentrations. In this respect the close analogy between molecular diffusion and heat conduction [8] appears to break down.

With high concentrations of dye in solution, the surface concentration may remain almost constant throughout most of the adsorption. With decreasing concentration, however, the rate may be governed by diffusion through the fiber, although the surface concentration decreases continually.

It is impossible to obtain a formal solution of the diffusion equation for the general case where the surface concentration is a given function of the bath concentration. Recently, however, solutions have been given for a linear relation between concentrations in the two phases. Barrer [5] has considered diffusion into a sphere in a constant-volume system, adapting the solution of the general diffusion equation given by Paterson [30], which deals with transference of heat to and from spheres in a stirred liquid. From the complete solution Barrer derived the following approximation:

$$\frac{Q_t}{Q_\infty} = \frac{6}{a}\frac{K'+1}{K'}\sqrt{\frac{D_i}{\pi}},$$

where $\frac{1}{K'} = \frac{\text{Amount of solute absorbed}}{\text{Amount of solute remaining in solution}}$, and a is the radius of the sphere. From this simple relation, the following conclusions may be drawn:

(*a*) For an exhausting dye bath the value of $t_{\frac{1}{2}}$ is independent of initial concentration.

(*b*) The curves of Q_t plotted against $\sqrt{t}$ are approximately linear.

It will be observed that the value of $t_{\frac{1}{2}}$ increases slowly with increase in concentration, this tendency most probably being due to the variation in K'. It is found that a curve showing the relationship between Q_t and $\sqrt{t}$ is linear (see Figure 7) in the

initial stages of the process. Thus, a qualitative explanation may be given for the results for the concentration region of 75 to 250 mg. of dye per liter.

The analogous case of diffusion into a cylinder has been treated by Wilson [46] and Crank [9] on the basis of diffusion with adsorption according to a linear isotherm. In this case the dye is considered to exist within the fiber as mobile or adsorbed dye, the concentrations of the two being related by the adsorption isotherm between solution and fiber. It was found that the shape of the kinetic curve predicted by this theory does not agree with that of the experimental curve, except in the initial stages of the process (see Figure 9).

The diffusion-with-adsorption theory of Crank and Wilson assumes that there is a continual equilibrium between the dye in solution and the dye on the fiber, which depends upon instantaneous adsorption *and desorption*. The disparity between the theoretical and the experimental rate curves indicates that the rate of adsorption in the later stages of the process is much greater than the predicted rate. This implies that dye penetrates a limited distance into the fiber (so that a greater diffusion gradient is maintained) owing to extremely slow desorption and redistribution of the dye throughout the whole of the fiber. Thus, in the course of a kinetic experiment, a state of apparent equilibrium is reached, with most of the dye adsorbed on the outer portion of the fiber, followed subsequently by redistribution of the dye throughout the whole of the fiber, leading to thermodynamic equilibrium. In the course of this redistribution, a readjustment in the concentration of dye in solution occurs, but this change is small compared with the change in concentration which occurs during adsorption, owing to the very high value of the distribution coefficient.

This explanation is supported by the visual observation of dyed fibers. Thus, after a dye bath has almost exhausted, it may be seen that most of the dye is concentrated on the outside of the fiber [25, 33]. It then requires considerable time for the bound dye to be redistributed uniformly in the fibers.

This picture of the process was used to derive a semi-epirical relation which is applicable to dyeing from an exhausting dye bath, assuming instantaneous adsorption on specific sites and very slow desorption. Values for the diffusion coefficient are of the expected order of magnitude and agree with the approximate values derived from the Wilson equation for small adsorptions.

The effects of temperature, stirring rate, and dye concentration are considered in detail in the light of the following results, which agree with a theoretical interpretation of diffusion with adsorption on fixed sites within the fiber.

Experimental Procedure

Two-gram samples of knitted wool fabric were wetted out in 0.01*N* solutions of hydrochloric acid overnight and rotated until each sample contained its own weight of acid solution. Each sample was fitted to a glass frame stirrer and rotated at a known speed in 280 ml. of dye solution containing 0.01*N* hydrochloric acid. During adsorption the pH remained between 2.1 and 2.2. The rate measurements were made by a procedure similar to that already described in detail for the reaction between wool and chlorine solutions [2]. Five-ml. samples of the solution were withdrawn periodically and estimated colorimetrically by means of a Spekker photometer. The concentration of dye in each sample was then obtained from a calibration graph.

In the experiments where the liquid was stirred with a paddle stirrer, a 1-in. paddle was attached to the electric motor, which had a series of gears to provide various constant stirring speeds, and the fabric was held on a fixed frame inside which the paddle was fixed.

All experiments were conducted in a thermostat which provided temperature control to within 0.1°C. The dye used throughout was Acid Orange 2G (Color Index No. 27).

Results

The effect of stirring on $t_{\frac{1}{2}}$ is shown graphically in Figures 1 and 2 for dye concentrations of 125 and 500 mg./l. At the lower concentration the rate of reaction is highly stirring-dependent, becoming independent of stirring only when the wool is rotated faster than 300 r.p.m. It is seen from a comparison of Figures 1 and 2 that rotation of the fabric in solution causes much greater agitation than stirring the solution does. With the higher concentrations, however, the rate of reaction is almost independent of agitation, which was also observed by Speakman and Smith [39]. These observations indicate that at the higher concentration the rate of reaction is controlled entirely by

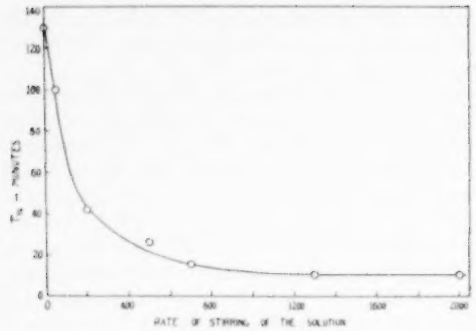

FIG. 1. *Effect of stirring the solution on $t_{\frac{1}{2}}$ at 25°C for dye concentration of 125 mg./l.*

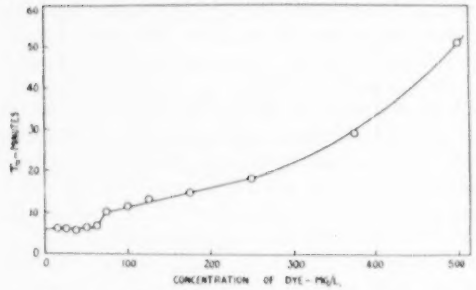

FIG. 3. *Effect of initial concentration of dye on $t_{\frac{1}{2}}$ at 25°C, stirring the wool at 200 r.p.m.*

diffusion within the fiber, whereas at the lower concentration either mechanism may predominate, depending on the degree of agitation.

Concentration affects the diffusion rate, as shown in Figure 3, where $t_{\frac{1}{2}}$ is plotted against concentration of dye in mg./l. These measurements were made by rotating the wool at 200 r.p.m. at 25°C with 1 g. of wool in contact with 140 ml. of solution. This liquor-wool ratio was employed in all of these experiments. The graph may be divided arbi-

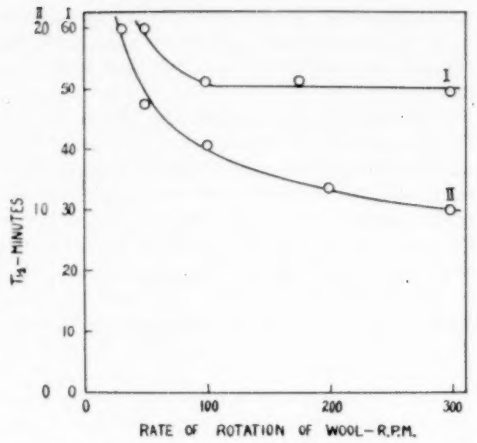

FIG. 2. *Effect of stirring the wool on $t_{\frac{1}{2}}$ at 25°C for dye concentrations of 500 mg./l. (I) and 125 mg./l. (II).*

trarily into three sections: (I) concentrations < 62.5 mg./l., where $t_{\frac{1}{2}}$ is completely independent of concentration; (II) concentrations > 250 mg./l., where $t_{\frac{1}{2}}$ increases rapidly and nonlinearly with increase in concentration; (III) intermediate concentrations (75–250 mg./l.), where $t_{\frac{1}{2}}$ increases very slowly with increase in concentration.

The break in the curve at 62–75 mg./l. dye concentration indicates a change in mechanism which is supported by the change in temperature coefficient. Table I gives calculated values for the activation energy for various temperatures and extreme conditions of stirring. It is seen that results corresponding to Section I give low calculated activation energies for low and high stirring rates. For Section III a low activation energy is obtained for low stirring rates (*i.e.*, stirring the solution) and a high value for high stirring rates (*i.e.*, rotating the wool), whereas for Section II high activation energies are obtained for all stirring rates.

TABLE I. ACTIVATION ENERGY (KG.-CAL./MOLE) CALCULATED FROM $t_{\frac{1}{2}}$ VALUES AT LOW AND HIGH STIRRING RATES

Initial conc. of dye (mg./l.)	Fast stirring, 200 r.p.m. (wool)					Slow stirring, 200 r.p.m. (liquid)				
	$t_{\frac{1}{2}}$ (0°C)	$t_{\frac{1}{2}}$ (25°C)	$t_{\frac{1}{2}}$ (35°C)	E (0°–25°C)	E (25°–35°C)	$t_{\frac{1}{2}}$ (0°C)	$t_{\frac{1}{2}}$ (25°C)	$t_{\frac{1}{2}}$ (35°C)	E (0°–25°C)	E (25°–35°C)
37.5	17.5	5.5	4.5	7.3	4.0	—	25.0	—	—	—
62.5	25	6.5	5.0	8.5	4.5	100	33.5	—	6.4	—
125	78	12.0	5.5	12.0	13.0	135	42.0	—	6.4	—
250	—	18.0	9.0	—	12.0	—	57.5	24.5	—	14.0
500	—	50.0	22.0	—	13.0	—	77.5	41.0	—	13.0

Discussion

Interpretation of Results

The rate measurements discussed in the preceding section refer to the case, usually employed in dyeing practice, of an exhausting bath. From the rate curves it was found that in each case the final dye concentration in solution could be neglected in comparison with the initial concentration. Thus, except at high concentrations, it follows that the concentration of dye at the fiber surface, governing the rate of diffusion into the fiber, decreases during the dyeing. Before the mechanism is considered in detail the significance of the three cases outlined in the Results section must be considered.

Diffusion Across a Liquid Layer (I).—At low concentrations it is observed that the rate is highly stirring-dependent and that the experimental activation energy is of the order of 4–6 kg.-cal./mole for all stirring rates. With increasing concentration the range of stirring rate for which a value for the activation energy of this order is obtained gradually decreases. This value is of the same order as that of diffusion of ions in aqueous media for the corresponding temperature range, although being somewhat higher in all cases. This has been shown to be due to the change in the thickness of the diffusion layer (δ) with temperature [2]. It is interesting to observe that E decreases rapidly with increase in temperature (Table I), which is characteristic for diffusion in aqueous media in the 0°–40°C temperature range. The rate of the reaction controlled by diffusion across a liquid layer at the surface of a solid is given by the general relation

$$D_l = \frac{\delta V}{At} \log_e \frac{c}{c - x},$$

V being the volume (in cc.) of solution in contact with area A of fibers, c and $c - x$ being the concentrations of dye at times 0 (zero) and t.

The graph in Figure 4 shows the effect of stirring on rate of dyeing for low concentrations of dye, where diffusion in solution is expected to govern the rate. It is seen that even for rapid stirring a logarithmic relation between concentration in solution and time is maintained. At higher concentrations, however, the logarithmic plots (Figure 5) are not linear for high degrees of agitation. Thus, over the extensive solution stirring range 50 to 2,000 r.p.m. it is observed that the graphs are nonlinear at very high and very low stirring rates. At high

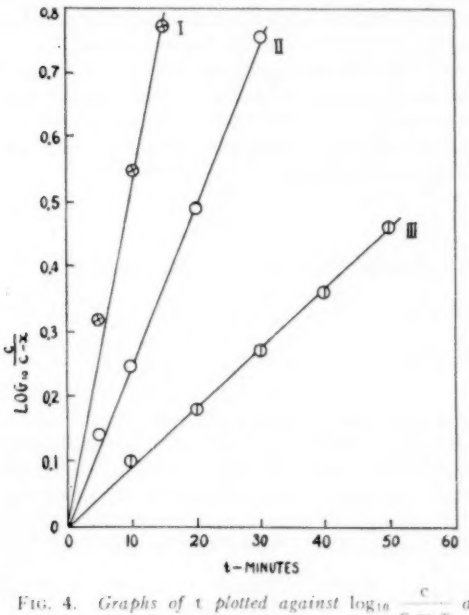

FIG. 4. *Graphs of* t *plotted against* $\log_{10} \frac{c}{c - x}$ *at 25°C for dye concentration of 62.5 mg./l. under the following conditions of stirring: (I) wool, 200 r.p.m.; (II) wool, 50 r.p.m.; (III) solution, 200 r.p.m.*

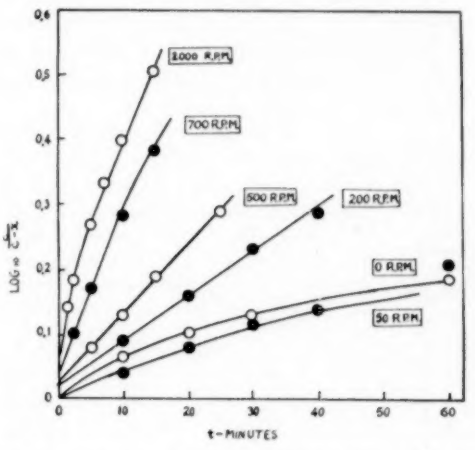

FIG. 5. *Graphs of* t *plotted against* $\log_{10} \frac{c}{c - x}$ *at 25°C for dye concentration of 125 mg./l., stirring the solution at various rates.*

stirring rates the concentration at the fiber surface becomes appreciable, so that the rate is governed by diffusion within the fiber. At very low stirring rates deviations are due to variation in thickness of the diffusion layer with concentration changes [1, 15, 17, 18].

The change in mechanism with concentration at low stirring rates is shown by the curves of Figure 6. It is seen that for concentrations of 37.5 and 62.5 mg./l. the curve of $\log_{10} \frac{c}{c-x}$ against t is linear. Deviations are observed with a concentration of 125 mg./l., whereas with 250 mg./l. and 500 mg./l. the relationship is not linear.

It should be noted that the above logarithmic relation holds only if the concentration of dyeing solution at the surface is negligible compared with the bulk concentration in solution. This arises from the extremely high distribution coefficient in dyeing and in dilute solution most of the dye is absorbed instantaneously on the surface of the fibers, thus maintaining the concentration in adjacent solution at approximately zero.

From the rate measurements (Figure 5) values of δ may be calculated for various stirring rates (Table II), assuming the D_t value for the azo dye to be 5.35×10^{-6} cm.²/sec. [42]. It can be seen that δ varies inversely with stirring rate, which is often found to be the case for these processes [1, 15, 17, 18, 22].

Diffusion in Fiber from Constant Surface Concentration (II).—Before considering the conditions of intermediate concentrations (represented by Section III under Results, p. 483) the rate data for high dye concentrations will be considered. The conditions employed here are similar to those used by Speakman and Smith [39], who considered reaction to proceed from a surface layer of constant concentration.

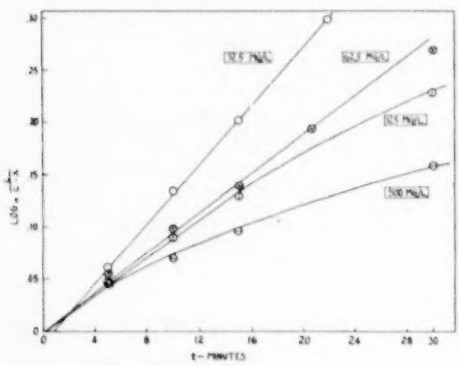

FIG. 6. *Graphs of* t *plotted against* $\log_{10} \frac{c}{c-x}$ *at 25°C for different dye concentrations, stirring the solution at 200 r.p.m.*

TABLE II. VALUES OF THE THICKNESS OF THE APPARENT DIFFUSION LAYER FOR VARIOUS STIRRING RATES AT LOW CONCENTRATION, ASSUMING THE REACTION TO BE CONTROLLED BY DIFFUSION IN SOLUTION

Rate of stirring (r.p.m.)	$k \times 10^4$ sec.$^{-1}$	δ (cm.)
2,000	8.9	1.8×10^{-2}
700	4.25	4.0×10^{-2}
500	1.8	9.2×10^{-2}
200	1.15	14.3×10^{-2}

Stirring the liquid; conc. of dye 0.125 g./l. at 25°C

$k = \frac{1}{t} \log_{10} \frac{c}{c-x}$. $A = 10^3$ cm.²/g.

$V = 140$ ml. $D = 5.35 \times 10^{-6}$ cm.²/sec.

It has been shown that for all conditions of agitation, with 250 mg./l. and 500 mg./l. of dye, an activation energy of the order of 13 kg.-cal./mole is calculated from the rate data. Thus, the over-all rate of reaction is controlled totally by diffusion within the fiber. For diffusion into a semi-infinite solid from a surface concentration C_s when a quantity Q_t has diffused in time t, the following approximate relation, which has already been discussed, may be considered to be true in the early stages of the reaction:

$$Q_t = 2C_s A \sqrt{\frac{D_s t}{\pi}}.$$

If dyeing proceeds almost to exhaustion, then

$$\tfrac{1}{2} c V = 2C_s A \sqrt{\frac{D_s t_{\frac{1}{2}}}{\pi}},$$

so that

$$t_{\frac{1}{2}} \propto c^2.$$

It is seen from Figure 3 that this relation is approximately obeyed as $t_{\frac{1}{2}} \propto c^{1.6}$. The square relationship does not hold exactly for the data of Speakman and Smith. Thus, it may be concluded that diffusion proceeds from an almost constant surface concentration for at least half of the process. The curves of $\sqrt{t}$ plotted against $\frac{Q_t}{Q_\infty}$ given in Figure 7 show that this law is obeyed at the beginning for approximately 40–50% of the reaction, depending on the initial dye concentration [13, 43]. It is

TABLE III. CALCULATED VALUES OF THE DIFFUSION COEFFICIENT, ASSUMING CONSTANT SURFACE CONCENTRATION, AND ASSUMING ALL THE DYE WITHIN THE FIBER TO BE MOBILE

Concentration (mg./l.)	D_s values (cm.²/sec.) (25°C)	(35°C)	E (25°–35°C) (kg.-cal./mole)
250	0.7×10^{-11}	1.40×10^{-11}	12.7
500	0.845×10^{-11}	1.95×10^{-11}	15.6

observed that at the higher concentrations deviations are greater, which is in agreement with increased penetration into the cylinder [8]. From the initial slopes values of D_s are calculated, assuming that the surface concentration C_s is given by the saturation value for acid adsorption—*i.e.*, approximately 88 millimoles/g. [34, 40] (Table III).

Diffusion Through the Fiber from a Varying Surface Concentration (III).—Attention may now be turned to the concentration range in which high and low activation energies are observed, depending on the rate of stirring. It is observed here that the rate of reaction is approximately proportional to the concentration of dye in solution—*i.e.*, $t_{\frac{1}{2}}$ is almost independent of initial concentration, although a slight increase is observed (Figure 3). By analogy with similar processes [2] this indicates that diffusion proceeds from a decreasing surface concentration (see page 482). The semi-empirical treatment considered below is an attempt to treat this condition in which it is assumed that dye already sorbed on specific sites according to a linear isotherm is not desorbed during the course of the kinetic determination.

Semi-Empirical Treatment for Diffusion in the Fiber

The process of dyeing may be regarded as a heterogeneous chemical reaction, similar to the oxidation of metals [26, 44] or the reduction of oxides. The chief difference is in the density of the product formed, for in the case of a metal the volume penetrated by reactant has reacted completely. In the present reaction, however, this will probably not be the case, owing to the relatively wide separation of sites.

The following assumptions lead to a simple treatment of this problem.

1. The rate of adsorption on sites is instantaneous; the rate of desorption (leveling) is small compared with the observed rate of dyeing (see photomicrographs in references [25] and [33]).

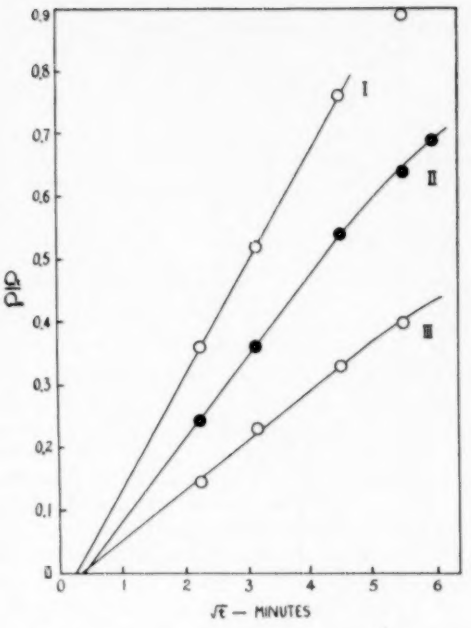

FIG. 7. *Graphs of* $\sqrt{t}$ *plotted against* $\frac{Q_t}{Q_\infty}$, *stirring the wool at 200 r.p.m. for the following dye concentrations: (I) 250 mg./l. at 35°C; (II) 250 mg./l. at 25°C; (III) 500 mg./l. at 25°C.*

2. Diffusion proceeds by way of mobile dye, the concentration of which at the surface approximately equals that within the liquid.

3. The concentration of mobile dye decreases linearly with penetration into the fiber.

4. The concentration of adsorbed dye within the volume penetrated either (*a*) is constant and equal to the maximum acid-combining capacity at high concentrations, or (*b*) decreases linearly with penetration and at the surface the concentration of adsorbed dye is given by $K \cdot c$. These two possibilities will be analyzed separately.

Booth [6] shows that by making an assumption similar to 4(*a*) (*i.e.*, a high density of product) the concentration gradient with respect to the depth of penetration is linear. The rate of removal of dye from solution at any instant is given by

$$\frac{d(xV)}{dt} = D_i A \frac{c - x}{d},$$

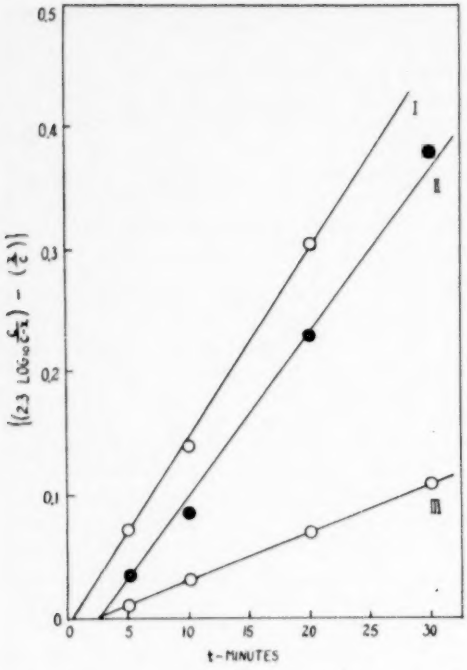

FIG. 8. *Graphs of* t *plotted against* $\left(2.3 \log_{10} \frac{c}{c-x} - \frac{x}{c}\right)$ *at 25°C, stirring the wool at 200 r.p.m., for the following dye concentrations: (I) 125 mg./l.; (II) 250 mg./l.; (III) 500 mg./l.*

where d is the distance penetrated when the initial concentration c has been reduced to $c - x$.

From assumption 4(*a*):

$$C_s = \frac{xV}{Ad},$$

so that

$$\frac{dx}{dt} = C_s D_s \frac{A^2}{V^2} \cdot \frac{c-x}{x};$$

i.e. (expression (*a*)),

$$D_s = \frac{c}{C_s}\left(\frac{V}{A}\right)^2 \cdot \frac{1}{t} \cdot \left[\log_e \frac{c}{c-x} - \frac{x}{c}\right].$$

From assumption 4(*b*), as the surface concentration of sorbed dye $= K \cdot c$,

$$\tfrac{1}{2}Kc = \frac{xV}{Ad};$$

TABLE IV. VALUES OF THE DIFFUSION COEFFICIENT CALCULATED USING THE SEMI-EMPIRICAL TREATMENT, ASSUMING DIFFUSION WITH ADSORPTION

Concentration (mg./l.)	D_s values (cm.²/sec.) (25°C)	‡(35°C)
500*	0.19×10^{-8}	0.45×10^{-8}
250*	0.25×10^{-8}	0.52×10^{-8}
125†	0.3×10^{-8}	0.65×10^{-8}
100†	0.33×10^{-8}	
75†	0.36×10^{-8}	
	$K = 4 \times 10^3$	

* Using expression (*a*).
† Using expression (*b*).

i.e.,

$$d = \frac{2xV}{KcA}.$$

Thus

$$\frac{dx}{dt} = \frac{D_s A^2 Kc}{2V^2} \cdot \frac{c-x}{x};$$

i.e. (expression (*b*)),

$$D_s\left(\frac{A^2K}{2V^2}\right) \cdot t = \left[\ln \frac{c}{c-x} - \frac{x}{c}\right]$$

or

$$KD_s = \frac{2}{t}\left(\frac{V}{A}\right)^2 \left[\ln \frac{c}{c-x} - \frac{x}{c}\right].$$

It is seen from these relationships that

1. $\left(\ln \frac{c}{c-x} - \frac{x}{c}\right) \propto t$. It should be noted that a linear plot of this type approximates a linear $\sqrt{t}$-Q_t relationship in the initial stages (see page 482).

2. The value of $t_{\frac{1}{2}}$ is independent of initial concentration in the case 4(*b*) and directly proportional to initial concentration in 4(*a*).

3. For a given concentration, $t_{\frac{1}{2}} \propto \left(\frac{V}{A}\right)^2$.

Figure 8 shows that graphs of $\log_e \frac{c}{c-x} - \frac{x}{c}$ against t are linear for most of the reaction within the 125–250 mg./l. range for high stirring rates. Moreover, it has been shown that over the concentration range 62.5–250 mg./l. of dye in solution, $t_{\frac{1}{2}}$ remains approximately constant. Thus, expression (*b*) was used to calculate values of D_s in this case (Table IV). For concentrations of 250 mg./l. and greater, $t_{\frac{1}{2}}$ increases with concentration, so that the requirements of expression (*a*) are approximately obeyed. The values of D_s calculated from this

expression for concentrations of 250 and 500 mg./l. are also included in Table IV, from which it is seen that the two sets of values agree satisfactorily. These values are much greater than those calculated assuming all the dye ions within the fiber to be mobile (see Table III).

The Diffusion Mechanism

The calculated diffusion coefficient D_s of the order of 10^{-11} cm.^{2}/sec. at 25°C appears to be exceedingly small when compared with values for other simpler ions and molecules [2, 16]. This may, of course, be due merely to the size of the dye anion, as diffusion within the solid is subject to greater restriction than aqueous diffusion, which suggests that the diffusing unit must force a path through more or less rigidly held molecules, so that a high activation energy is required. It is observed, however, that the activation energy for dyeing, where a slow-moving dye ion replaces a chloride ion which is already within the fiber, is close to corresponding values for exchange of much smaller units within the fiber. Table V summarizes the D_s values, which were calculated by using the approximate equation for diffusion from constant surface concentration, assuming a completely mobile diffusing species (*i.e.*, as for Table III), and gives calculated activation energies for the exchange of various simple ions with the bisulfite ion [16].

The apparently very low mobility of the dye ions may be due to interaction of ions with the fiber in such a way that the majority of ions within the fibers are held on specific sites; diffusion proceeds by way of a small fraction of mobile dye ions, thus giving an apparently very low value for D_s. This is the basis of the diffusion-with-adsorption theories of Standing *et al.* [45], Morton [23], Wilson [46], and Crank [10]. Here it is assumed that dye diffusing through pores containing solution is adsorbed on particular sites according to an adsorption isotherm. It is possible that application of equilibrium data in order to obtain a relationship between concentration of dye adsorbed and mobile dye during a kinetic process may not be valid, owing to the rapid adsorption of dye on available sites during a kinetic experiment with subsequent slow redistribution (leveling) in an equilibrium experiment. This two-stage process may be observed directly by taking photomicrographs [25, 33], from which it can be seen that a thick deposit of dye is confined to an outside film of the fiber during the time taken for a kinetic determination, the subsequent equilibration requiring several days. In addition, at high temperatures an even distribution of dye is obtained more readily than at lower temperatures [39], so that care should be taken in applying equilibrium data to kinetic processes of this kind.

TABLE V. RELATIONSHIP BETWEEN ANION AFFINITY AND APPARENT DIFFUSION COEFFICIENT FOR ION-EXCHANGE PROCESSES, INCLUDING DYEING

Exchange process	$D_s \times 10^6$ (cm.^{2}/sec.) (18°C)	E (0°–18°C) (kg.–cal./mole)	Anion affinity ($\Delta\mu$)*
NO_3^-—HSO_3^-	2.97	9.9	0.75
Cl^-—HSO_3^-	1.89	10.2	0
$C_6H_5SO_3^-$—HSO_3^-	0.87	12.4	0.80
$H_2PO_4^-$—HSO_3^-	0.47	14.2	0
Acid Orange 2G—Cl^-	0.005	13.0	4.0

* $\Delta\mu$ for HSO_3^- = 1.21.

The semi-empirical treatment given in the preceding section is based on the assumption that rapid adsorption occurs on specific sites, thus effectively removing dye from the sphere of diffusion. This treatment considers the diffusion front to proceed in the form of a well-defined band [13], with complete saturation with adsorbed dye of the volume penetrated at the higher concentration. It is important to note that dye concentrations of 0.25 and 0.5 g./l. correspond to final equilibrium concentrations with the fiber of only 13.5 and 27 milliequivalents/100 g., respectively. The kinetic results, however, agree with a process of diffusion from a constant surface concentration or with a process of varying surface concentration, with complete saturation within the volume that is penetrated. This is a consequence of the very high distribution coefficient between fiber and solution; thus a surface in contact with the dye remains saturated with adsorbed dye throughout most of the process.

The semi-empirical treatment and the complex treatment of Wilson [46] and Crank [9] suffer from the postulate that the concentration of *free* mobile dye within the fiber is equal to the bath concentration. This is probably not true, owing to membrane effects [24, 31, 32], although the two concentrations would be expected to vary proportionally as a first approximation. The value calculated using the semi-empirical treatment (Table IV) agrees with the value of 10^{-9} cm.^{2}/sec. at 25°C calculated by the method of Wilson [46] for the

initial stages of the process, where the theoretical and experimental curves approximately coincide (Figure 9). These values of D_i are of the same order as those obtained directly for the diffusion of simple ions within the fiber [16].

The above discussion suggests that only part of the dye within the fiber is mobile and governs the rate of diffusion. The mode of diffusion through the wool structure may occur in one of two ways. The fiber may be considered to be a homogeneous gel of relatively low water content, or a heterogeneous system of solid phase peneterated by innumerable pores of relatively large diameter, compared with molecular dimensions, which are filled with solvent which is held by capillary attraction. For a random distribution of pores with respect to the fiber axis, the measured diffusion would appear to be isotropic. Diffusion in this system would proceed via the macropores, with a velocity comparable to that in a purely aqueous phase, but it would be measurably less, owing to the small proportion of the geometrical surface area occupied by pores. The majority of dye ions would be adsorbed on the pore surface and would not participate further in the diffusion process. Several factors discount this theory. If it is true that diffusion proceeds in the aqueous medium of a macropore, it is difficult to account for the high activation energy of 13 kg.-cal./mole compared with the value of about 5 kg.-cal./mole for dyes in aqueous solution [42]. In a similar system Boyd, Adamson, and Myers [7] showed that diffusion of ions through a resin swollen to an extent similar to wool fibers is not controlled by diffusion in the macropores but by diffusion through the solid. In addition, it was shown by these workers that in order for this mechanism to hold the diffusion coefficient should vary inversely with the affinity of the ion for the fiber. It has recently been shown that for simple ions diffusing through wool fibers this condition is not satisfied (see Table V).

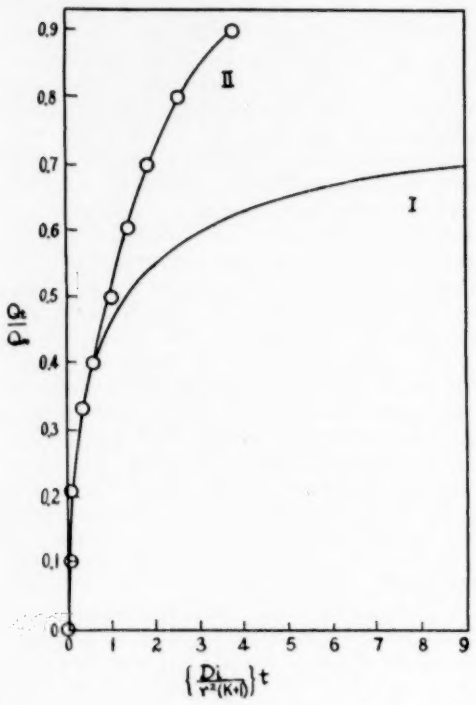

FIG. 9. *Graphs of* $\frac{Q_t}{Q_\infty}$ *plotted against* $\left(\frac{D_i}{r^2(K+1)}\right).t.$ *(I) Calculated by the method of Wilson [46]. (II) Experimental curve for 125 mg./l. at 25°C. stirring the wool at 200 r.p.m.*

The high activation energy suggests that diffusion requires deformation of the keratin structure with hole formation [29], which could be the case only if the ions diffused through pores of molecular dimension. A process of this type can hardfy be regarded as a two-phase diffusion; it becomes equivalent to a migration of ions through the swollen fiber structure, which is regarded as a uniform gel of low water content. This mechanism is also supported by the fact that very simple ions require a high activation energy, approximately 10 kg.-cal./mole [6], even though these ions are highly mobile within the fiber (see Table V).

List of Symbols

A = Surface area of 1 g. of fibers
c = Initial concentration of dye in solution
C_s = Surface concentration of dye on the fiber
d = Distance penetrated
D_i = Diffusion coefficient of dye in solution
D_a = Apparent diffusion coefficient within the fiber (all the dye considered mobile)
D_s = Internal diffusion coefficient (for diffusion with adsorption)
δ = Thickness of diffusion layer in solution at fiber surface
E = Activation energy
k = First-order velocity constant

K = Distribution coefficient of dye in the fiber and in solution
K' = Quantity of solute in solution divided by the quantity of solute adsorbed at equilibrium
Q_t = Quantity of dye adsorbed at time t
Q_∞ = Total quantity of dye adsorbed at infinity
r = Fiber radius
t = Time
$t_{\frac{1}{2}}$ = Half-life period
T = Temperature
V = Volume of solution in contact with 1 g. of fibers
x = Change in concentration in solution after time t
$\Delta\mu$ = Relative anion affinity [11]

Acknowledgment

The authors wish to thank the Messrs. Wolsey Ltd., Leicester, for financial support which made this investigation possible, and Prof. H. V. A. Briscoe for his help and interest.

Literature Cited

1. Agar, J. N., *Faraday Society Discussion No. 1*, 1947, p. 26.
2. Alexander, P., Hudson, R. F., and Gough, D., *Trans. Faraday Soc.* **45**, 1058, 1109 (1949).
3. Alexander, P., and Hudson, R. F., *J. Phys. Chem.* **53**, 733 (1949).
4. Barrer, R. M., "Diffusion In and Through Solids," London, Cambridge University Press, 1941.
5. Barrer, R. M., *Trans. Faraday Soc.* **45**, 358 (1949).
6. Booth, F., *Trans. Faraday Soc.* **44**, 796 (1948).
7. Boyd, G. E., Adamson, A. W., and Myers, L. S., *J. Am. Chem. Soc.* **69**, 2836 (1947).
8. Carslaw, H. S., and Jaeger, J. C., "Conduction of Heat in Solids," Oxford University Press, 1947.
9. Crank, J., *Phil. Mag.* **39**, 140 (1948).
10. Crank, J., *J. Soc. Dyers and Colourists* **64**, 386 (1948).
11. Gilbert, G. A., *Proc. Roy. Soc.* **183A**, 167 (1944).
12. Hanson, J., Neale, S. M., and Stringfellow, W. A., *Trans. Faraday Soc.* **31**, 1718 (1935).
13. Hermans, P. H., *J. Colloid Sci.* **2**, 387 (1947).
14. Hill, A. V., *Proc. Roy. Soc.* **104B**, 39 (1929).
15. Hixson, A. W., and Crowell, J. H., *Ind. Eng. Chem.* **23**, 1160 (1931).
16. Hudson, R. F., and Schmeidler, G. A., *J. Phys. Chem.* **54** (1950) (in press).
17. King, C. V., and Schack, M., *J. Am. Chem. Soc.* **57**, 1212 (1935).
18. King, C. V., and Bravermann, M. N., *J. Am. Chem. Soc.* **54**, 1744 (1932).
19. Kunin, R., and Myers, R. J., *J. Phys. Chem.* **51**, 1111 (1947).
20. Lemin, D. R., and Vickerstaff, T., in "Symposium on Fibrous Proteins," Bradford, England, Soc. Dyers and Colourists, 1946, p. 129.
21. Lemin, D. R., and Vickerstaff, T., in "Symposium on Recent Advances in the Theory and Practice of Dyeing," Bradford, England, Soc. Dyers and Colourists, 1947, p. 32.
22. Levich, B., *Faraday Discussion No. 1*, 1947, p. 37.
23. Morton, T. H., *Trans. Faraday Soc.* **31**, 262, 283 (1935).
24. Morton, T. H., in "Symposium on Fibrous Proteins," Bradford, England, Soc. Dyers and Colourists, 1946, p. 155.
25. Morton, T. H., *Textil-Rundschau* **4**, 39 (1949).
26. Mott, N. F., and Gurnay, R. W., "Electronic Processes in Ionic Crystals," Oxford University Press, 1940, Chap. VIII.
27. Neale, S. M., and Stringfellow, W. A., *Trans. Faraday Soc.* **29**, 1167 (1933).
28. Neale, S. M., *Trans. Faraday Soc.* **31**, 282 (1935).
29. Neale, S. M., *Trans. Faraday Soc.* **44**, 1027 (1949).
30. Paterson, S., *Proc. Phys. Soc.* **59**, 50 (1947).
31. Peters, L., and Speakman, J. B., *J. Soc. Dyers and Colourists* **65**, 63 (1949).
32. Proctor, H. R., and Wilson, J. A., *J. Chem. Soc.* **109**, 307 (1916).
33. Royer, G. L., Fiddel, L. I., and Millson, H. E., *Am. Dyestuff Reptr.* **37**, 116 (1948).
34. Steinhardt, J., and Harris, M., *J. Research Natl. Bur. Standards* **24**, 335 (1940).
35. Steinhardt, J., Fuggit, C. H., and Harris, M., *J. Research Natl. Bur. Standards* **25**, 293 (1941); **29**, 417 (1945).
36. Speakman, J. B., *Proc. Roy. Soc.* **132A**, 167 (1931); *Trans. Faraday Soc.* **29**, 148 (1933).
37. Speakman, J. B., and Clegg, H., *J. Soc. Dyers and Colourists* **50**, 348 (1934).
38. Speakman, J. B., and Elliott, G. H., in "Symposium on Fibrous Proteins," Bradford, England, Soc. Dyers and Colourists, 1946, p. 116.
39. Speakman, J. B., and Smith, S. G., *J. Soc. Dyers and Colourists* **52**, 121 (1936).
40. Speakman, J. B., and Stott, E., *Trans. Faraday Soc.* **30**, 539 (1934); **31**, 1428 (1935).
41. Valko, E., *Trans. Faraday Soc.* **31**, 278 (1935).
42. Valko, E., *J. Soc. Dyers and Colourists* **55**, 173 (1939).
43. Vreedenberg, H. A., *Rec. trav. chim.* **67**, 839 (1948).
44. Wagner, C., and Grunewald, K., *Z. physik. Chem., B*, **40**, 455 (1938).
45. Willis, H. F., Warwicker, J. O., Standing, H. A., and Urquhart, A. R., *Trans. Faraday Soc.* **41**, 506 (1945).
46. Wilson, A. H., *Phil. Mag.* **39**, 48 (1948).

(*Manuscript received March 17, 1950.*)

INDUSTRIAL SECTION

Gloss Measurements on Fabrics*

Richard G. Quynn,† Edwin J. Bernet, and Earl K. Fischer‡

Contribution from Institute of Textile Technology, Charlottesville, Virginia

Abstract

The gloss or luster of a surface is essentially a subjectively evaluated property which is related to the manner in which the surface reflects light falling on it. Although the impression or sensation of glossiness is a matter of common experience, measurement of this property in physical terms and correlation of the measurements with its psychological aspects are extremely difficult. The most satisfactory physical measurement involves the use of a goniophotometer, an instrument which measures the amount of light reflected from a surface at various angles. Curves showing intensity of reflected light *vs.* the scanning angle exhibit a peak at the so-called specular angle for surfaces rated as being of high gloss. Surfaces of more complex structure, such as those of fabrics, show a displacement of maximum reflectance from the specular angle; the displacement is related to the angle of the incident light. The curve shape is characteristic for different fabrics.

This article describes the experimental measurement of reflectance by means of a goniophotometer for a group of fabrics. The results are presented in the form of curves, computed "gloss indexes" or "gloss numbers," and visual ratings by different observers.

Introduction

Certain fabrics have long been noted for their lustrous or glossy appearance, and their esthetic appeal and consequent economic value depend in large measure upon the consumer's evaluation of this property. A reliable and convenient measure of the reflectance of light from fabric surfaces would place the rating of gloss or luster on an impersonal or objective basis. Although studies of this kind have been made in the paper and paint industries, relatively little attention has been given to measurement of the gloss characteristics of textile materials. The objectives of the work described in this paper were: (1) to survey the capabilities of the instruments described in the literature; (2) to devise a simple goniophotometer of precision adequate for measurements on fabrics; (3) to examine photometrically a representative group of fabrics and to express their reflectance characteristics in a suitable record form; and (4) to determine to what extent the instrumental data could be correlated with visual ratings.

Gloss is generally regarded as a property of the surface which is related to its ability to reflect light specularly—*i.e.*, such that the angle of reflection equals the angle of incidence. On most gloss scales the "perfect" mirror is assigned the highest gloss value, since such a mirror theoretically reflects all of the light incident upon it in the manner prescribed by the law of regular reflection. Thus, a perfect mirror illuminated by a single "point" source of light

* This paper is based on a thesis submitted to the Institute of Textile Technology by Richard G. Quynn in partial fulfillment of the requirements for the degree of Master of Science. Presented at the 27th meeting of the Virginia Academy of Science, Richmond, Virginia, May 6, 1949.

† Present address: Textile Research Institute, Princeton, N.J.

‡ Present address: National Bureau of Standards, Washington 25, D. C.

appears bright for only a single direction of viewing (the specular angle) and shows no brightness for all other directions. The lowest gloss value is ordinarily assigned to the perfect matte surface, defined as one which reflects incident light in such a way that the brightness of the surface is the same for all directions of viewing and independent of the angle of incidence. A perfect matte surface is said to reflect light "diffusely," but it is important to understand that diffuse reflection is not a special type of reflection: a matte surface reflects light according to the same laws that govern specular reflection, and "diffuse" is only a term used to indicate that the surface is optically so irregular that reflected light leaves it in all possible directions.

All materials lie between the limits of a perfect mirror and a perfect matte surface, and one must commonly deal with surfaces with reflective properties intermediate between those of "ideal" surfaces. The gloss of actual surfaces is then determined in a general way by how much light they reflect "specularly" and how much they reflect "diffusely." Such a distinction, as will be seen later, is possible only in the case of certain surfaces near the upper end of the gloss scale—*e.g.*, polished metals—, and attempts to analyze light reflected from surfaces of low gloss into specularly reflected and diffusely reflected components meet with no success.

There is another aspect of gloss the importance of which, as far as the present investigations are concerned, is perhaps as great as the "physical" interpretation of gloss which has hitherto been considered. When an observer estimates the gloss of a surface by visual inspection, the sensation which he receives (described as "gloss," "sheen," "luster," or in other terms) is the result of the composite impression upon his receptor system of the scattered light as a whole: upon holding the surface to the light and rotating it about an axis in its plane, the observer notes the appearance of the sample not only at the specular angle, at which he perceives a flash of light, but at the other angles as well; he bases his estimate of gloss upon the appearance of the sample at all angles of observation. It is by no means clear that the process by which the observer arrives at his estimate is a physical one; nevertheless, a review of the literature on gloss reveals that a large number of investigations have been undertaken in which physical measurements of gloss have been made, and the results of these measurements compared with visual gloss, no allowance being made for psychological and physiological factors, which have the utmost importance in visual observation.

One purpose of the present investigations was to attempt a correlation of "objective" measurements with visual or "subjective" estimates of gloss; the extent to which physical measurements can be compared with visual sensations is a matter of the greatest complexity. A buyer who is seeking a fabric with, say, high gloss will base his choice upon what he sees, and not upon what he is told. If the physical indication of gloss disagrees with the buyer's estimate, the physicist's ratings will be held suspect.

In the sense in which the term will be used here, then, gloss is a visual sensation: it is not a property capable of direct instrumental measurement as temperature or length is. That this conception of gloss as essentially subjective in nature greatly increases the difficulties in its physical interpretation is indisputable, but we must not be led to believe that gloss in this sense is any less "real" than some physical characteristic of a surface which we might choose to denote by the term "gloss." Harrison [15] declares that any fancied "unreality" of gloss is simply a result of our present ignorance about its nature and our failure to measure it adequately.

The degree of precision adopted in the gloss measurements reported in this paper has been largely governed by the belief that the sacrifice to convenience and simplicity of measurement which more refined procedures would involve is not worth the usefulness of the greater precision. Refined measurements may, of course, be necessary when the data are to be used, for example, to keep strict control over a manufactured product. The connection between visual estimates and instrument readings in gloss work is at present one of only the loosest sort, and it is a matter of common experience that the eye judges gloss in only an approximate way. We are interested chiefly in the relative magnitudes and gross features of surface reflection, and the connection these have with visual estimates.

It should be noted that the physical properties of the materials studied in this work are essentially surface properties. We have not been concerned with bulk properties such as transmittance or index of refraction, except as these properties might affect incident light by internal reflection or multiple refraction so as to effect its re-emergence at the surface and hence its contribution to the gloss characteristics of the material.

Methods of Measurement

In the past the procedure for specifying the gloss of a certain material has been generally this: the material has been subjected to some physical measurement (usually, but not always, involving the intensity of reflected light) and the gloss of the material then has been expressed in terms of some combination of the measurements. In most cases the gloss values obtained have been functions of the manner in which the measurements have been made, and it is not surprising to find in the literature gloss values of comparable materials which do not agree, even when the various investigators used the same gloss scale. Not only do different instruments disagree on the numerical value of gloss, but they often disagree on the order in which samples of varying degrees of gloss are to be ranked; in other words, various instruments do not always agree upon which of two samples is the "glossier." The main reason for confusion in interpretation of data and nonstandardization of instruments is simply that no complete agreement has been reached upon what the term gloss shall denote physically, much less psychologically. The American Society for Testing Materials has made some progress in the matter of standardization of instruments and units, but only for one type of surface—namely, paint finishes [4].

The complete physical measurement of gloss involves essentially the measurement of the intensity of light reflected at all possible angles from the material under consideration; physical description of the reflecting properties of the surface could in theory be presented in terms of spherical coordinates, the origin of the radius vector being the point at which a single incident beam struck the surface. The mechanical difficulties involved in such a complete specification of gloss are prohibitive, and the usual practice is to consider only the reflections which are in the plane containing the incident ray and the normal to the surface. This method of gloss measurement is called goniophotometry (Greek: *gonio-*, angle), and it is the method which has been adopted in the present work. Goniophotometric results may be presented on rectangular coordinates or by a polar diagram in which the length of the radius vector is proportional to the intensity of light reflected at any given angle. Attention should be called to the optical convention of measuring angles in the direction from the normal to the surface. Although this convention has not been adopted in the experimental work reported in this paper, previous work in gloss is so expressed unless otherwise stated.

Harrison [15] has compiled an excellent survey of the literature. In his book all pertinent papers on gloss from about 1750 to 1945, with but few omissions, receive critical attention. Hunter has published several bibliographies on gloss [20, 21]. The photometric concepts and nomenclature which form the basis of all gloss measurement have been summarized by McNicholas [38, 39] and Moon [41]. Useful reports on instrumentation have been prepared by The Institute of Paper Chemistry [27–30]. Adderley [1] has presented a survey of the physical causes of luster in cotton. A short discussion of physical and psychological problems of gloss measurement has recently been given by Smith [55]. Derrett-Smith [11] has described glossmeters which have been used in routine textile work. Buck and McCord [9] have recently published a comprehensive survey of the luster of cotton and have appended an extensive bibliography.

It will be convenient to divide the attempts at practical gloss measurement into five sections according to the method employed; single-angle viewing methods, two-angle viewing methods, goniophotometric methods, polarization methods, and special methods.

Single-Angle Viewing Methods

In the single-angle viewing method, as the name indicates, the sample to be investigated is illuminated by a collimated beam at a fixed angle, and light reflected from the sample is measured by a receptor which is also at a fixed angle with respect to the sample, usually the specular angle. Various angles of incidence have been used, but 45 degrees seems to be the most frequent choice. This type of instrument has been used widely in routine control measurements, and has been applied to a variety of surfaces, including textile fabrics [14], paint panels [17], and asphaltic bitumen [5].

In Pfund's instrument [45] the angles of incidence and viewing may be varied, but in such a way that the two are always equal. Specular reflection is all that is considered, and the test object is given a cylindrical form in order to suppress diffuse reflection. The receptor is a small optical pyrometer, and the arbitrarily chosen gloss standard is a highly polished cylinder of soda glass, blackened on its inner surface. Measurements are expressed in terms of "objective gloss," defined as the ratio of the intensity of light

reflected specularly from the material in question, at a specific angle of incidence, to the intensity of light reflected specularly from a perfectly polished surface of the same material at the same angle of incidence. Pfund recommends for his instrument an incident angle of about 75 degrees for most surfaces, 5 degrees for very high-gloss surfaces, and 85 degrees for very matte surfaces.

The Pfund glossmeter has been applied to the measurement of "objective gloss" of paints and lacquers by Haslam and Grady [17]. A Salford Electrical Instruments, Ltd., [51] phototube device was first placed over a standard white surface such as magnesium oxide and then placed over the sample; the difference in phototube readings was taken as a measure of gloss. Derrett-Smith [11] has described a photometric method for routine gloss measurements of textile materials in which brightness of the surface is compared simultaneously with that of a standard lamp. The Photovolt Corporation [46] and the Henry A. Gardner Laboratory, Inc., [13] have offered commercial instruments which measure specular reflectance for an incident angle of 60 degrees.

Two-Angle Viewing Methods

This method of measurement consists of illumination of the sample at a fixed angle and measurement of the light reflected at two angles of viewing, one of which is usually the specular angle. The gloss value of the sample is often expressed as the difference between or ratio of the two measurements, or as a combination of these with the measurement of some standard surface.

Schulz [52] has described a glossmeter made by Goerz. This instrument consists of two totally internally reflecting prisms which are arranged so that the intensities of light reflected at the specular angle and light reflected at 90 degrees from the specular angle are viewed in the head of a comparison photometer. The angle of incidence is not stated. Schulz computed a gloss number from the photometric measurements, and then used the logarithm of this number as a measure of visual sensation; the logarithm is used as a consequence of the rather questionable Weber-Fechner law, which states that differences in brightness as judged by the eye are proportional to the logarithms of the intensities of light reflected in the two cases.

In the method of Klughardt [35], the sample is illuminated at an angle of 45 degrees and its brightness determined, when viewed normally, by comparison with a baryta white (barium oxide) standard; the sample is then tilted in 5-degree steps, and its brightness measured in each position against the standard. Klughardt, who has given considerable attention to the theoretical aspects of gloss measurement, expresses his "gloss number," γ, as follows:

$$\gamma = \frac{H' - H}{H_o}, \qquad (1)$$

where H_o is the brightness of the sample in the initial (horizontal) position, H' is the brightness in the tilted position, and H is a theoretical quantity which can be computed from Lambert's law * in the manner shown [35] and which corresponds to the reading which would have been obtained from an ideal matte surface at the given angle of tilt, having a brightness H_o in the horizontal position. Values of γ are presented for various angles of tilt for a series of gray paper samples. In another paper [36], Klughardt notes that rotation of a textile fabric in its own plane influences the brightness and hence the gloss number, but he gives no data.

Desbleds [12] has described a glossmeter for textile materials in which reflectance is measured at the specular angle and at another angle displaced a few degrees from the specular angle, the difference in the two values being taken as a measure of gloss.

Goniophotometric Methods

Jones [32] may be regarded as having established the basis for the goniophotometric method of gloss measurement, which involves illumination of the sample at some fixed angle and measurement of the intensity of light reflected from the sample as a function of the viewing angle. As a result of an investigation of the gloss characteristics of photographic papers, Jones concluded that the most favorable and comfortable conditions for viewing photographic papers are obtained when the line of sight is normal to the surface and the illumination is incident at approximately 45 degrees. He showed quantitatively that use of collimated illumination provides a more extended gloss scale, thereby permitting measurement of smaller differences in gloss than would be possible when the source subtends a larger angle.

* Lambert's law, which is frequently used in gloss measurements, states that the intensity of light from a surface element of a diffuse radiator or reflector is proportional to the cosine of the angle between the direction of emission and the normal to the surface.

Curves for matte, semimatte, semiglossy, and glossy photographic papers are presented which correspond to collimated illumination normal to the surface. Jones has pointed out the necessity for care in mounting the samples, and states that variations in planeness of the samples seriously affect gloss values, particularly those of high-gloss specimens, a conclusion that Harrison [15] has reached by mathematical analysis. Shook [53] has used a modification of Jones' apparatus, in which the specimen is illuminated at 45 degrees; the relative brightness at 45 degrees and at 0 degrees is taken as an indication of gloss.

Barratt [7] has utilized a simple goniophotometer in a study of the luster of fibers, threads, and fabrics produced by mercerization. Reflectance is measured as a function of incident angle for a fixed viewing angle of 67.5 degrees. The same procedure is followed in the method of Adderley and Oxley [2], but a viewing angle of 45 degrees is maintained. Naumann [44] has studied gloss properties of textile fabrics with a goniophotometer based on Klughardt's work.

A Gaertner student spectrometer has been adapted to goniophotometry by Wetlaufer and Scott [59]. They have investigated a variety of high-gloss paint panels, and state that good correlation with visual gradings has been obtained. Murty [42] has presented curves for various photographic papers, in which relative reflectance is expressed as a function of viewing angle for an incident angle of 45 degrees.

A novel goniophotometric method has been devised by Preston [47]. In his apparatus a photographic film is mounted in a cylindrical frame about the sample, thereby allowing simultaneous recording of reflections at all angles. The angle of incidence is 45 degrees. Preston discusses the luster of textile materials, and points out that the luster of fabrics is a more complicated phenomenon than that of individual fibers, the luster of fabrics being affected by the original luster of the fibers, the structure of the yarn and of the fabric, and by the mechanical finishing operations—*e.g.*, schreinering. Slater [54] has used a photographic method similar to that of Preston.

Moon and Laurence [40] have described the construction and testing of an elaborate research goniophotometer which is power-driven and which records automatically. A direct-vision photometer has been used by Benford and Ruggles [8] for measuring the reflective properties of metal mirrors at various angles of incidence and reflection. Harrison [16] has recently made a careful comparison of several commercial instruments with respect to agreement of results with visual estimates. As a result of work with a series of nine printing papers, he concludes that the most satisfactory correlation is obtained by measurements of the intensity of light reflected when angles of incidence and viewing are 45 degrees.

The method of Ransom and Edelstein [49] involves motion of the light source rather than of the receptor about the sample and a fixed viewing angle of 45 degrees. A few data are given for yarns and for one fabric. A commercial goniophotometer known as the Aminco-Scott Glossmeter was at one time available from the American Instrument Company [3].

Polarization Methods

It is well known that light reflected from many nonmetallic surfaces is polarized, the extent of polarization depending upon the angle of the incident (unpolarized) beam and the refractive index of the surface [31, 50]; this dependency forms the basis of the polarization method of gloss measurement. For glass there is one angle of incidence—namely, 57.5 degrees—at which polarization is practically complete —*i.e.*, for which the reflected beam is almost wholly plane-polarized. For other substances there is always an angle of maximum polarization, i, given by Brewster's law:

$$\tan i = n, \qquad (2)$$

n being the refractive index of the material.

Ingersoll [25] found experimentally that 57.5 degrees was also the polarizing angle for paper. A modified form of his instrument, known as the Glarimeter [26], measures gloss in terms of the fraction which is polarized of the intensity of light reflected at 57.5 degrees, this angle also being the incident angle. Ingersoll expresses gloss values simply by readings on the circular scale which is associated with the rotating Nicol prism which is used in polarization measurements.

Horsfield [18] has patented a polarization type of glossmeter. Laurence [37] has investigated the polarizing action of paper, several worsted fabrics, and one metallic surface; he finds that dark worsteds cause little depolarization, whereas light worsteds depolarize almost completely. Schulz, an early

worker in gloss, has stated that polarization methods are inadequate for gloss specification of fabrics, since the angle of maximum polarization is not constant over the fabric surface [52].

Special Methods

Hunter [20] has distinguished six types of gloss according to visual characteristics: "specular gloss," which is largely the property of shininess exhibited by high-gloss surfaces; "sheen," which corresponds to surface shininess apparent at grazing angles of incidence and viewing; "contrast gloss," which is identified by contrasts in brightness between specularly reflecting areas of the surface and other areas; "absence-of-bloom gloss," which is characterized by freedom from reflection haze or smear adjacent to reflected highlights; "distinctness-of-image gloss," identified by the distinctness or sharpness of images reflected in the surface; and "absence-of-surface-texture gloss," which appears as a lack of surface texture and surface blemishes. Judd [33] has attempted more precise definitions of five of these gloss types.

In an effort to analyze "distinctness-of-image gloss," Hunter [19] has adopted the following empirical procedure: a target pattern is mounted on the face of a goosenecked desk lamp which illuminates test paint panels at an angle of approximately 45 degrees. A photograph of the panels is taken by a camera mounted at about the same angle to the test surfaces. The target pattern is a photographic negative consisting of concentric rings which vary from fine lines to wide bands, and the narrowest lines which are perceptible after reflection from a surface are used as the criterion of the "distinctness-of-image gloss" of that surface. Hunter concludes from a study of paint panels that reflected images become more distinct as the viewing angle approaches grazing angles, and therefore that many very flat, matte surfaces reflect distinguishable images at near-grazing incidence; this behavior has been recognized in the paint industry for some time.

A modification of Hunter's "distinctness-of-image gloss" procedure has been used by Myers [43]. Vernon [58] has employed reflectance measurements to investigate tarnishing of metal surfaces under various atmospheric conditions. A glossmeter for the comparison of smoothness of machine-finished surfaces has been described by Hunter [24], who has also designed a photoelectric reflectometer [21]; the latter instrument has been evaluated by The Institute of Paper Chemistry [30]. In another paper [23], Hunter reviewed gloss problems in connection with camouflage paints; this paper also contains a comparison of several commercial instruments according to the A.S.T.M. specifications for specular gloss of paint finishes [4].

Bancroft and Allen [6] have examined the psychophysical aspects of metallic luster. The preparation of reproducible gloss standards has been discussed recently by Smith and Mahoney [56, 57]. McNicholas [39] has used a specially designed sphere reflectometer in a general study of goniophotometry. Judd [34] and Hunter [22] have commented upon optical and geometrical specifications in the definitions of specular and contrast gloss. Dench [10] has devised a goniophotometer in which the sample is rotated in synchronization with the sweep circuit of an oscilloscope.

Numerical Gloss Specification

As the literature survey indicates, numerical gloss specification has taken many forms, depending upon the method of measurement employed, the gloss standard adopted, and the use for which the specification was intended. It will be convenient to generalize some of the more widely used expressions by disregarding the types of receptor (photometer, barrier-layer cell, vacuum or gas phototube, etc.), the particular illuminants, and the detailed geometry of the various measurements. If we let G_i be the numerical gloss value corresponding to some fixed angle of incidence or illumination i, S_i be the intensity of reflected light measured at the corresponding specular angle i, and D_r be the intensity of reflected light measured at some other "diffuse" viewing angle r, then representative, simple gloss values may be expressed as follows:

$$G_i = S_i, \tag{3}$$

$$G_i = \frac{S_i}{D_r}, \tag{4}$$

$$G_i = S_i - D_r, \tag{5}$$

$$G_i = \frac{S_i - D_r}{D_r}, \tag{6}$$

where all angles are measured from the normal. These expressions will be used later for computation of gloss numbers from the experimental data.

Comments upon Various Methods

If it is taken as a working hypothesis that visual perception of the gloss of a surface is largely a function of the reflective properties of the surface, it is clear that reflectance measurements at single or limited angles of illumination and viewing afford only restricted knowledge of the gloss properties of the surface. The usefulness of the reflectance value at a single angle of viewing, for instance, decreases as the surface tends less and less to reflect preferentially at this angle. More precisely, the validity of a numerical gloss value based upon measurement at a single angle of viewing (for a given incident angle) is greatest when the reflectance angle *vs.* viewing angle curve of the surface exhibits a sharp peak at this single angle, and decreases as the curve broadens out, so far as gloss specification of the entire surface is concerned; in any case, measurement of specular reflectance alone leaves the shape of the remainder of the curve quite indefinite. We may thus conclude that single-angle and two-angle viewing methods are satisfactory only when the surfaces examined exhibit a fairly well-defined specular reflectance; such surfaces are generally those which would be near the top of a visual gloss scale. This conclusion has been reached by many investigators [11, 15, 20, 36], the most notable exception being The Institute of Paper Chemistry, which in an early report [27] recommended a fixed-angle instrument, for paper surfaces at least. Single-angle instruments are useful for certain restricted purposes, of course, and they have the advantages of simplicity and speed of operation.

Polarization methods of measurement, although valuable as a means for investigation of a particular surface property, suffer from the disadvantage that the state of polarization of a reflected light beam has no necessary connection with the visual gloss sensation. The eye cannot distinguish degree of polarization, and it is not clear to what extent the changes in the state of polarization correspond to degrees of gloss as perceived by the eye [15].

Hunter's "distinctness-of-image gloss" procedure has definite advantages in the case of surfaces which are smooth and glossy enough to reflect distinguishable images; textile fabrics (even the glossiest ones), however, simply do not reflect distinguishable images, and yet they display distinct differences in luster. Empirical methods such as these nevertheless have considerable usefulness, as is evidenced by their rather widespread acceptance in certain industries.

Goniophotometry thus appears to be the most satisfactory physical method of gloss measurement; it does not involve the assumption that maximum reflection occurs at the specular angle, it yields reflectance values not only at the specular angle but at all other angles as well, thereby determining the shape as well as the peak value of the reflectance curve, and from the results may be computed the various gloss ratios and indexes determined by fixed-angle instruments. Measurements at various angles of illumination also provide a means for determining the illuminating angle at which correlation of reflectances with visual gloss ratings is most satisfactory.

Instrument Design

A goniophotometer was designed and constructed for the experimental work described in this paper. It was intended that the instrument meet the following requirements: (1) that it afford precise measurements of the intensity of light reflected from textile fabrics at various angles of viewing for various incident angles; (2) that it be relatively inexpensive, flexible, convenient to operate, and capable of giving reproducible results with minimum adjustments; (3) that its optical and geometrical system be simple and easy to construct; (4) that its receptor response to color approximate that of the human eye and be approximately linear over the range of light intensities encountered; (5) that it form the basis for an instrument which could be applied readily to control work in various operations of the textile industry—*e.g.*, finishing.

Mechanical System

A schematic view of the instrument is shown in Figure 1; this diagram is a top view, and the scale

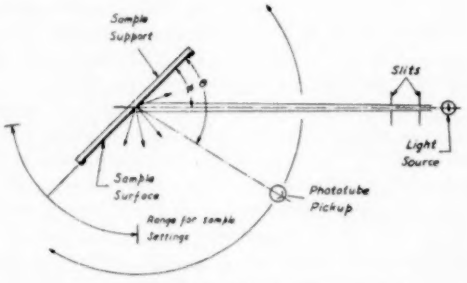

FIG. 1. *Diagram showing geometry of goniophotometer.*

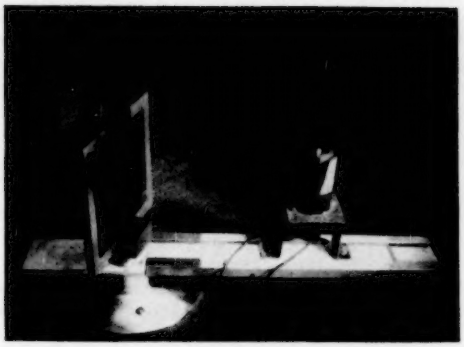

FIG. 2. *View of goniophotometer showing sample holder, phototube mounted on supporting arm, and bearing.*

is somewhat distorted. Light from a source of constant intensity passes through two slits (which collimate and at the same time reduce the intensity of the beam) and falls on the fabric sample; the sample is mounted in such a way that it can rotate about an axis perpendicular to the plane of the paper and can be oriented at any angle ϕ with respect to the incident beam. A phototube (one component of an electrical circuit) is mounted on an arm which rotates about the sample in such a way that the phototube can record the intensity of light reflected at any angle θ with respect to the sample, except in the vicinity of the angle of incidence (where the phototube would block out the incident light). Sample and receptor are both enclosed in a light-tight housing. Figure 2 shows the essential parts of the instrument: the sample holder, the phototube mounted on its arm, and the bearing by which rotation about a common axis is accomplished. These design features can be seen in detail in Figure 3, which is a side-view diagram drawn to scale, with the goniophotometer bearing shown in cross section for greater clarity.

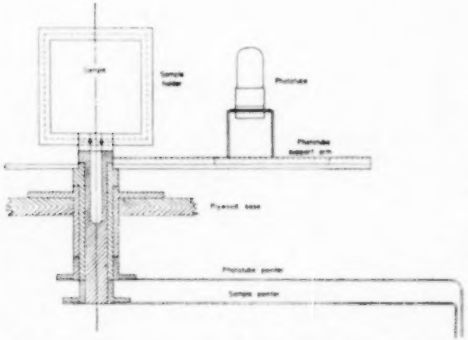

FIG. 3. *Diagram showing essential design features of goniophotometer including central sleeve bearing, support for phototube, sample holder, and pointers.*

Machined from solid brass stock, the bearing consists of a central cylindrical shaft 6½ in. long, about which a system of sleeves rotates. The central axis of this shaft is the axis of rotation of all the movable parts of the bearing, sample holder, and phototube arm. The phototube arm is rigidly attached to the upper end of the long, innermost sleeve, and to the lower end of this sleeve is set-screwed a smaller sleeve which carries a brass pointer. To the lower end of the central shaft is set-screwed another sleeve which carries the pointer for the sample. The phototube pointer and the sample pointer indicate respectively the angles θ and ϕ (of Figure 1) on a circular scale which is mounted horizontally beneath the bearing. The whole bearing assembly is supported by the outermost upper sleeve, which is rigidly attached to a plywood base.

The sample holder consists of a brass frame 5 in. by 5 in., the base of which is a brass block which fits into a 3-in.-deep hole drilled into the center of the bearing. The metal frame of the sample holder reduces the exposed area of the sample to 4 in. by 4 in., and is so constructed that when the fabric sample is inserted in place the front face of the sample coincides with the plane of the axis of rotation. Fabric samples are mounted on Bristol board, inserted in place, and backed up by a fiberboard sheet which is fastened securely by clips on the back of the holder.

The phototube arm, constructed from $\frac{3}{16}$-in. aluminum, is 16 in. by 2 in. in over-all dimensions. The side carrying the phototube measures 12 in. from the axis of rotation, the other 4 in. providing space for any necessary counterweights. On the long side of the arm are mounted $\frac{1}{16}$-in. brass "L" bars which serve as ways along which the phototube support may slide; the latter is constructed from sheet steel and is rigidly attached to a polystyrene block which slides lengthwise along the phototube arm.

The two pointers, constructed from sheet brass, extend roughly 16 in. from the axis of rotation; they are bent down as shown in Figure 3 in order to meet a circular scale of approximately 16 in. in radius. The circular scale, which is ruled in degrees from

0 to 360, is attached with photographic dry mounting tissue to a lower plywood base. Angular measurements can be made to within ± 0.5 degree.

Optical System

It has long been recognized that goniophotometric measurements are functions of the geometry of the optical system under which they are carried out, and much of the disagreement in gloss values determined by various instruments can be traced to nonuniformity in geometrical arrangement [23]. Construction of any goniophotometer necessitates fixing of some geometrical system, and realization of the fact that measurements may be varied by changing this system. Conflicting requirements in this work were the greatest possible collimation of the incident beam, the greatest possible resolution, and the necessity for illumination of the sample sufficient to activate the phototube. ("Resolution" means here the narrowness of illumination at the sample face.) When it is realized that the incident beam (and hence the illumination at the sample) and also the surface of the phototube cathode have finite dimensions, reference to Figure 1 will show that a reflectance measurement at some angle θ can be the result of reflection of light not only from the single, central point of incidence but also from points to either side, provided that reflected rays from these points are directed toward the receptor surface. The situation cannot be otherwise, since it is, of course, impossible to construct a phototube with an infinitely narrow sensitive surface, or a light source which will illuminate an infinitely narrow portion of the sample.

The optical system of the goniophotometer consists of the light source, its housing, and two narrow slits. The positions of these elements with respect to one another can be seen in Figure 4, which is drawn approximately to scale.

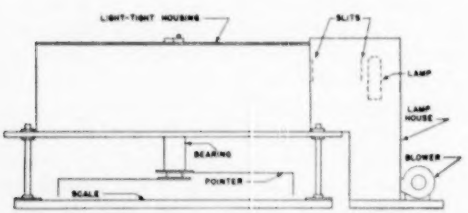

FIG. 4. *Diagram of exterior of goniophotometer.*

It was necessary in the present work to obtain the greatest possible degree of collimation consistent with the requirements that the patch of light at the sample face be narrow, intense, equally bright over its area, and sharp—*i.e.*, have no "fuzzy" edges. Considerable experimentation was carried out before it was decided that a double-slit system met these requirements more completely than any lens or lens-slit system which could be devised. The essential dimensions of the system adopted were as follows:

Distance from lamp filament to source slit: 5.2 cm.
Distance from source slit to second slit: 9.7 cm.
Distance from second slit to sample face: 33.0 cm.
Distance from sample face to receptor surface: 10.0 cm.
Height and width of source slit: 2.0 cm. × 0.2 cm.
Height and width of second slit: 1.5 cm. × 0.3 cm.
Height and width of sample illumination: 12.0 cm. × 2.0 cm.
Height and width of receptor surface: 2.1 cm. × 1.6 cm.

(By "source slit" is meant the slit nearest the light source.) These dimensions result in a divergence of the incident beam of 1 degree 30 minutes—*i.e.*, the angle between either outermost ray (see Figure 1) and the horizontal is this amount, the origin being taken at the second slit. Dimensions of the receptor surface are, of course, fixed by the phototube manufacturers.

The light source employed is a 750-watt, 115-volt Mazda projection lamp with bayonet base. The lamp is mounted in a housing constructed for this work and supplied with a spherical reflector and holder for the source slit. Voltage at the lamp terminals is held at 115 volts A.C. through a Sola Constant Voltage Transformer. The lamp is oriented so that the plane of its filaments coincides with the plane of propagation. Because of its high wattage, the lamp requires considerable cooling, and this is provided by a blower which is mounted beneath the open housing.

The source slit was constructed by soldering two razor-blade halves to a brass frame. Construction of this slit from metal was dictated by its proximity to the heated lamp. The second slit, cut from smooth Bristol board, is mounted on the side of the light-tight housing which surrounds the apparatus and may be seen to the right in Figure 2. Dimensions of this slit determine the dimensions of the il-

luminated portion of the sample—12.0 cm. × 2.0 cm. Both slits are mounted with their longer sides vertical, thus effecting a long, rectangular patch of light at the face of the sample.

The light-tight housing consists of a plywood box which is hinged at the top and which is painted on its inner surface with a very flat black paint.

Electrical Circuit

The receptor, chosen after considerable experimentation with vacuum phototubes, gas phototubes, and barrier-layer cells, is an RCA 929 vacuum phototube. Vacuum-type phototubes, generally speaking, have higher internal resistances, more constant sensitivity, and less susceptibility to damage by accidental operation than gas types, and are therefore preferable for many light-measurement applications. The Weston Photronic cell, although possessing a spectral response curve more nearly like that of the human eye (when equipped with the Weston Viscor filter), was discarded in favor of the 929 tube because of the extremely low output current of the former; use of the Photronic cell over the range of light intensities encountered would have required more elaborate electrical apparatus than was thought suitable for a simple goniophotometer.

The phototube is connected through a D.C. voltage supply of 105 volts to the input terminals of an RCA VoltOhmyst. The VoltOhmyst, essentially a vacuum tube voltmeter, measures the D.C. voltage drop across its constant 10-megohm input resistance which is produced by the phototube output current. Since the current output of the phototube is linearly related to the intensity of light incident upon it, D.C. volts indicated by the VoltOhmyst are directly proportional to intensities. Linearity of the phototube with respect to light intensities was checked with a series of Bausch and Lomb neutral-tint glass filters placed near the second slit; the results are shown in Figure 5, where the ordinate is D.C. voltage as indicated by the VoltOhmyst. The anode supply voltage of 105 volts, obtained from three Burgess "B" batteries, was checked with the VoltOhmyst at the beginning of each run; such precautions were considered necessary in order to be certain that the system was functioning correctly. Precise voltage control during each run, however, was unnecessary, since the output current of the 929 phototube is essentially constant over a wide range of anode voltages [48].

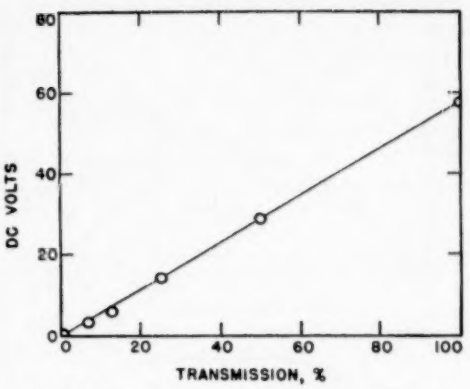

FIG. 5. *Experimental values showing linearity of phototube response.*

While in operation, the phototube is supplied with a small paper shield (see Figure 2) on its back side in order to prevent illumination of the back of its cathode when the tube is rotated past the incident beam. All measurements were taken with the light-tight housing in place, and the VoltOhmyst was "zeroed in" at the beginning of each run in order to insure that no light-leakage contribution to tube output would be measured.

The 929 phototube has the RCA S-4 spectral response curve, which peaks at 3750 Å.; the tube is therefore more responsive to violet light than the eye is, but the two curves are of similar shape, and the difference in response was not considered to outweigh the other advantages of this tube.

Experimental Procedure and Data

The experimental procedure involved in the determination of the goniophotometric curves presented in Figures 6 to 23 was as follows: the fabric sample was inserted in the sample holder, care being taken that the sample exposed as flat a surface as possible. The sample was oriented at some angle, ϕ, with respect to the incident beam by means of the sample pointer; this angle ϕ was maintained while the phototube arm was rotated (by means of its pointer) through various scanning angles θ. The term "scanning angle" was used on the plotted curves in place of "viewing angle," since the latter expression has a subjective implication; "scanning angle" is synonymous with "viewing angle" as the latter expression has been used in previous sections.

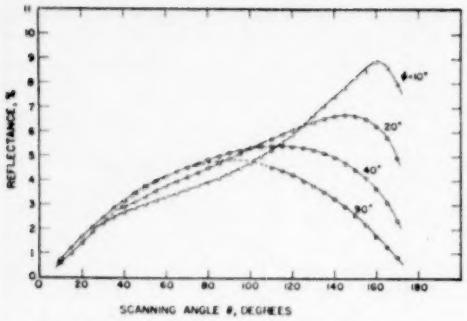

FIG. 6. *Reflectance curves for light-yellow Oxford fabric.*

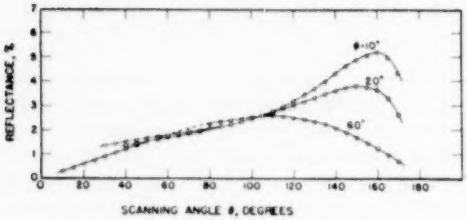

FIG. 7. *Reflectance curves for blue-green Oxford fabric.*

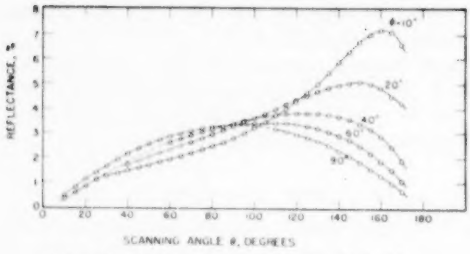

FIG. 8. *Reflectance curves for light-blue Oxford fabric.*

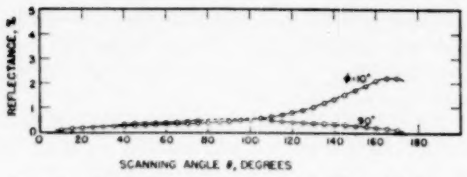

FIG. 9. *Reflectance curves for red Oxford fabric.*

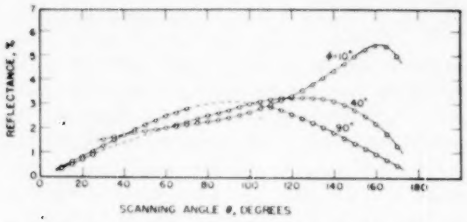

FIG. 10. *Reflectance curves for pink Oxford fabric.*

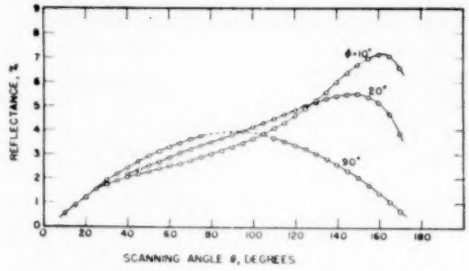

FIG. 11. *Reflectance curves for gray Oxford fabric.*

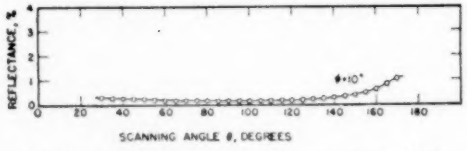

FIG. 12. *Reflectance curve for red velvet fabric.*

D.C. volts were converted to percent reflectance by dividing by the voltage produced when the incident beam struck the phototube head-on with the sample removed. This figure also served as a check on the constancy of the lamp emission. The term "% reflectance" thus means the percentage of the intensity of incident light reflected toward and recorded by the phototube at an angle θ.

Each set of curves corresponds to a particular fabric, except in the case of one ribbed fabric, where it was of interest to determine curves for two orientations of the same fabric in its own plane. Each individual curve corresponds to a particular value of ϕ, the angle of incidence. It should be kept in mind that both θ and ϕ are measured from the sample (see Figure 1) and not from the normal; the angle of mirror reflection (the specular angle) for any ϕ then falls at 180 degrees minus ϕ.

Actual measurements were made on most of the samples for ten values of ϕ—from ϕ equal to 10 de-

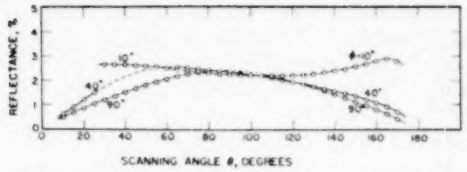

FIG. 13A. *Reflectance curves for tan corduroy fabric with ribs parallel to plane of incidence.*

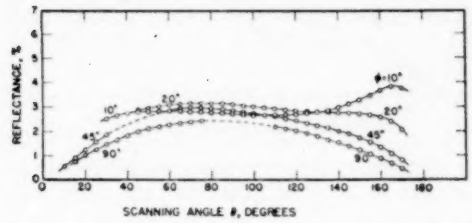

FIG. 13B. *Reflectance curves for tan corduroy fabric with ribs perpendicular to plane of incidence.*

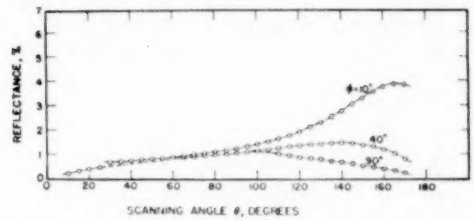

FIG. 14. *Reflectance curves for green poplin fabric.*

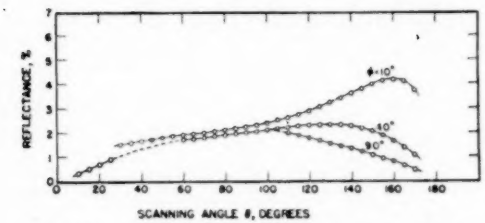

FIG. 15. *Reflectance curves for tan poplin fabric.*

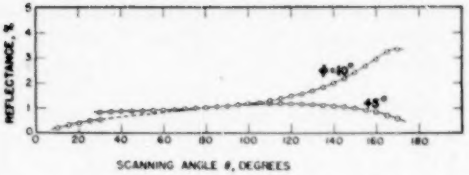

FIG. 16. *Reflectance curves for blue imitation butcher-linen fabric.*

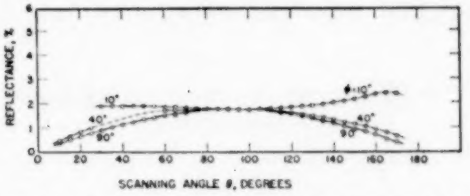

FIG. 17. *Reflectance curves for pink flat-crepe fabric.*

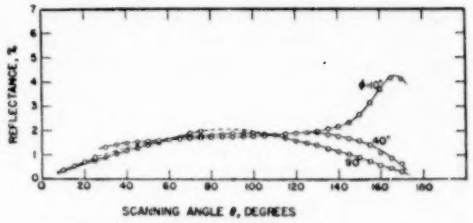

FIG. 18. *Reflectance curves for yellow upholstery fabric.*

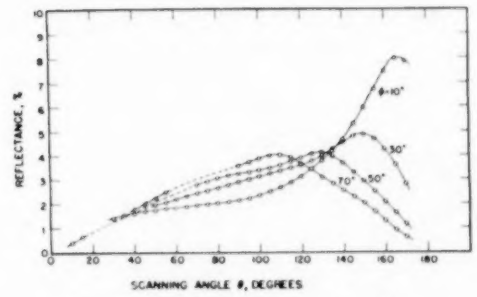

FIG. 19. *Reflectance curves for yellow fancy-rayon fabric.*

grees to 90 degrees in steps of 10 degrees plus a value of ϕ equal to 45 degrees. All of these curves were not plotted, particularly in cases where the trend of behavior was apparent and where confusion would have resulted from plotting many curves on the same graph. For samples showing very low reflectance, curves for only a few values of ϕ are presented, and in one case only one value of ϕ is shown. The size of the receptor surface made impossible measurements at values of θ lower than 10 degrees or higher than 170 degrees.

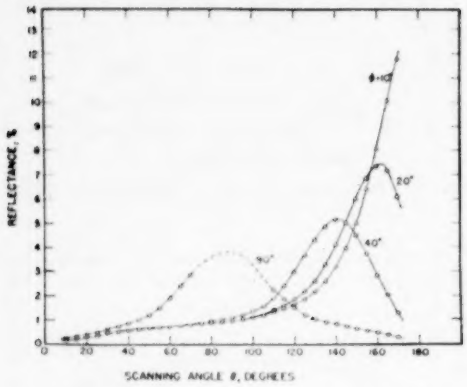

FIG. 20. *Reflectance curves for gray rayon coat-lining fabric.*

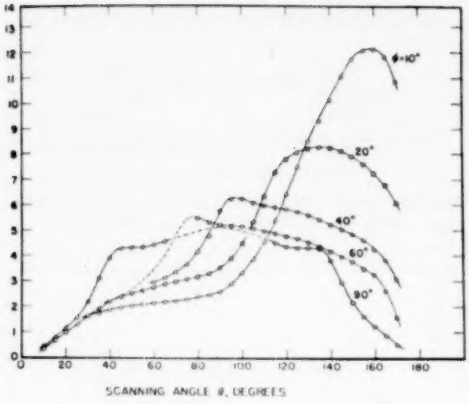

FIG. 21. *Reflectance curves for light-yellow taffeta fabric.*

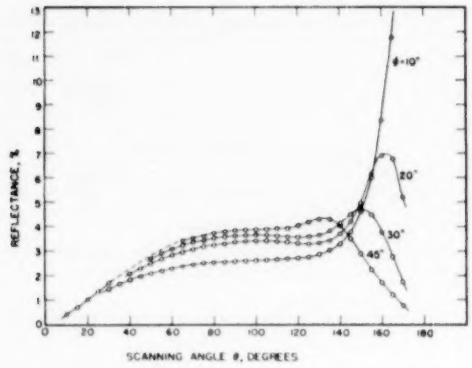

FIG. 22. *Reflectance curves for white, semimatte photographic paper.*

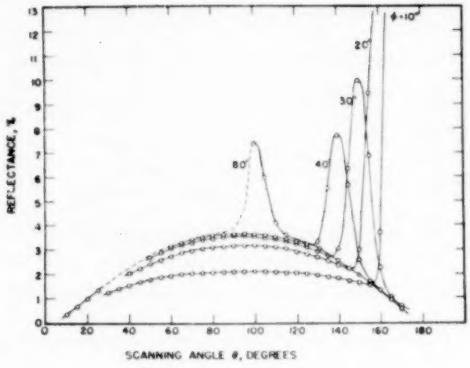

FIG. 23. *Reflectance curves for white, glossy photographic paper.*

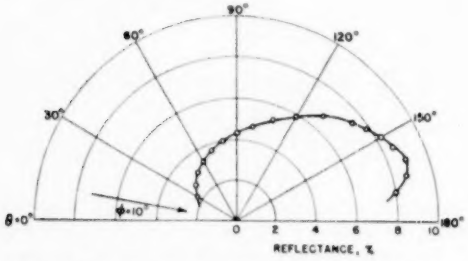

FIG. 24. *Reflectance curve of sample number 6, using polar coordinates.*

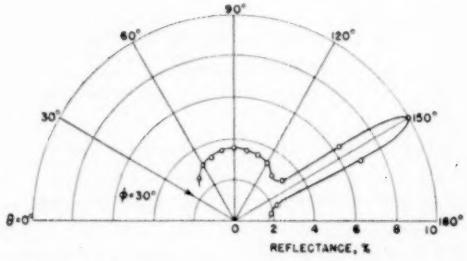

FIG. 25. *Reflectance curve of sample number 23, using polar coordinates.*

It will be noted that the curves contain dotted lines, indicating that no measurements were made in these intervals. These values of θ correspond to positions where the phototube blocked out the incident light—that is, positions in the vicinity of θ equal to ϕ. The present authors have taken the liberty of drawing in the missing portions, not only for the sake of continuity but also because the dotted lines help to distinguish curves corresponding to various values of ϕ when many of the curves fall close together.

Rectangular rather than polar coordinates were employed because of the general unfamiliarity of the latter, and subsequent difficulty in their interpretation. In goniophotometric work, however, polar coordinates have the advantages that angular relationships are more apparent, and the coordinate system suggests the manner in which actual measurements were made; two curves plotted in this way are shown in Figures 24 and 25. In these figures arrows indicate the direction of the incident beam.

The fabric samples were chosen to illustrate the effect on gloss of color, weave, and type of the fiber. It was not intended to investigate exhaustively any one of these variables, but rather to study a variety of fabric types, disregarding their detailed specifications. Several photographic papers were included in the investigations, since they possess interesting gloss properties and have been rather extensively studied in the past [*32*].

Specifications for the fabric samples and photographic papers investigated are given in Table I; fabric samples are numbered to correspond to the figures representing their gloss behavior—sample number 6 corresponds to Figure 6, and so on. Detailed information about some of the fabrics was not available, since many were purchased at local retail stores.

Interpretation of Results and Correlation with Visual Ratings

Inspection of Figures 6 through 23 reveals that all the samples have certain reflectance characteristics in common. The peaks of the reflectance curves, with but few exceptions, shift to the left along the abscissa as the angle of incidence, ϕ, increases, a behavior which is simply a consequence of the law of regular reflection. All curves representing values of ϕ equal to 90 degrees exhibit symmetry about an ordinate corresponding to θ equal to 90 degrees. This

TABLE I. FABRIC AND PHOTOGRAPHIC PAPER SPECIFICATIONS

Sample No.	Type of material	Color	Remarks
6	Oxford	Light yellow	Sanforized, mercerized
7	Oxford	Blue-green	Sanforized, mercerized
8	Oxford	Light blue	Sanforized, mercerized
9	Oxford	Red	Sanforized, mercerized
10	Oxford	Pink	Sanforized, mercerized
11	Oxford	Gray	Sanforized, mercerized
12	Velvet	Red	Cotton
13A	Corduroy	Tan	Measured with ribs parallel to plane of incidence
13B	Corduroy	Tan	Same fabric as No. 13A; measured with ribs perpendicular to plane of incidence
14	Poplin	Green	Sanforized, mercerized cotton; measured with filling perpendicular to plane of incidence
15	Poplin	Tan	Sanforized, mercerized cotton; measured with filling perpendicular to plane of incidence
16	Imitation butcher linen	Blue	Cotton
17	Flat crepe	Pink	Measured with warp parallel to plane of incidence
18	Upholstery material	Yellow	Saran warp, cotton filling
19	Fancy dress goods	Yellow	All filament rayon; delustered warp; all-over novelty pattern
20	Coat lining	Gray	All acetate filament; twill weave; measured with filling parallel to plane of incidence
21	Taffeta	Light yellow	All acetate filament; measured with ribs (filling) parallel to plane of incidence
22	Semimatte photographic paper	White	Eastman Kodak Co. Kodabromide Grade E, designated "white, fine grained, lustre"
23	Glossy photographic paper	White	Eastman Kodak Co. Kodabromide Grade F, designated "white, smooth, glossy"

behavior is also to be expected, since a homogeneous surface illuminated normally will show the same reflectance at the same scanning position on either side of the normal.

The curves show a decrease in peak values as ϕ increases; in other words, samples show the greatest reflectance at near-grazing incidence and, generally, declining reflectance maxima as the angle of incidence is increased. Samples with the highest over-all reflectances—*e.g.*, samples *20*, *22*, *23*—show the sharpest decline; the curve of peak values *vs.* θ appears to be exponential, but actually it is not. This behavior may very well correspond to the subjective impression of "sheen"—high reflectance at near-grazing angles of illumination and viewing. Decrease in reflectance with increase in angle of incidence is characteristic of nonmetallic substances in general [31]. Glass, for example, specularly reflects about 4% of ordinary visible light at normal incidence; at other angles of incidence the reflecting power increases with decreasing angle, at first slowly and then more rapidly until at ϕ close to 0 degrees (grazing incidence) all incident light is reflected. The closest approach to complete reflection reached in this work was a reflectance of about 36% at θ equal to 170 degrees and ϕ equal to 10 degrees for sample number *23*. (This point is not shown in Figure *23*.)

Figures 6–11 and Figures 14 and 15 show the effect of color changes upon reflectances. The samples represented in Figures 6–11 are alike in every respect but color, and the same is true for samples 14 and 15; it is seen that color influences the relative magnitudes but not the shapes of the reflectance curves. Changes in magnitudes with color are, of course, the result of the spectral response of the phototube.

A most important characteristic of many of the curves (one clearly shown in Figures 6–11) is that maximum reflection does not always occur at the specular angle. For an incident angle of ϕ equal to 10 degrees, for example, the corresponding specular angle is 180 degrees minus ϕ, or θ equal to 170 degrees; the curve of Figure 6 corresponding to a value of ϕ equal to 10 degrees, however, peaks at θ equal to 160 degrees, 10 degrees displaced from the specular angle. Displacement from the specular position decreases with increasing ϕ (with the exception of sample *21*), until at ϕ equal to 90 degrees the positions of maximum reflectance and specular reflectance coincide. Noncoincidence of maximum and specular reflectance at low incident angles is exhibited to a greater or lesser degree by all the fabric samples except sample *20*; the photographic papers (samples *22* and *23*), however, show all their peaks at the corresponding specular angles. This point is of considerable importance in the design of instruments to be used for gloss measurements of fabrics, or any surfaces with regular structures; maximum reflectance cannot be assumed to occur at the specular angle. It is interesting that several investigators have obtained goniophotometric curves for fabrics in which the point of maximum reflectance does not coincide with the specular angle, but none has commented on this fact [2, 47, 49].

It is apparent that each type of fabric has a characteristic set of reflectance curves; in general, the greater the degree of structural difference between two fabrics, the greater will be the difference between the shapes of their reflectance curves. The surface structure of the series of Oxford fabrics (Figures 6–11) and that of the two poplin fabrics (Figures 14 and 15) are similar, and the curves in the two cases are of similar shape. The unusual shapes shown in Figures 13A, 13B, and *21* may very well be explained in a similar fashion. These two fabrics have a surface structure unlike any of the other samples. The corduroy fabric, of course, has distinct and relatively large ribs across its face and a rough pile surface. The taffeta fabric (Figure *21*) is also ribbed, but the ribs are much smaller and more uniform; in addition, the taffeta fabric, being made of rayon exclusively, has an over-all smoothness much greater than that of the corduroy.

Quite different reflectance characteristics are shown by the two photographic papers (Figures *22* and *23*) since their surfaces are unlike any of the fabrics. These surfaces, particularly that of sample *23*, illustrate the reflectance characteristics of surfaces approaching those of mirror-like reflectors. The curves of both for ϕ equal to 10 degrees may be taken to represent the closest approach to mirror reflection—constant reflectance at all scanning angles but the specular, and, at this single angle, very high reflectance.

It will be observed that sample *23* exhibits, most noticeably for values of ϕ equal to 20, 30, and 40 degrees, a decline in reflectance just before specular reflection takes place. In Figure *22* there is a suggestion of the same behavior, but in none of the curves for fabrics is this trend apparent. The authors have

been unable to explain this on the basis of present experimental data, but believe that it is associated with the very different nature of the surface of photographic papers: a reflectance curve like that of Figure 23 might be considered to be the sum of two reflectance curves, one corresponding to diffuse reflection from the lower, rough layer of the paper, and the other corresponding to specular reflection from the thin, top, high-gloss film. Reflectance at low incident angles from relatively low-gloss surfaces (see Figure 7) falls off rapidly once the position of maximum reflectance is passed, and maximum reflectance is displaced toward the left for low-incident angles. If it happened that the diffuse reflectance decreased more rapidly at values of θ approaching the specular angle than the specular reflectance increased at these same values of θ, the resultant curve might be expected to exhibit a decline in reflectance just before specular reflectance occurs. Jones [32] did not observe this phenomenon, presumably because his observations were made at normal incidence (ϕ equal to 90 degrees).

Visual rating of the samples was conducted under a 150-watt Mazda blue daylight bulb in a blackened box. Eight observers, including the present authors, attempted to rank the samples according to visual gloss. Little experience was necessary to indicate the difficulties involved in such estimates. An initial attempt was made to classify the samples into the following groups: high gloss, medium gloss, and low gloss. Samples 23, 21, 20, 19, and 22 were placed in the high-gloss group, and were ranked according to decreasing gloss, in the order given. Samples 18, 17, 14, 15, and 16 were placed, in that order, in the medium-gloss group. The set of Oxfords as a whole (samples 6 to 11) was judged to be the highest of the low-gloss group and below it were ranked samples 13A, 13B, and 12, in that order. Within the set of Oxfords, sample 8 appeared to be the glossiest, but no difference was perceptible among other members of this set. This general classification was agreed upon by a majority of observers; one observer, however, ranked samples 12, 13A, and 13B higher in gloss than the set of Oxfords. Several observers disagreed with the authors' ranking of sample 22, placing it in the medium-gloss group.

Ranking within the groups led to occasional agreement. All observers decided that sample 23 was by far the glossiest of the samples. Disagreement arose over sample 21; it was decided that this sample showed a distinct "sheen," particularly when viewed with its ribs horizontal, but agreement was not reached on the question of its rank with samples 19 and 20. Disregarding the position of sample 22, the observers agreed that sample 18 possessed the lowest gloss of the high-gloss group. No other agreement was reached concerning samples within this group, except that already mentioned for sample 23, nor were definite conclusions reached about rankings within the medium-gloss group.

Within the group of low-gloss samples, the initial ranking was generally accepted. Samples 12, 13A, and 13B were considered the lowest of all the samples. Within the group of Oxfords, all observers agreed that little difference was apparent among individual members of the group, except that sample 8 (the light-blue Oxford) might be considered slightly higher. No reason could be given for this choice. Little change in the gloss appearance of the corduroy fabric was perceptible on rotation of the sample through 90 degrees in its plane, and it is seen that the curves in Figures 13A and 13B are quite similar in shape.

Despite the lack of agreement of visual ratings of the samples, several conclusions may be drawn from the attempted correlation. Within a group of samples which differ in color but not in surface structure, similarity in the shapes of the reflectance curves apparently accounts for their equal visual gloss (see Figures 6 through 11). Pile surfaces may be considered the closest approach to perfect "diffusors"

TABLE II. COMPUTED GLOSS NUMBERS

Sample No.	D_o (%)	S_{45} (%)	S_{45}/D_o	$S_{45}-D_o$ (%)	$(S_{45}-D_o)/D_o$
6	4.96	4.83	0.97	−0.13	−0.03
7	2.24	2.58	1.15	0.34	0.15
8	3.44	3.58	1.04	0.14	0.04
9	0.52	0.55	1.06	0.03	0.06
10	2.79	3.10	1.11	0.31	0.11
11	3.95	3.96	1.00	0.01	0.00
12	0.17	0.17	1.00	0.00	0.00
13A	2.38	1.60	0.67	−0.78	−0.33
13B	2.79	2.08	0.75	−0.71	−0.25
14	1.05	1.38	1.31	0.33	0.31
15	2.04	2.20	1.08	0.16	0.08
16	1.05	1.09	1.04	0.04	0.04
17	1.76	1.38	0.78	−0.38	−0.22
18	1.84	1.71	0.93	−0.13	−0.07
19	3.20	4.15	1.30	0.95	0.30
20	1.19	4.85	4.07	3.66	3.08
21	6.04	5.01	0.83	−1.03	−0.17
22	3.86	4.33	1.12	0.47	0.12
23	3.74	7.38	1.97	3.64	0.97

in the realm of textile fabrics; both their reflectance and their visual gloss are low.

One difficulty in the physical measurement of gloss of low-gloss fabrics is illustrated by Figures 9 and 13A or 13B; the over-all reflectance of the Oxford is seen to be lower than that of the corduroy, yet the Oxford was generally ranked higher in visual gloss. The subjective impression of gloss is apparently affected considerably by surface structure in the case of samples which lack gloss "contributors," such as highly lustrous fibers.

The inadequacy of gloss specification for a fabric by a single numerical expression is illustrated in Table II. Gloss numbers in this table have been computed from the experimental data for i equal to 45 degrees and r equal to 0 degrees by means of the formulas outlined previously. It is seen that only measurement of specular reflectance at a scanning angle of 45 degrees from the normal places sample 23 in its position as the highest-gloss sample according to visual ratings. This method, however, ranks sample 6 considerably higher in gloss than sample 18, a ranking which is the reverse of the visual estimate; other disagreements may be easily seen. Moreover, none of the various gloss numbers indicate that the Oxford fabrics have approximately the same visual gloss.

Summary and Conclusions

1. Measurement of the reflectance of incident light from various surfaces as a function of scanning angle is a practical means for obtaining data of greater physical significance than subjective viewing and rating of gloss by observers.

2. Reflectance curves are obtained which are characteristic of different surfaces. Generally, fabric specimens of the same construction provide curves of similar shape; color affects the total reflectance (and hence the position of the curve) but not the shape of the curve. The greatest scattering of incident light is obtained with pile fabrics, which also exhibit very low visual gloss.

3. At an incident angle of 90 degrees the reflectance curve is symmetrical. At small incident angles (near 10 degrees) the peak reflectance is greatest, corresponding to the subjective impression of "sheen."

4. It is not always true that maximum reflectance occurs at the specular angle, and for low-gloss specimens it seldom does. Displacement of maximum reflectance from the specular position is a function of incident angle.

5. Considered as a group, and compared with other surfaces such as coated papers, enameled panels, etc., fabric specimens are of low gloss, or luster, both when measured physically and when estimated visually.

6. The correlation of physical measurements with the subjective sensation of gloss was considered as only a secondary objective of this work, mainly because of the complexities and imponderables of psychophysical analyses. It appears, however, that the analysis of gloss in physical terms requires consideration of many factors, including the following: the brightness of the sample (*i.e.*, total reflectance); the shape of the goniophotometric curve, particularly the sharpness of its peak and its shift with incident angle; and the color of the sample.

7. Successful expression of gloss in adequate terms by a simple numerical expression derived from physical measurements appears extremely unlikely, and all "gloss numbers" serve merely as convenient but not necessarily valid empirical ratings. For industrial and quality control records, goniophotometric data provide an objective measure of certain important optical properties of the surface, and are therefore of considerable value.

Acknowledgments

The authors wish to acknowledge the assistance of Mr. S. P. Hunt in designing the goniophotometer bearing assembly, and of Mr. J. C. Burnett and Mr. H. A. Loving in part of the photographic work.

Literature Cited

1. Adderley, A., *J. Text. Inst.* **15**, T195–206 (1924); *Shirley Inst. Mem.* **2**, 189–93 (1923).
2. Adderley, A., and Oxley, A. E., *J. Text. Inst.* **16**, T167–84 (1925); *Shirley Inst. Mem.* **4**, 17–34 (1925).
3. American Instrument Co., Bulletin No. 2115, entitled "Aminco-Scott Glossmeter," Silver Spring, Md., May, 1943.
4. American Society for Testing Materials, Standard D523–48T for Specular Gloss of Paint Finishes, Philadelphia, 1948.
5. Anderson, A. P., and Reamer, T. E., *Ind. Eng. Chem., Anal. Ed.* **12**, 423–4 (1940).
6. Bancroft, W. D., and Allen, R. P., *J. Phys. Chem.* **28**, 588–610 (1924); **29**, 564–86 (1925).
7. Barratt, T., *Trans. Faraday Soc.* **20**, 240–50 (1924).
8. Benford, F., and Ruggles, W. A., *J. Optical Soc. Am.* **32**, 174–84 (1942).

9. Buck, G. S., Jr., and McCord, F. A., TEXTILE RESEARCH JOURNAL **19**, 715–54 (1949).
10. Dench, E. C., U. S. Patent 2,388,727 (Nov. 13, 1945).
11. Derrett-Smith, D. A., *J. Text. Inst.* **28**, T293–8 (1937).
12. Desbleds, L. B., *Dyer* **64**, 515–17, 583–5 (1930).
13. Gardner, H. A., and Sward, G. G., "Physical and Chemical Examination of Paints, Varnishes, Lacquers, and Colors," Bethesda, Md., Henry A. Gardner Laboratory, Inc., 1950.
14. Hampson, R. E. V., and Richards, H. W., *J. Text. Inst.* **25**, T106–21 (1934).
15. Harrison, V. G. W., "Definition and Measurement of Gloss," London, Printing and Allied Trades Research Assoc., 1945.
16. Harrison, V. G. W., *J. Sci. Instruments* **26**, 84–90 (1949).
17. Haslam, G. S., and Grady, L. D., Jr., *Ind. Eng. Chem., Anal. Ed.* **2**, 346–8 (1930).
18. Horsfield, W. R., Brit. Patent 438,798 (May 23, 1934) (through *J. Text. Inst.* **27**, A79–80 (1936)).
19. Hunter, R. S., *J. Optical Soc. Am.* **26**, 190–6 (1936); *J. Research Natl. Bur. Standards* **16**, 359–66 (1936).
20. Hunter, R. S., *J. Research Natl. Bur. Standards* **18**, 19–39 (1937).
21. Hunter, R. S., *J. Optical Soc. Am.* **30**, 536–59 (1940).
22. Hunter, R. S., *J. Optical Soc. Am.* **31**, 758 (1941).
23. Hunter, R. S., *Metal Finishing* **42**, 519–22 (1944).
24. Hunter, R. S., *J. Optical Soc. Am.* **36**, 178–82 (1946).
25. Ingersoll, L. R., *Elec. World.* **63**, 645 (1914).
26. Ingersoll, L. R., *J. Optical Soc. Am.* **5**, 213–17 (1921).
27. Institute of Paper Chemistry, "Report on Gloss," Appleton, Wisc., Nov. 20, 1934.
28. Institute of Paper Chemistry, "A Comparative Study of the Bausch and Lomb Glossmeter and the Ingersoll Glarimeter," Appleton, Wisc., Nov. 20, 1935.
29. Institute of Paper Chemistry, "Report on the Modified Oxford Glarimeter," Appleton, Wisc., Jan. 10, 1945.
30. Institute of Paper Chemistry, *Paper Trade J.* **107**, 29–40 (Dec. 22, 1938).
31. Jenkins, F. A., and White, H. E., "Fundamentals of Physical Optics," New York, McGraw-Hill Book Co., Inc., 1937.
32. Jones, L. A., *J. Optical Soc. Am.* **6**, 140–61 (1922).
33. Judd, D. B., *Am. Dyestuff Reptr.* **26**, 234–5 (1937).
34. Judd, D. B., *J. Optical Soc. Am.* **27**, 225–7 (1937).
35. Klughardt, A., *Z. tech. Physik* **8**, 109–19 (1927).
36. Klughardt, A., *Melliand Textilber.* **8**, 620 (1927).
37. Laurence, J., *J. Optical Soc. Am.* **31**, 9–13 (1941).
38. McNicholas, H. J., *J. Research Natl. Bur. Standards* **1**, 29–73 (1928).
39. McNicholas, H. J., *J. Research Natl. Bur. Standards* **13**, 211–36 (1934).
40. Moon, P., and Laurence, J., *J. Optical Soc. Am.* **31**, 130–9 (1941).
41. Moon, P., *J. Optical Soc. Am.* **32**, 348–62 (1942).
42. Murty, N. N., Indian Lac Research Inst., Bulletin No. 37, 1940.
43. Myers, R. J., *Ind. Eng. Chem., Anal. Ed.* **12**, 678–81 (1940).
44. Naumann, H., *Z. tech. Physik* **8**, 239–43 (1927).
45. Pfund, A. H., *J. Optical Soc. Am.* **20**, 23–6 (1930).
46. Photovolt Corporation, Bulletin on the Photovolt Photoelectric Glossmeter, New York, May, 1943.
47. Preston, J. M., *J. Soc. Dyers and Colourists* **47**, 136–43 (1931).
48. Radio Corporation of America, "RCA Tube Handbook HB-3," Vol. 1–2, Harrison, N. J., 1947.
49. Ransom, H., and Edelstein, S. M., *Am. Dyestuff Reptr.* **26**, 432–7 (1937).
50. Robertson, J. K., "Introduction to Physical Optics," 3rd Ed., New York, D. Van Nostrand Co., Inc., 1941.
51. Salford Electrical Instruments, Ltd., *Textile Recorder* **53**, 38 (1935) (through *J. Text. Inst.* **27**, A27 (1936)).
52. Schulz, H., *Melliand Textilber.* **5**, 25–7 (1924).
53. Shook, G. A., *J. Optical Soc. Am.* **9**, 61–3 (1924).
54. Slater, J. M., *J. Optical Soc. Am.* **25**, 218–23 (1935).
55. Smith, D., *Interchem. Rev.* **7**, 95–108 (1948–9).
56. Smith, D., and Mahoney, M. M., *Paper Trade J.* **128**, 29–30 (Jan. 13, 1949).
57. Smith, D., and Mahoney, M. M., *J. Optical Soc. Am.* **38**, 86–90 (1949).
58. Vernon, W. H. J., *Trans. Faraday Soc.* **19**, 839–934 (1923–24).
59. Wetlaufer, L. A., and Scott, W. E., *Ind. Eng. Chem., Anal. Ed.* **12**, 647–52 (1940).

(*Manuscript received February 21, 1950.*)

The Influence of Sodium Carboxymethyl Cellulose on the Suspending Power of Built Soap Solutions

C. H. Bayley and A. S. Weatherburn

Division of Applied Chemistry, National Research Laboratories, Ottawa, Canada

Abstract

The influence of sodium carboxymethyl cellulose (CMC) on the ability of soap solutions to prevent the deposition of carbon black on fabric during the detergent process has been studied. It was found that the presence of alkaline builders (sodium carbonate, modified soda, sodium metasilicate, and sodium orthosilicate) resulted in a decrease in the suspending power of soap solutions. The addition of CMC to such built soap solutions compensated to a considerable extent for this reduction in suspending power caused by the builder, although in no case did the suspending power equal that of the unbuilt soap. The maximum improvement in suspending power was obtained with a CMC concentration of 0.005%; *i.e.*, 5% of the weight of soap used. In general, those builders which caused the greatest depression in the suspending power of the soap solution also showed the greatest improvement in suspending power on the addition of CMC.

THE SIGNIFICANCE of the soil redeposition factor in the detergent process has been discussed previously [3], and it was pointed out that the suspending power of a detergent solution is of considerable importance in determining its over-all detersive efficiency. It was further shown that the addition of alkaline builders to a soap solution resulted in a decrease in the suspending power of the latter [4].

Sodium carboxymethyl cellulose (CMC) has been used recently in conjunction with synthetic detergents of the alkyl aryl sulfonate type to increase their suspending power, and considerable improvement not only in suspending power but in over-all detergency has been reported [2]. While the addition of CMC to unbuilt soap solutions was found to have very little effect on their suspending power, its use with soap solutions built with sodium metasilicate was found to be advantageous since it compensated, to a considerable extent, for the reduction in suspending power caused by the builder [1].

The present paper gives data relating to the effect of CMC on the suspending power of soap solutions built with sodium carbonate, sodium sesqui-carbonate (modified soda), sodium metasilicate, and sodium orthosilicate.

Materials and Methods

Materials

Soap: a commercial laundry flake soap, analyzed as follows, was used:

Moisture	5.6%
Total fatty acid	86.7%
Free fatty acid	0.16%
Sodium chloride	0.26%
Sodium sulfate	0.18%
Saponification value of fatty acids	206
Iodine number	55.5
Titer	37.3°C

Sodium carbonate: reagent grade.

Sodium bicarbonate: reagent grade.

Modified soda: A 1:1 molar mixture of sodium carbonate and sodium bicarbonate of the grade listed above (55.8% and 44.2% by weight, respectively).

Sodium metasilicate: "Metso, granular," obtained from National Silicates Limited, New Toronto, Ontario. Na_2O, 29.4%; SiO_2, 28.3%; H_2O (by difference), 42.3%; ratio $Na_2O:SiO_2 = 1.01:1$.

Sodium orthosilicate: "Pensal," obtained from Canadian Industries Limited, Montreal, Quebec.

Na_2O, 61.5%; SiO_2, 29.1%; H_2O (by difference), 9.4%; ratio $Na_2O : SiO_2 = 2.04 : 1$.

Carboxymethyl cellulose: "Carboxel L.V.," a low-viscosity sodium carboxymethyl cellulose supplied by the Standard Chemical Co., Toronto, Ontario.

Methods

The suspending-power measurements were carried out by the method in current use in these laboratories, as follows: A suspension composed of 0.25 g. of carbon black (Standard Micronex, supplied by Binney & Smith Co., 41 E. 42nd St., New York) and 250 ml. of the detergent solution under test was shaken for 20 min. at 70°C. The suspension was contained in 400-ml. vacuum bottles to provide temperature control, and was shaken by means of a shaking machine having a reciprocating motion with a 3-in. stroke and a speed of 105 cycles per min. After the preliminary shaking, one piece of fully bleached, desized cotton fabric (nainsook, 2.7 oz./sq. yd., thread count 100 × 100) measuring 3 in. × 4 in. was added to each bottle and the shaking was continued for 20 min. At the end of this time, the cotton test piece was removed, a second white test piece was added to the same suspension, and the shaking was continued for another 20 min. After removal from the suspension, the test pieces were rinsed lightly in distilled water at 70°C, dried, and ironed, and the reflectance of each side was determined with a Hunter reflectometer. Each experimental value recorded was based on at least 4 replicate determinations (16 reflectometer readings). The suspending power was calculated as follows:

$$\text{Suspending power } \% = \frac{B - B_w}{B_o - B_w} \times 100,$$

where B = average reflectance of test pieces after shaking in detergent suspension; B_w = "water value"

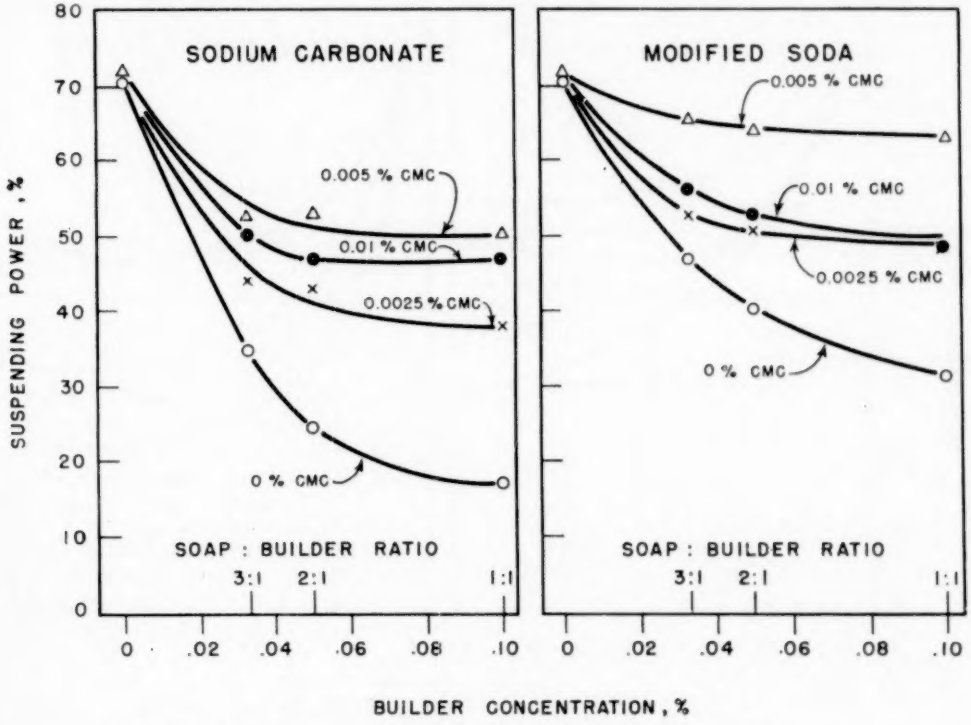

FIG. 1. *Effect of CMC on the suspending power of carbonate-built soap solutions.*

(*i.e.*, average reflectance of test pieces after shaking in a suspension of carbon in distilled water); B_o = average reflectance of original white cotton fabric.

On this scale, 100% suspending power represents no deposition of soil, and 0% represents the suspending power of distilled water.

Stock solutions of the various materials to be tested were made up and diluted as required for use, distilled water being used throughout. The CMC was conditioned at 70 ± 2°F and 65 ± 2% relative humidity prior to weighing.

Data and Discussion

Suspending power measurements were carried out on (*a*) 0.1% soap solution; (*b*) solution containing 0.1% soap + 0.005% CMC; (*c*) solutions containing 0.1% soap + each of the builders, in soap: builder ratios of 1:1, 2:1, and 3:1 for the carbonate builders, and ratios of 1:1, 3:1, and 5:1 for the silicate builders; (*d*) each of the solutions listed in (*c*) with the addition of 0.0025%, 0.005%, and 0.01% CMC (equal to 2.5%, 5%, and 10% of the weight of the soap, respectively). The results are given in Figures 1 and 2 and in Table I.

It may be seen that the suspending power of the unbuilt soap solution was relatively high, and that the addition of 0.005% of CMC to the solution caused only a negligible increase in the suspending power. The addition of increasing amounts of any of the builders studied to the soap solution in the absence of CMC resulted in a progressive decrease in the suspending power of the solution, the more alkaline builders in each group (i.e., carbonate group and silicate group) causing the greater reduction. In every case the addition of CMC to built soap solutions resulted in an improvement in the suspending power, although in no case did the suspending power equal that of the unbuilt soap.

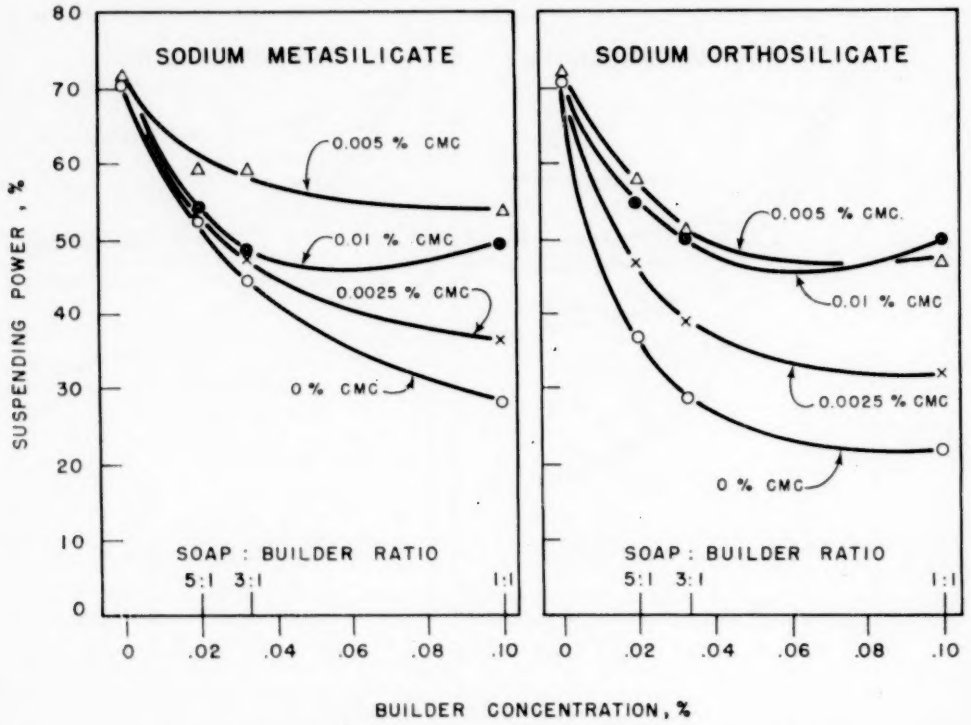

FIG. 2. *Effect of CMC on the suspending power of silicate-built soap solutions.*

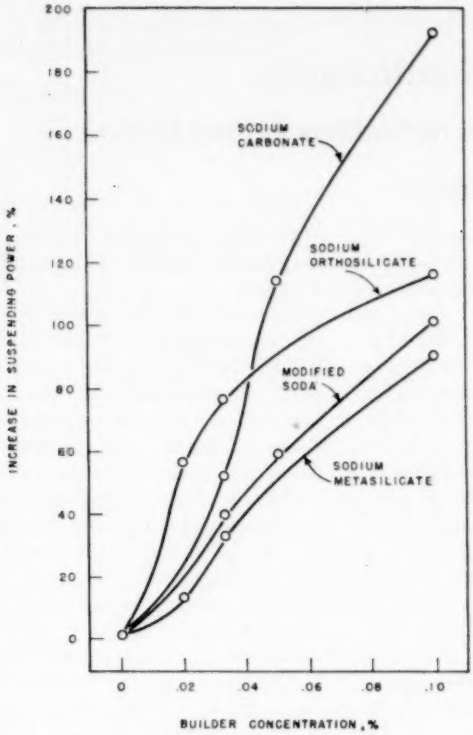

FIG. 3. *Increase in the suspending power of built soap solutions due to the addition of 0.005% CMC.*

Of the three CMC concentrations studied, the maximum improvement in suspending power was obtained with 0.005% CMC, or 5% of the weight of soap, indicating that an optimum CMC concentration exists, and that the use of amounts of CMC in excess of this optimum concentration is not only undesirable from the standpoint of economy but actually results in poorer suspending power, and hence probably in poorer detergent efficiency.

Figure 3 shows the percent increase in suspending power * of various built soap solutions in the presence of 0.005% of CMC. It may be noted that the effectiveness of the CMC in improving the suspending power increases with increasing builder concentration, and that in each group the greater improvement is obtained with the more alkaline builder.

It may be concluded, in general, that the addition of CMC has little effect when the initial suspending power is high, as in unbuilt soap solutions, but that when the initial suspending power tends to be low owing to the use of builders the addition of CMC in the correct proportion results in considerable improvement, the improvement being most pronounced in those cases in which the reduction in suspending power due to the builder has been the greatest.

TABLE I. EFFECT OF CMC ON THE SUSPENDING POWER OF BUILT AND UNBUILT SOAP SOLUTIONS *

Builder Type	Conc'n (%)	Suspending power (%) CMC Concentration (%): 0	0.0025	0.0050	0.0100
None	—	70.5	—	71.7	—
Sodium carbonate	0.033	34.9	44.2	53.0	50.3
	0.050	24.7	43.0	53.0	47.0
	0.100	17.2	38.0	50.3	47.0
Modified soda	0.033	47.0	52.7	65.7	56.1
	0.050	40.2	50.7	64.0	52.7
	0.100	31.3	48.4	62.9	48.4
Sodium metasilicate	0.020	52.4	52.7	59.7	53.9
	0.033	44.7	47.6	59.3	48.4
	0.100	28.4	36.8	53.9	49.4
Sodium orthosilicate	0.020	36.9	46.6	57.6	54.7
	0.033	28.8	38.9	50.8	49.8
	0.100	21.7	31.8	46.9	49.4

* All solutions contained 0.1% of soap.

Acknowledgment

The authors wish to express their thanks to Mr. J. L. Dicaire, who carried out the suspending-power measurements reported in this paper.

Literature Cited

1. Bayley, C. H., Weatherburn, A. S., and Rose, G. R. F., *Laundry and Dry Cleaning J. Can.* **28**, No. 12, 16–18, 36 (Dec. 1948).
2. Vaughn, T. H., and Smith, C. E., *J. Am. Oil Chemists' Soc.* **25**, 44–51 (1948).
3. Weatherburn, A. S., Rose, G. R. F., and Bayley, C. H., The Suspending Power of Detergent Solutions, I: Pure Soaps, *Can. J. Research* **F28**, 213–25 (1950).
4. Weatherburn, A. S., Rose, G. R. F., and Bayley, C. H., The Suspending Power of Detergent Solutions, II: Soap-Builder Solutions, *Can. J. Research* (in press).

(*Manuscript received March 31, 1950.*)

* $\frac{B_c - B}{B} \times 100$ = % increase in suspending power, where B = suspending power of built soap solution and B_c = suspending power of the same solution to which CMC has been added.

Laboratory Techniques

Colorimetric Determination of Sodium Hypochlorite

Guy R. Wallin*

A COLORIMETRIC METHOD for the determination of sodium hypochlorite is offered as a possible alternative to the standard sodium thiosulfate titration procedure. This method depends upon the amount of blue color developed when phenol, ammonium hydroxide, and sodium hypochlorite react. It represents an adaptation to a specific use of a general method developed by Tarugi and Lenci [3] and described by Snell and Snell [2] for determining $-NH_2$ and $=NH$ groups which depends upon the reaction of phenol and sodium hypochlorite with these groups. This method has also been adapted to the qualitative determination of these groups associated with textile materials [4]. Chloramine T has been used as a substitute for NaOCl [1].

Experimental Procedure and Discussion

By holding the phenol and ammonia constant it has been found that the depth of blue color formed in solution when sodium hypochlorite is added is proportional to the amount of available chlorine over a range of 10 mg. of available chlorine per 100 ml., with adherence to Beer's law, as shown in Figure 1.

The quantities of NH_4OH and phenol which would give ideal results were determined by experiment. It is essential to neutralize all free acid. In order to obtain a complete reaction within a reasonable length of time, heat is necessary. The time of heating which is most desirable for reproducible results was also determined by experiment. It was found that with prolonged periods of heating the color of the solution changes from blue to green and then to greenish yellow. The original color reappears upon cooling.

The formation of the blue color is evidently associated with the oxidizing potential of NaOCl. If one substitutes H_2O_2 for NaOCl one obtains a greenish yellow color with a maximum absorption at 415 mμ. The maximum absorption band with NaOCl as determined with a Leitz Rouy-Photrometer is at 640 mμ, as shown in Figure 2.

Phenol and NH_4OH will react over a protracted period of time, with the formation of a blue color. The development of this color is believed to be associated with exposure to ultraviolet light. Owing to the length of time required for the development of this blue color, it does not interfere with the determination of NaOCl. Upon heating in boiling water for 10 min. the colored complex separates from the aqueous phase; the complex has a greater density and an oily, droplet-like formation. It is not affected by alkalies or reducing agents.

The pH of the solution being tested is important. The method was developed for solutions of NaOCl with the usual alkalinity and pH. There is not a sufficient amount of NH_4OH to compensate for lack of alkalinity of the test solution. If the solution has

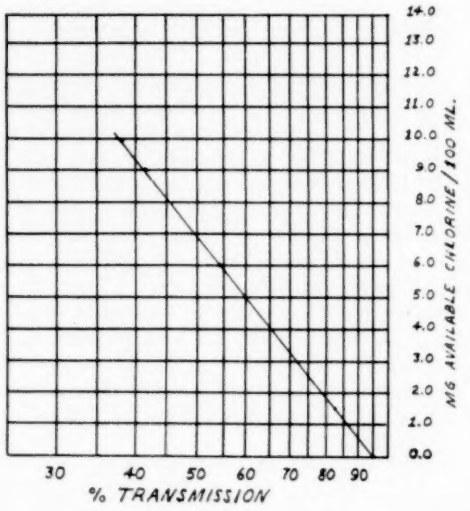

FIG. 1. *Calibration curve.*

* Present address: Burlington Mills Corp., Greensboro, North Carolina.

pH below 11 it must be brought up to this point with alkali before analysis is begun.

Reagents

26% NH_4OH, or equivalent, and 90% phenol, or equivalent.

Procedure

Take 10 ml. of unknown which has a pH of 11 and dilute to 100 ml. with distilled water. Place 2 ml. of 26% NH_4OH and 1 ml. of 90% phenol in a 100-ml. flask. Transfer 2 ml. of diluted unknown to this flask. This must follow the addition of the reagents. Mix and allow the blue color to develop. Immerse flask in boiling water for *exactly* 1 min. Dilute to mark with distilled water and allow to stand for exactly 5 min. Set colorimeter to zero with distilled water, using a filter covering 640 mμ. Read unknown at end of 5-min. period of standing. See Table I for results.

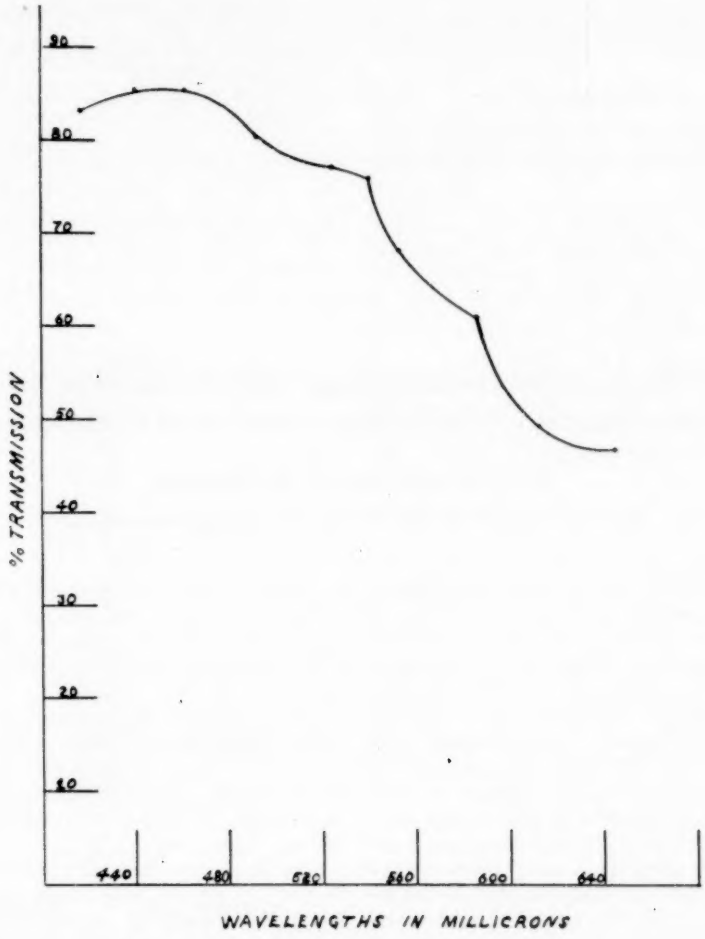

FIG. 2. *Absorption curve, using NaOCl, as determined with a Leitz Rouy-Photrometer.*

TABLE I. ANALYSES OF KNOWN AMOUNTS OF NaOCl USING COLORIMETRIC PROCEDURE

Amount in solution (mg. of available chlorine)	Amount found (mg. of available chlorine)	Recovery * (%)
3.0	3.0	100.0
3.0	3.0	100.0
3.0	3.0	100.0
6.0	6.0	100.0
6.0	6.0	100.0
6.0	5.9	100.0
9.0	9.2	102.2
9.0	9.1	101.1
9.0	9.0	100.0

* The greatest error in recovery was 2.2%, which is well within the range of error tolerable for colorimetric procedures.

Summary

This is a simple, fast, and accurate method which compares favorably with the sodium thiosulfate titration procedure. A determination may be completed in 7 or 8 min. Only 2 reagents are required, and they are of the type which will be on hand at all times, whereas sodium thiosulfate, which is used in the standard procedure, is difficult to standardize and to keep.

Literature Cited

1. Crismer, *Bull. soc. chim. biol.* **19**, 1000–9 (1937) (through *Chem. Abstr.* **31**, 7796 (1937)).
2. Snell, F. D., and Snell, C. T., "Colorimetric Methods of Analysis," 3rd ed., New York, D. Van Nostrand Co., 1948.
3. Tarugi and Lenci, *Boll. chim. farm.* **50**, 907 (1912); Merck Index, 3939.
4. Wallin, G. R., *Am. Dyestuff Reptr.* **38**, 746 (Oct. 17, 1949).

(*Manuscript received January 27, 1950.*)

Rapid Method for Determining Mildew Susceptibility of Materials and Disinfecting Activity of Compounds

R. G. H. Siu and G. R. Mandels

Quartermaster General Laboratories, Philadelphia, Pennsylvania

A SIMPLE METHOD has been developed in the Quartermaster General Laboratories which minimizes the difficulties inherent in the tests used currently for evaluation of resistance of materials to microorganisms. In many cases tests can be completed overnight. Furthermore, the same apparatus can be used for testing a variety of materials, such as cotton, wool, leather, and plastics. Once the apparatus has been set up and adjusted for the particular test to be used, the method can be executed by the average technician. A brief description of the technique is given in this paper. Detailed experimental results involving various materials are being published elsewhere.

Millions of individual assays are conducted annually on the bactericidal and fungicidal activity of chemical compounds. Since the last war considerable emphasis has been laid on testing the susceptibility of various materials, such as cotton, wool, leather, paper, and plastics, to microorganisms for purposes of research and procurement. Here again the number of tests is very large.

One of the objectionable features of most of these testing procedures is the length of time required. In the case of cotton textiles the period varies between 14 and 45 days. For plastic films [5] about 30 days are required. Leather [2] demands an equally long period of incubation.

Another difficulty lies in the fact that different apparatus and conditioning rooms are required for different materials. In the case of cotton textiles, for example, the conditioning room is maintained at 70°F and 60% relative humidity; a Scott Tensile

Tester is used to determine the decline of fabric strength. In contrast to the conditions required for cotton textiles, plastic films are conditioned at 73°F and 50% relative humidity; a Clark Flexibility Tester is employed to measure increased stiffness of the film.

The method proposed here is based upon a measurement of the growth of the microorganism by means of a manometric determination of the total oxygen absorbed during growth. This is the basic difference between this method and those manometric methods previously proposed [1, 4, 6], which involve a measurement of the effect of a particular substance upon the respiration of a given quantity of organisms. A basic shortcoming of such techniques is that growth can be inhibited by concentrations of substances which may have little or no effect upon the immediate respiration. The converse situation has not been observed. Since the main interest is in preventing growth, the difficulty is obvious. It should also be pointed out that it would be easy to overlook an effective compound by relying upon such methods. In the method described here the cumulative respiration of the mass of organism which has grown in the presence of the inhibitor is measured. The basic assumptions are: (1) the amount of growth in a given period is a function of the effect of the inhibitor; (2) the cumulative respiration of the organism during growth is determined to a much greater degree by the quantity of organism than by the effect of the substance on respiration.

TABLE I. MILDEW-RESISTANCE OF TREATED COTTON FABRICS AS DETERMINED BY 2 TESTING METHODS

Pure-culture method			Manometric method		
Time (days)	% copper naphthenate as copper	Strength loss (%)	Time (hrs.)	% copper naphthenate as copper	Pressure change (mm.)
3	0.00	45	20	0.00	53
	0.01	23		0.01	48
	0.04	7		0.04	22
	0.16	0		0.16	6
	0.64	0		0.64	2
7	0.00	87	30	0.00	114
	0.01	87		0.01	102
	0.04	32		0.04	50
	0.16	0		0.16	10
	0.64	0		0.64	1
11	0.00	100	40	0.00	192
	0.01	100		0.01	177
	0.04	90		0.04	73
	0.16	0		0.16	18
	0.64	0		0.64	4

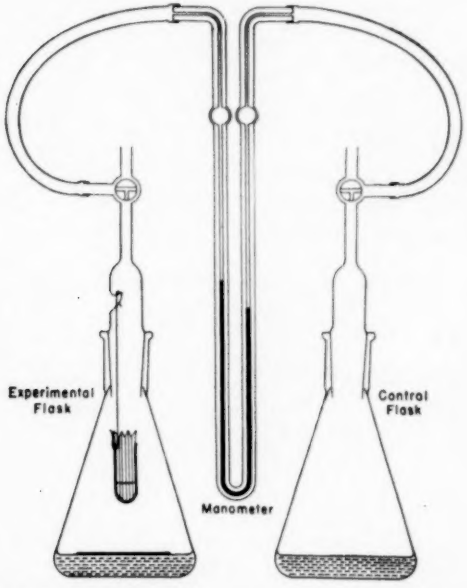

FIG. 1. *Differential manometer for evaluation of microbiological susceptibility.*

The apparatus (Figure 1) is, essentially, a Barcroft differential manometer. The manometer proper is constructed of capillary tubing of 2 mm. bore, with arms about 300 mm. long which are partially filled with Brodie's solution [3]. The bulbs have a capacity several times the volume of the manometric fluid. The culture vessels are 250-ml. Erlenmeyer flasks fitted with 24/40 standard tapered joints and attached to the manometer arms by flexible plastic tubing. Each flask contains 50 ml. of mineral-salts agar. Suspended in the flask is a cup containing 1.5 ml. of 10% potassium hydroxide and a filter-paper wick. In our laboratory the apparatus is placed in an incubator at 30°C. Actually, only the flasks need be in the incubator.

The method can be illustrated by the following procedure for cotton textiles. A fabric disc, 7 cm. in diameter, is placed on the agar surface in the experimental flask and inoculated with 1 ml. of a spore suspension of *Myrothecium verrucaria*, USDA 1334.2. Both experimental and control flasks are then attached to the manometer by the connectors (the

joints should be carefully sealed with stopcock lubricant). After an equilibration period of 3 hrs. the stopcocks are closed. During growth the organism absorbs oxygen from the gas space in the flask, which causes a decrease in pressure. The carbon dioxide produced is absorbed by the alkali in the well. Periodic readings are taken of pressure changes in the manometers. These changes are used as the criterion of susceptibility to mildew.

A comparison of data obtained by this method and by the standard pure-culture technique is provided by values given in Table I. Cotton khaki twill fabrics containing different amounts of copper naphthenate were used. The correlation between results obtained by the two procedures is excellent.

In tests of greater duration it is advisable to have wells containing alkali as well as the same agar medium in both experimental and control flasks. Both flasks are inoculated. Respiration due to growth of the organism on the agar, which contains significant quantities of assimilable impurities, is thus canceled out.

Acknowledgment

Acknowledgment is made to Miss T. M. Powers for her technical assistance in the development of the method, and to Messrs. L. Boor, A. McQuade, and M. Packard for supplying some of the materials.

Literature Cited

1. Bronfenbrenner, J., Hershey, A. D., and Doubly, J., *J. Bact.* **37**, 583 (1939).
2. Day, D., *J. Am. Leather Chemists' Assoc.* **44**, 558 (1949).
3. Dixon, M., "Manometric Methods," Cambridge University Press, 1943.
4. Ely, J. O., *J. Bact.* **38**, 391 (1939).
5. Harvey, J. V., "Testing the Fungal Resistance of Plastic-Coated Fabrics and Plastic Film," Research Report, Microbiology Series No. 13, Philadelphia, Pa., Quartermaster General Laboratories, Apr. 22, 1949.
6. Nickerson, W. J., *Science* **103**, 484 (1946).

(Manuscript received May 1, 1950.)

TEXTILE RESEARCH INSTITUTE, INC.

LABORATORIES AND GENERAL OFFICES

KINGSTON-PRINCETON ROAD, PRINCETON, N. J.

PUBLICATIONS DEPARTMENT

10 EAST 40TH STREET, NEW YORK 16, N. Y.

OFFICERS

A. G. Ashcroft, *President*
Kenneth Wilson, *Vice-President*
Richard T. Kropf, *Treasurer*
P. C. Alford, Jr., *Secretary*

BOARD OF DIRECTORS

Term Expires 1952	*Term Expires 1951*	*Term Expires 1950*
Norman C. Armitage	F. Eugene Ackerman	A. G. Ashcroft
Andre Blumenthal	Joseph H. Brant	Robert Burns
Ephraim Freedman	Miles A. Dahlen	W. J. Fullerton
Thomas G. Hawley, Jr.	Bertrand W. Hayward	J. B. Goldberg
G. P. Hoff	Richard T. Kropf	Henry Herrmann
Jules Labarthe, Jr.	H. Wickliffe Rose	C. H. Masland, II
Donald H. Powers	Leonard Smith	Edward T. Pickard
W. Bailey Sellars	Kenneth Wilson	H. Gordon Smith

EXECUTIVE COMMITTEE

Andre Blumenthal, *Chairman*

A. G. Ashcroft	Richard T. Kropf	H. Gordon Smith
J. B. Goldberg	H. Wickliffe Rose	Kenneth Wilson

DIRECTOR OF RESEARCH

John H. Dillon

DEPARTMENT HEADS

James H. Wakelin, *Associate Director of Research*
P. C. Alford, Jr., *Administrative Assistant to Director of Research*
K. Lanse Turner, *Assistant to Director of Research, Field Engineer*

Julian S. Jacobs, *Director of Publications*
10 East 40th Street
New York 16, New York

Edward T. Pickard, *Advisor on Economic Research and Education*
Kent, Connecticut

RESEARCH ADVISORY COMMITTEE

Miles A. Dahlen, *Chairman*	Karl T. Compton	Richard T. Kropf
William D. Appel	Robert E. Doherty	G. K. Lake
A. G. Ashcroft	Warren E. Emley	Donald H. Powers
F. Bonnet	J. B. Goldberg	Hugh S. Taylor
Joseph H. Brant	M. E. Heard	Werner von Bergen
Lyman J. Briggs	G. P. Hoff	Albert C. Walker
Vannevar Bush	Donald H. Howard	R. Y. Winters
Malcolm E. Campbell	H. Y. Jennings	